



北京大学

# 博士研究生学位论文

题目： 基于 SUN 分布的 Thurstone-Mosteller  
排序模型的共轭贝叶斯学习方法

姓 名： 李臻

学 号： 1601110060

院 系： 数学科学学院

专 业： 统计学

研究方向： 统计机器学习

导 师： 姚远

二〇二四年三月

# 版权声明

任何收存和保管本论文各种版本的单位和个人，未经本论文作者同意，不得将本论文转借他人，亦不得随意复制、抄录、拍照或以任何方式传播。否则，引起有碍作者著作权之问题，将可能承担法律责任。







## 摘要

成对比较法在基于成对比较 (Pairwise Comparison) 数据推导出排序 (Ranking) 的过程中扮演着关键角色，尤其在众包 (Crowdsourcing) 环境下更是如此。在此种情况下，贝叶斯决策过程为采集现实世界数据提供了一个可行且充满希望的手段，特别是在线 (Online) 环境，数据是序列化采集的，并且整个采集过程受到严格的预算限制。然而，现有的方法往往因为近似误差而性能受损。例如，近似知识梯度法 (Approximated Knowledge Gradient) 依赖矩匹配 (Moment Matching) 来估计每轮迭代后的后验分布，这种做法导致了结果的不精确性。

本研究提出了一种创新方法来弥补这一不足，该方法采用了 SUN (Unified Skew-Normal) 分布作为后验，并且具有闭式解。在广泛应用的经典排序模型——Thurstone-Mosteller 模型中，本文发现如果参数的先验是高斯分布，则后验为 SUN 分布。本文的定义的最优排序是基于 Kendall's  $\tau$  相关系数的后验期望最大化，并在文中展示了，在一些轻微的基于实践观察的假设下，该封闭形式的后验导出的最优排序恰好就是后验均值排序。

本研究的框架不仅从贝叶斯视角丰富了频率学派的成对比较法，他也可以被无缝推广到一个动态的在线排名系统中，并享有闭式后验的优势。将本研究的框架与知识梯度 (Knowledge Gradient) 策略结合，本文把主动采样 (Active Sampling) 策略转化为一个贝叶斯马尔可夫决策过程 (Bayesian Markov Decision Process)。该决策系统的目标函数是固定样本数量的情况下最大化 Kendall's  $\tau$  后验期望，并基于知识梯度策略每一步选择相应的成对数据 (Pair) 进行比较。此整合显著提升了采样效率，并减少了精确推断排序所需的成对比较样本数量。

针对大规模数据集所带来的计算挑战，本文采用了平均场变分推断 (Mean-field Variational Inference, MFVI) 方法来有效近似后验分布，并保持局部收敛的特性，同时维持 Kendall's  $\tau$  的精度。

本文在模拟和现实世界的数据集上进行了广泛实验，以验证了本研究方法的有效性和计算效率。模拟数据集的研究强调了本研究的框架在不同数据生成模型（如 Thurstone-Mosteller 或 Bradley-Terry-Luce 模型）下的适应能力，确保了其稳健性和有效性。在现实世界数据的实验中，无论是阅读难度评估、图像质量评价还是视频质量评价，本文的框架都展现了显著的性能。特别是在阅读难度评估（教育领域），本文的算法实现了最优的 Kendall's  $\tau$  表现，彰显了其在个性化学习体验上的潜力，即通过匹配不同难度的教育材料和学习者的对应阅读能力，以此来提高教学效率。在图像和视

频质量评价方面，本研究的方法在多个场景中实现了最先进的 Kendall's  $\tau$  性能，显示了其在优化压缩参数和提升用户满意度方面的应用潜力。考虑到图像和视频质量评估数据集中的基准分数是通过 HodgeRank 估计的，这进一步证明了该框架的稳健性。

综上所述，本论文提出了一个全新的贝叶斯共轭排序框架，显著推动了成对比较方法的发展，并提供了解决现实应用中关键挑战的新颖解决方案。同时，本文展示了该框架在多个领域应用中的稳健性和实用性。

关键词：Thurstone-Mosteller 模型，贝叶斯共轭框架，主动采样，成对比较，统一偏态正态分布，知识梯度，平均场变分推断。

# Conjugate Bayesian Ranking for Thurstone-Mosteller Model via Unified Skew-Normal Distributions

Zhen Li (Statistics)

Directed by Prof. Yuan Yao

## ABSTRACT

Pairwise ranking methods play a crucial role in inferring rankings from pairwise comparison data, particularly in crowdsourcing contexts. Bayesian decision processes offer a promising avenue for handling real-world data collection, especially in online settings with sequential data acquisition and budget constraints. However, existing methods often suffer from approximation errors, diminishing their performance. For instance, approximated knowledge gradient methods rely on moment matching to approximate the posterior distribution per iteration, introducing inaccuracies.

This dissertation addresses this gap by proposing a novel approach that leverages the closed-form posterior derived from the Unified Skew-Normal (SUN) distribution. We observe that under the Thurstone-Mosteller model, a widely-used classical ranking model, the posterior follows the SUN distribution with Gaussian priors. Demonstrating under empirically observed assumptions, this closed-form posterior facilitates optimal ranking inference based on the expected Kendall's  $\tau$  correlation coefficient via posterior mean sorting.

Our framework not only supplements frequentist pairwise comparison methods from a Bayesian perspective but also extends seamlessly to an active online ranking framework enjoying a closed-form nature. By integrating our framework into the knowledge gradient policy as a Bayesian Markov Decision Process for active sampling, strategic selection of pairs for comparison is enabled, maximizing expected Kendall's  $\tau$  over the known form of posterior. This integration enhances sampling efficiency and reduces the number of pairwise comparisons required for accurate ranking inference.

To address computational challenges associated with large-scale datasets, we employ Mean-field Variational Inference (MFVI) method, efficiently approximating the posterior distribution with local convergent property while maintaining Kendall's  $\tau$  accuracy.

Extensive experimental validation on both simulated and real-world datasets underscores

the efficacy and computational efficiency of our proposed approach. In simulated datasets, our research highlights the adaptability of our framework across different data generation models (Thurstone-Mosteller or Bradley-Terry model), ensuring robustness and effectiveness regardless of the underlying model. In real-world data experiments, our framework shows its remarkable performances in a variety of applications, including reading difficulty assessment, image quality assessment, and video quality assessment. In the education domain (reading difficulty), our algorithm achieves highest Kendall's  $\tau$  performance, highlighting its ability to offer personalized learning experiences by matching educational materials to learners' proficiency levels, enhancing educational effectiveness. In image and video quality assessment, our approach achieves state-of-art Kendall's  $\tau$  performance in many cases, highlighting its utility to optimizing compression parameters and enhancing user satisfaction. Considering the ground-truth scores are estimated via HodgeRank in imagine an video quality assessment datasets, this fact further emphasizes the robustness of our framework.

Additionally, we provide insights into the computational trade-offs between our original framework and a more computationally efficient version (MFVI approximated version), offering practitioners flexibility in balancing computational speed and accuracy.

In summary, this dissertation significantly advances pairwise comparison methodologies with a conjugate Bayesian framework, providing novel solutions that address critical challenges in real-world applications and shows its robust practical utility with applications spanning diverse domains.

**KEYWORDS:** Thurstone-Mosteller model, Bayesian conjugate framework, active ranking, pairwise comparisons, unified skew-normal distribution, knowledge gradient, mean field variational inference.

## Contents

<b>Chapter 1 Introduction.....</b>	<b>1</b>
1.1 Problem Background.....	1
1.2 Main Contributions .....	4
1.3 Organization.....	6
1.4 Notations .....	7
<b>Chapter 2 The Unified Skew-Normal (SUN) Distribution.....</b>	<b>9</b>
2.1 Multivariate Normal Distribution.....	9
2.1.1 Some Properties of Multivariate Normal Distribution .....	10
2.2 Multivariate Skew-Normal Distribution.....	11
2.2.1 Derivation of Multivariate Skew-Normal Distribution.....	12
2.2.2 Some Properties of Multivariate Skew-Normal Distribution .....	12
2.3 The Unified Skew-Normal Distribution .....	13
2.3.1 Derivation of Unified Skew-Normal Distribution .....	13
2.3.2 Some Properties of Unified Skew-Normal Distribution.....	14
2.3.3 Applications of the Unified Skew-Normal Distribution .....	16
2.4 Chapter Summary .....	17
<b>Chapter 3 Conjugate Bayesian Framework for Thurstone-Mosteller Model .....</b>	<b>19</b>
3.1 Introduction .....	19
3.2 Pairwise Comparison Methods .....	19
3.3 Bayesian Ranking Framework .....	21
3.4 Conjugate Bayesian for Thurstone-Mosteller Model.....	25
3.5 Monte Carlo Estimation of $\text{Pred}_T(i > j)$ and $\mu_T$ .....	31
3.6 Convergence of SUN Ranking Algorithm.....	33
3.7 Chapter Summary .....	36
<b>Chapter 4 Proofs of the Conjugate Bayesian Framework.....</b>	<b>37</b>
4.1 Preliminaries .....	37
4.2 Proof of Theorem 3.1 for the Estimated Ranking .....	38
4.3 Proof of Proposition 3.1 for the CDF form of $\text{Pred}_T(i > j)$ .....	47
4.4 Proof of Lemma 3.1 for the Derivation of SUN Distribution.....	51

---

4.5 Proof of Theorem 3.2 on Convergence Property .....	52
<b>Chapter 5 Conjugate Bayesian Active Online Ranking .....</b>	<b>57</b>
5.1 Introduction .....	57
5.2 Previous Online Ranking Frameworks and Their Defects .....	57
5.3 Bayesian Markov Decision Process.....	59
5.4 Knowledge Gradient Policy and SUN Active Ranking .....	60
5.5 Interesting Properties of SUN Active Ranking.....	62
5.6 Proofs in This Chapter .....	63
5.7 Chapter Summary .....	67
<b>Chapter 6 Approximation by Mean-Field Variational Inference.....</b>	<b>69</b>
6.1 Introduction .....	69
6.2 Variational Inference and Mean-Field Family.....	70
6.3 SUN Ranking with Mean-Field Variational Inference .....	71
6.4 SUN Active Ranking with Mean-Field Variational Inference .....	76
6.5 Proofs in This Chapter .....	77
6.6 Chapter Summary .....	79
<b>Chapter 7 Experimental Validation on Simulated Data.....</b>	<b>81</b>
7.1 Simulation Study for SUN Ranking Algorithm .....	81
7.1.1 Experimental Setting .....	81
7.1.2 Implementation Details.....	81
7.1.3 Compared Baselines.....	82
7.1.4 Kendall's $\tau$ Comparison.....	82
7.1.5 Computational Costs .....	83
7.2 Simulation Study for SUN Active Ranking Algorithm .....	84
7.2.1 Experimental Settings and Implementation Details .....	85
7.2.2 Compared Baselines.....	85
7.2.3 Kendall's $\tau$ Comparison.....	85
7.2.4 Computational Costs .....	87
7.3 Chapter Summary .....	88
<b>Chapter 8 Real-World Applications.....</b>	<b>91</b>
8.1 Real-World Applications for SUN Ranking Algorithm .....	91
8.1.1 Applications and Datasets.....	91

8.1.2	Implementation Details.....	92
8.1.3	Result Analysis for Reading Difficulty Dataset.....	93
8.1.4	Result Analysis for IQA and VQA Datasets .....	94
8.2	Real-World Experiments for SUN Active Ranking Algorithm .....	95
8.2.1	Implementation Details.....	96
8.2.2	Results Analysis .....	96
8.3	Chapter Summary .....	97
<b>Chapter 9</b>	<b>Conclusions and Future Work .....</b>	<b>101</b>
<b>References</b>	.....	<b>103</b>
<b>Appendix A</b>	<b>Code Implementation.....</b>	<b>109</b>
A.1	Implementation Description.....	109
A.2	Function Descriptions .....	109
A.3	Function Details .....	110
<b>Acknowledgment</b>	.....	<b>113</b>
<b>北京大学学位论文原创性声明和使用授权说明</b>	.....	<b>115</b>
<b>学位论文答辩委员会名单</b>	.....	<b>117</b>
<b>北京大学博士学位论文答辩委员会决议书</b>	.....	<b>119</b>
<b>提交终版学位论文承诺书</b>	.....	<b>121</b>



# Chapter 1 Introduction

## 1.1 Problem Background

Rank aggregation, originating from social choice theory [Borda, 1781], addresses the task of consolidating diverse rank orders into an optimized ranking. Its utility spans various domains, including recommendation systems [Baltrunas et al., 2010, Meena and Bharadwaj, 2013, Zehlike et al., 2022, Bałchanowski and Boryczka, 2023], web search algorithms [Dwork et al., 2001, Lempel and Moran, 2005, Lamberti et al., 2008], and competitive arenas like sports and gaming competitions [Ailon et al., 2008, Pelechrinis et al., 2016, Minka et al., 2018, Chen et al., 2022].

In the realm of ranking methodologies, estimating latent scores for items is crucial as they gauge various aspects such as relevance or quality. Researchers typically encounter two types of labels when estimating scores: one type pertains solely to individual items. For instance, users may assign ordinal scores ranging from 1 to 10 to rate a movie. However, scores from this type may be inconsistent due to variations in users' knowledge backgrounds or psychological states. For example, an optimistic user may rate all movies highly, while a pessimistic user may rate all movies low. The second type of labels is associated with a subset of items. For example, users are asked to choose their favorite movie from a set of movies. This approach can effectively reduce bias among users and is more widely used in academic research.

Empirical evidence consistently favors labels derived from pairwise comparisons over the simultaneous assessment of multiple items, as discussed by Chen et al. [2016]. Therefore, many works have been proposed in pairwise ranking, employing paired comparison data where workers are presented with each pair to choose which one is better. Typical examples include Jiang et al. [2011], Emerson [2013], Rajkumar and Agarwal [2014a], Negahban et al. [2012], Azari Soufiani et al. [2013], Chen et al. [2022].

While these methods exhibit strong performance on static datasets, it is crucial to acknowledge that real-world data collection often faces constraints imposed by budget or time limitations. To address this challenge, numerous active sampling strategies have been proposed [Li et al., 2018, Mikhailiuk et al., 2021, Xu et al., 2018a, Chen et al., 2013, 2016], with the goal of optimizing the efficiency of collecting samples in terms of ranking accuracy. Among these methods, most of them are based on Bayesian inference. For instance, Li et al. [2018] introduced the *Hybrid Minimum Spanning Tree* (Hybrid-MST), selecting a new pair via the

maximization of the expected information gain (EIG) based on the asymptotic distribution of Maximum Likelihood Estimator. Furthermore, Chen et al. [2016] aimed to maximize the expected Kendall's  $\tau$  correlation coefficient [Kendall, 1938], a direct measure of ranking accuracy, under the Bradley-Terry-Luce (BTL) model with a Dirichlet Prior. To determine the optimal sampling sequence, they introduced the *approximated knowledge gradient* (AKG) method, leveraging moment matching to approximate the posterior at each iteration.

A significant challenge faced by these methods lies in the occurrence of approximation errors, which can severely impact sampling efficiency and ranking accuracy. For instance, the asymptotic distribution of Hybrid-MST in Li et al. [2018] may not hold in early iterations, especially when the sample size is small. Additionally, the approximated posterior distribution via moment matching approach employed in AKG [Chen et al., 2016] may deviate from the ground-truth posterior since the target function for approximation is not the true posterior after more than one sample, leading to non-ignorable estimation errors. To illustrate this, consider the following example.

*Example 1.1.* Consider the ranking of  $N = 3$  items with scoring parameters  $\theta_1, \theta_2$ , and  $\theta_3$ . We examine the estimation error of three methods: AKG [Chen et al., 2016], utilizing an approximated posterior; Hybrid-MST [Li et al., 2018], utilizing asymptotic distribution; and our proposed method, denoted as SUN. The error is defined as:

$$\text{Error}_t = \sum_{i=1}^3 \sum_{j=i+1}^3 \left| \Pr(\theta_i - \theta_j > 0 | X_t, Y_t) - \widehat{\Pr}(\theta_i - \theta_j > 0 | X_t, Y_t) \right|,$$

where, at the  $t$ -th iteration,  $X_t$  is the design matrix of pairwise comparisons, and  $Y_t$  is generated by the Thurstone-Mostelle (TM) or BTL models.  $\Pr(A)$  denotes the probability of event  $A$  from the ground-truth posterior, and  $\widehat{\Pr}(A)$  denotes the probability of event  $A$  from the distribution used in each method. To ensure fair comparison, we maintain the same  $X_t$  and  $Y_t$  across all methods. The average error over 25 trials under both models is shown in Fig. 1.1. Our method consistently yields the lowest errors, while AKG and Hybrid-MST may exhibit larger errors.

In this thesis, we resolve this problem by providing the closed-form posterior in the Bayesian inference framework. Inspired by recent findings in Durante [2019], we establish that the posterior distribution under the commonly utilized Thurstone-Mosteller (TM) model, coupled with a Gaussian prior, conforms to the *unified skew-normal* (SUN) distribution [Arellano-Valle and Azzalini, 2006]. By incorporating this novel posterior into the Bayesian framework originally proposed by Chen et al. [2016], we demonstrate that, under mild conditions, the estimated ranking, based on the expectation of Kendall's  $\tau$  correlation

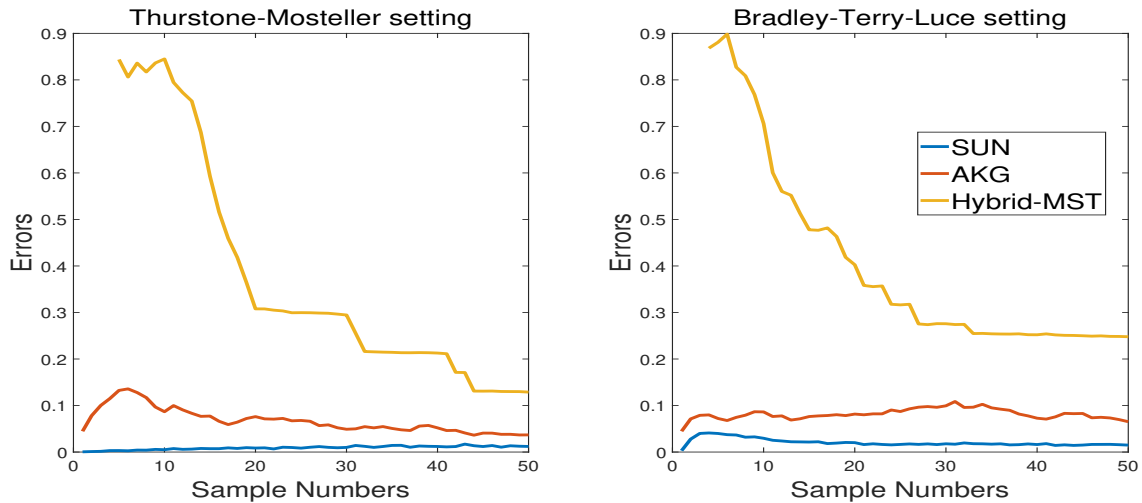


Figure 1.1 Demonstration of Estimation Errors in the Toy Example

coefficient over the posterior, is optimal. Moreover, the corresponding estimated ranking is simply the sorting of the posterior mean. Thus, we derive our Conjugate Bayesian framework for Thurstone-Mosteller ranking for batched data. This Bayesian approach not only supplements existing frequentist methods from a Bayesian perspective but also possesses convergence properties based on the Maximum Likelihood Estimator. We evaluate this batched version on both simulated and real-world data, achieving state-of-the-art results.

Subsequently, we integrate our framework into the knowledge gradient policy and extend it to an online ranking scenario. Leveraging the known form of the SUN distribution, our approach differs from previous online ranking methods by consistently utilizing the ground-truth posterior throughout the entire process. At each iteration, the knowledge gradient policy selects the next pair for comparison, aiming to maximize the expected increment of Kendall's  $\tau$  correlation coefficient. This Bayesian online ranking framework is well-formulated as it directly optimizes the index for ranking accuracy, i.e. Kendall's  $\tau$  correlation coefficient, rather than utilizing indirect indices such as expected information gain, as seen in numerous active online ranking frameworks. We evaluate this online ranking framework on simulated data, where it achieves state-of-the-art results.

To mitigate the computational burden in our framework, stemming from the intricate complexity of the SUN distribution, particularly when dealing with large sample numbers, we introduce an approximate version of our framework using the Mean-field Variational Inference (MFVI) method. This approximation is applicable to both the batched and online versions of our framework. In the MFVI method, we introduce a simple multivariate normal distribution to

approximate the complex SUN distribution. The proposed optimal ranking is then obtained by sorting the posterior mean of this simple distribution. We demonstrate the utility and efficiency of MFVI on both synthetic datasets and real-world datasets, showing that this approximated version not only significantly reduces computational time but also maintains comparable results to the original method.

## 1.2 Main Contributions

In this section, we summarize our contributions as follows:

- **Bayesian Conjugate Framework for Efficient Thurstone-Mosteller Ranking.** We employ the Bayesian framework introduced by Chen et al. [2016], facilitating the derivation of closed-form posteriors, which follow a unified skew-normal distribution under the classical Thurstone-Mosteller model. We establish that, under mild and empirically observed conditions, the estimated ranking derived from maximizing the expectation of Kendall’s  $\tau$  [Kendall, 1938] over the posterior, despite being an NP-hard problem, can be efficiently induced via simple sorting of the posterior mean. Our work extends the classical Thurstone-Mosteller model into a conjugate Bayesian framework and renders it tractable for practical employment. To obtain the posterior mean or other statistics, we propose the Monte Carlo integration method to be carried out.
- **Knowledge Gradient Policy Integration for Active Learning in Ranking:** We seamlessly integrate our framework with the knowledge gradient policy, extending it to the active sampling scenario. Leveraging Bayesian Markov Decision processes as proposed by Chen et al. [2016], our approach distinguishes itself by offering a closed-form posterior throughout the entire sampling process. Through iterative maximization of the expectation of Kendall’s  $\tau$ , we can improve sampling efficiency, particularly under limited sampling constraints. Notably, while many existing active sampling strategies prioritize maximizing the expected information gain, our work targets a different objective—optimizing Kendall’s  $\tau$ . Our experimental evaluations demonstrate that this alternative objective leads to superior performance, especially with a small number of samples, showcasing the effectiveness and practical relevance of our approach.
- **Mean-field Variational Inference for Scalable Bayesian Ranking.** The intricate sophistication in the unified skew-normal distribution poses challenges in its efficient application in scenarios involving large samples. To address this challenge, we approximate the posterior using the Mean-field Variational Inference method, which not

only enjoys the property of local convergence [Wang and Titterington, 2012] but also effectively addresses computational burdens via a closed-form simple iterative scheme. We prove that the estimated ranking from the multivariate normal distribution (as an approximation to the posterior) is simply the sorting of its mean, further enhancing the tractability of this strategy.

- **Empirical Evaluation and Real-world Applications of Bayesian Ranking Methods.**

Evaluated via Kendall’s  $\tau$ , we employ our framework on simulated data, achieving state-of-the-art results compared to other methods. Similarly, on real-world datasets, our approach yields state-of-the-art or comparable results to competitive baselines. In the simulated setting, our work demonstrates robustness regardless of whether outcomes are generated from the Thurstone-Mosteller or Bradley-Terry-Luce models, and it showcases efficiency under limited sample numbers. We also apply our approach to real-world applications, including:

- **Reading Difficulty Dataset.** Pairwise comparison data on reading difficulty finds applications in various fields, particularly in education. For example, such data can assist in the development of educational materials and exercises by providing learners with texts that match their current proficiency level, thereby offering more effective learning experiences. Our algorithm achieves the best performance in this dataset, underscoring its utility in the education field where personalized learning experiences are crucial for effective education delivery.
- **Image Quality Assessment.** Pairwise comparison data in image quality assessment is indispensable for evaluating and improving the quality of images across various domains such as medical imaging, multimedia content delivery, and advertising. By comparing the perceived quality of compressed images with their originals, developers can fine-tune compression parameters to minimize quality loss while reducing file sizes. In this context, our work achieves state-of-the-art results in the original version and comparable results in the active online learning version, demonstrating the robustness and effectiveness of our algorithms in applications where image quality is paramount. Importantly, considering that the ground-truth scores of items are estimated via HodgeRank rather than the ground-truth score itself, our algorithm’s robustness is further highlighted.
- **Video Quality Assessment.** Similarly, pairwise comparison data in video

quality assessment plays a crucial role in refining video compression algorithms and encoding techniques. By assessing the perceived quality of compressed videos relative to their original versions, developers can optimize compression settings to achieve high-quality video playback while minimizing bandwidth usage and storage requirements. In this context, our work attains state-of-the-art results in the original version and comparable results in the active online learning version, highlighting the effectiveness of our algorithms in applications where video quality directly impacts user experience, such as video streaming services and surveillance systems. Furthermore, considering that the ground-truth scores of items are estimated via HodgeRank rather than the ground-truth score itself, our algorithm's robustness is further underscored.

It is noteworthy that while our original version excels in Kendall's  $\tau$  performance, it may incur a significant computational burden. On the other hand, the Mean-field Variational Inference version offers computational efficiency, albeit with a slight drawback in Kendall's  $\tau$ . Therefore, in practice, the choice between the original version and the approximated version depends on whether computational speed or accuracy in Kendall's  $\tau$  is prioritized. All the experimental results in this thesis have reproducible code downloadable at

[https://github.com/zhenlipku/sun\\_ranking](https://github.com/zhenlipku/sun_ranking).

### 1.3 Organization

The remainder of this dissertation is structured into three main parts, each reflecting the key contributions outlined above, followed by the final conclusion chapter:

- **Foundational Framework Development:** This part encompasses our primary contribution and comprises three chapters as outlined below:
  - **Chapter 2: Preliminaries on Distributions:** This chapter establishes the foundational concepts by providing essential preliminaries on the multivariate normal distribution and its skewed extension, the SUN distribution.
  - **Chapter 3: Conjugate Bayesian Framework:** Here, we introduce our Conjugate Bayesian framework, which relies on the SUN-distributed posterior. This chapter elucidates the theoretical foundations and computational procedures of our approach.
  - **Chapter 4: Proofs of Theoretical Results:** In this chapter, we present the

proofs of Lemmas, Propositions, and Theorems introduced in Chapter 3, providing rigorous mathematical justification for our framework.

- **Active Sampling Strategy and Approximation Technique:** This part constitutes the second and third contributions and comprises two chapters:
  - **Chapter 5: Active Online Ranking Version:** This chapter discusses our active online ranking version, detailing its formulation and implementation for efficient sampling in dynamic environments.
  - **Chapter 6: Approximated Versions via MFVI Method:** Here, we introduce approximated versions of our algorithm using the MFVI method, addressing computational challenges associated with large-scale datasets.
- **Empirical Validation and Practical Applications:** This part demonstrates the practical utility of our framework, with the following application chapter:
  - **Chapter 7: Experimental Evaluation on Simulated Data:** This chapter evaluates our Conjugate Bayesian framework using simulated data under different comparison models, i.e., Thurstone-Mosteller model or Bradley-Terry-Luce model, to verify its efficiency and robustness in different scenarios.
  - **Chapter 8: Experimental Evaluation on Real-World Applications:** This chapter evaluates our Conjugate Bayesian framework in different real-world applications as mentioned in the main contributions section, i.e., reading difficulty assessment, image quality assessment, and video quality assessment.
- **Conclusions and Future Work:** Finally, **Chapter 9** presents the conclusions drawn from our work, highlighting key findings, contributions, and avenues for future research.

## 1.4 Notations

In this dissertation, unless otherwise stated, all vectors are assumed to be column vectors, denoted by small bold letters, while matrices are denoted by capital letters. The following notation is consistently used throughout the entire dissertation:

- $\mathbb{R}^+$ : Positive real numbers.
- $\mathbb{R}^N$ :  $N$ -dimensional real space.
- $\mathbf{0}$ : Zero vector or matrix, the dimension of which depends on the context.
- $\mathbf{0}_N$ :  $N$ -dimensional vector with all elements set to 0.
- $\mathbf{1}_N$ :  $N$ -dimensional vector with all elements set to 1.
- $A(i, j)$ : The entry in the  $i$ -th row and  $j$ -th column of matrix  $A$ .

- $A(i, :)$ : The  $i$ -th row of matrix  $A$ .
- $A^\top$ : Transpose of matrix  $A$ .
- $\alpha^\top$ : Transpose of vector  $\alpha$ .
- $I_N$ :  $N$ -dimensional identity matrix.
- $\text{diag}(\alpha)$ : A diagonal matrix expanded by the vector  $\alpha$ .
- $|S|$ : The cardinality of set  $S$ .
- $\times$ : Multiplication.
- $\phi(x)$ : Density of a standard normal distribution evaluated at  $x$ .
- $\phi(x; a, b)$ : Density of a normal distribution with mean  $a$ , variance  $b$ , evaluated at  $x$ .
- $\Phi(x)$ : Distribution function of a standard normal distribution evaluated at  $x$ .
- $\Phi(x; a, b)$ : Distribution function of a  $\phi(x; a, b)$  random variable evaluated at  $x$ .
- $\Phi(x; b)$ : Distribution function of a  $\phi(x; 0, b)$  random variable evaluated at  $x$ .
- $\mathcal{N}_N(\mu, \Sigma)$ :  $N$ -dimensional multivariate normal distribution with mean  $\mu$  and variance-covariance or correlation matrix  $\Sigma$ . We omit  $N$  in the subscript when  $N = 1$ .
- $\Phi_T(\gamma)$ : Distribution function of  $\mathcal{N}_T(\mathbf{0}_T, I_N)$  evaluated at  $\gamma$ . In this dissertation, we do not differentiate between  $\gamma$  being represented as a row vector or a column vector in the context of multivariate normal cumulative distribution functions.
- $\Phi_T(\gamma; \Sigma)$ : Distribution function of  $\mathcal{N}_T(\mathbf{0}_T, \Sigma)$  evaluated at  $\gamma$ .
- $\Phi_T(\gamma; \mu, \Sigma)$ : Distribution function of  $\mathcal{N}_T(\mu, \Sigma)$  evaluated at  $\gamma$ .
- $\left. \frac{df(t)}{t} \right|_{t=0}$ : Derivative of  $f(t)$  with respect to vector  $t$  when it is a zero vector.
- CDF: Cumulative distribution function.
- CGF: Cumulant generating function.
- i.i.d.: Independent and identically distributed.
- KL: Kullback-Leibler.
- Kendall's  $\tau$ : Kendall's  $\tau$  rank correlation coefficient.
- MGF: Moment generating function.
- MLE: Maximum likelihood estimator.
- PDF: Probability density function.
- SUN: Unified skew-normal.

## Chapter 2 The Unified Skew-Normal (SUN) Distribution

Although the normal distribution has been widely utilized in academic works, real-world data often exhibit asymmetry. For instance, human life data typically displays negative skewness because most people tend to die after reaching an average age, with few individuals passing away too soon or too late. To model such skewed data, researchers have proposed various skew-normal distributions. For the sake of generality, we focus on the multivariate case, considering the univariate distribution as a special case. Numerous multivariate skew-normal distributions have been introduced by researchers [Azzalini and Valle, 1996, Azzalini and Capitanio, 1999, Gonza et al., 2004, Gupta and Chen, 2004]. Arellano-Valle and Azzalini [2006] subsequently proposed the *unified skew-normal* distribution, abbreviated as SUN. This distribution extends the multivariate skew-normal distribution, and they demonstrate that the SUN distribution encompasses or is at least equivalent to earlier versions of skew-normal distributions.

This chapter provides an overview of this newly introduced distribution, beginning with the multivariate normal distribution (Sec. 2.1), followed by the multivariate skew-normal distribution (Sec. 2.2). Subsequently, we present derivations and properties of random vectors distributed according to the SUN distribution (Sec. 2.3). We illustrate that the SUN distribution preserves many intriguing properties of the multivariate normal distribution.

### 2.1 Multivariate Normal Distribution

The multivariate normal distribution stands as one of the most prominent distributions in academic research, prized not only for its ease of tractability but also for its widespread use as an approximation in many cases, courtesy of the central limit theorem. Moreover, it serves as the cornerstone of the skew-normal family. In this section, we introduce the basic setup and properties of the multivariate normal distribution pertinent to our study.

Specifically, we denote a  $N$ -dimensional multivariate normal distributed random vector  $\boldsymbol{\theta} = (\theta_1, \theta_2, \dots, \theta_N)^\top$  as:

$$\boldsymbol{\theta} \sim \mathcal{N}_N(\boldsymbol{\mu}, \Sigma),$$

where  $\boldsymbol{\mu} = (\mu_1, \mu_2, \dots, \mu_N)^\top \in \mathbb{R}^N$ , and  $\Sigma$  is an  $N \times N$  positive definite variance-covariance

matrix. The probability density function (PDF) of  $\boldsymbol{\theta}$  is expressed as:

$$p(\boldsymbol{\theta}) = \frac{\exp\left(-\frac{1}{2}(\boldsymbol{\theta} - \boldsymbol{\mu})^\top \Sigma^{-1}(\boldsymbol{\theta} - \boldsymbol{\mu})\right)}{\sqrt{(2\pi)^N |\Sigma|}}, \quad (2.1)$$

where  $|\Sigma|$  denotes the determinant of  $\Sigma$ , representing the generalized variance [Kocherlakota and Kocherlakota, 2004].

### 2.1.1 Some Properties of Multivariate Normal Distribution

Here, we introduce several properties of the multivariate normal distribution relevant to our investigation. Proofs are omitted due to their widespread familiarity and accessibility, readily found in resources such as Wikipedia.

- The cumulative distribution function (CDF) of Eq. (2.1) is

$$F_{\boldsymbol{\theta}}(\mathbf{x}) = \Pr(\boldsymbol{\theta} \leq \mathbf{x}) = \Phi_N(\mathbf{x} - \boldsymbol{\mu}; \Sigma), \text{ with } \boldsymbol{\theta} \sim \mathcal{N}_N(\boldsymbol{\mu}, \Sigma),$$

- The moment generating function (MGF) of Eq. (2.1) is

$$M(\mathbf{t}) = \exp\left(\boldsymbol{\mu}^\top \mathbf{t} + \frac{1}{2}\mathbf{t}^\top \Sigma \mathbf{t}\right),$$

where  $\mathbf{t} \in \mathbb{R}^N$ . Additionally, the CGF (cumulant generating function) of Eq. (2.1) is

$$K(\mathbf{t}) = \boldsymbol{\mu}^\top \mathbf{t} + \frac{1}{2}\mathbf{t}^\top \Sigma \mathbf{t}$$

- Closed under conditional distribution. If  $\boldsymbol{\theta}$  is partitioned as  $\boldsymbol{\theta} = \begin{pmatrix} \boldsymbol{\theta}_1 \\ \boldsymbol{\theta}_2 \end{pmatrix}$ , with size  $\begin{pmatrix} s \\ N-s \end{pmatrix}$ . We then assume  $\boldsymbol{\mu}$  is partitioned as  $\boldsymbol{\mu} = \begin{pmatrix} \boldsymbol{\mu}_1 \\ \boldsymbol{\mu}_2 \end{pmatrix}$ , with size  $\begin{pmatrix} s \times 1 \\ (N-s) \times 1 \end{pmatrix}$  and  $\Sigma$  is partitioned as  $\Sigma = \begin{pmatrix} \Sigma_{11} & \Sigma_{12} \\ \Sigma_{21} & \Sigma_{22} \end{pmatrix}$  with size  $\begin{pmatrix} s \times s & s \times (N-s) \\ (N-s) \times s & (N-s) \times (N-s) \end{pmatrix}$ . Then the conditional distribution  $(\boldsymbol{\theta}_1 | \boldsymbol{\theta}_2 = \mathbf{x})$  is multivariate normal distributed, i.e.

$$(\boldsymbol{\theta}_1 | \boldsymbol{\theta}_2 = \mathbf{x}) \sim \mathcal{N}_s(\boldsymbol{\mu}', \Sigma')$$

where  $\boldsymbol{\mu}' = \boldsymbol{\mu}_1 + \Sigma_{12}\Sigma_{22}^{-1}(\mathbf{x} - \boldsymbol{\mu}_2)$  and  $\Sigma' = \Sigma_{11} - \Sigma_{12}\Sigma_{22}^{-1}\Sigma_{21}$ .  $\Sigma_{22}$  is the generalized inverse of  $\Sigma_{22}$  and  $\Sigma'$  is the Schur complement of  $\Sigma_{22}$  in  $\Sigma$ .

- Closed under affine transformation. Let  $\boldsymbol{\theta}' = \mathbf{c} + B\boldsymbol{\theta}$ , where  $\mathbf{c}$  is a  $M \times 1$  constant vector,  $B$  is a  $M \times N$  constant matrix, then  $\boldsymbol{\theta}'$  is multivariate normal distributed, i.e.

$$\boldsymbol{\theta}' \sim \mathcal{N}_M(\mathbf{c} + B\boldsymbol{\mu}, B\Sigma B^\top).$$

- Closed under summation of independent multivariate normal distributions. If we have  $\boldsymbol{\theta}_1 \sim \mathcal{N}_N(\boldsymbol{\mu}_1, \Sigma_1)$ ,  $\boldsymbol{\theta}_2 \sim \mathcal{N}_N(\boldsymbol{\mu}_2, \Sigma_2)$  and  $\boldsymbol{\theta}_1$  and  $\boldsymbol{\theta}_2$  are independent, then  $\boldsymbol{\theta}_1 + \boldsymbol{\theta}_2$  is still multivariate normal distributed, i.e.

$$\boldsymbol{\theta}_1 + \boldsymbol{\theta}_2 \sim \mathcal{N}_N(\boldsymbol{\mu}_{1+2}, \Sigma_{1+2}),$$

where  $\boldsymbol{\mu}_{1+2} = \boldsymbol{\mu}_1 + \boldsymbol{\mu}_2$  and  $\Sigma_{1+2} = \Sigma_1 + \Sigma_2$ .

- Closed under marginalization. If  $\boldsymbol{\theta} = \begin{pmatrix} \boldsymbol{\theta}_1 \\ \boldsymbol{\theta}_2 \\ \boldsymbol{\theta}_3 \end{pmatrix}$  follows the multivariate normal distribution  $\mathcal{N}_N(\boldsymbol{\mu}, \Sigma)$ .  $\boldsymbol{\mu}$  is partitioned as  $\boldsymbol{\mu} = \begin{pmatrix} \boldsymbol{\mu}_1 \\ \boldsymbol{\mu}_2 \\ \boldsymbol{\mu}_3 \end{pmatrix}$ , with size  $\begin{pmatrix} s \\ k \\ t \end{pmatrix}$  satisfying  $s + k + t = N$ .  $\Sigma$  is partitioned as  $\begin{pmatrix} \Sigma_{11} & \Sigma_{12} & \Sigma_{13} \\ \Sigma_{21} & \Sigma_{22} & \Sigma_{23} \\ \Sigma_{31} & \Sigma_{32} & \Sigma_{33} \end{pmatrix}$ , with size  $\begin{pmatrix} s \times s & s \times k & s \times t \\ k \times s & k \times k & k \times t \\ t \times s & t \times k & t \times t \end{pmatrix}$ . Then the joint distribution of  $\begin{pmatrix} \boldsymbol{\theta}_1 \\ \boldsymbol{\theta}_3 \end{pmatrix}$  is also multivariate normal distributed, i.e.

$$\begin{pmatrix} \boldsymbol{\theta}_1 \\ \boldsymbol{\theta}_3 \end{pmatrix} \sim \mathcal{N}_{s+t} \left( \begin{pmatrix} \boldsymbol{\mu}_1 \\ \boldsymbol{\mu}_3 \end{pmatrix}, \begin{pmatrix} \Sigma_{11} & \Sigma_{13} \\ \Sigma_{31} & \Sigma_{33} \end{pmatrix} \right).$$

## 2.2 Multivariate Skew-Normal Distribution

Although the normal distribution has been widely used, real-world data often exhibit asymmetry. Apart from human life data mentioned earlier, income distribution typically follows a skewed pattern. This asymmetry arises because a large proportion of individuals in a given population belong to a low-income group, while only a few fall into the high-income bracket. Consequently, the mean of such data tends to be greater than other measures of central tendency, such as the median or mode. In such cases, the normal distribution may not be an appropriate choice for modeling. Researchers therefore turn to alternative distributions to better capture the skewness. One popular choice is the skew-normal family. The multivariate skew-normal distribution was initially proposed by Azzalini and Valle [1996] and subsequently refined by Azzalini and Capitanio [1999]. Gupta et al. [2004] further introduced the closed skew-normal distribution, which retains properties similar to the normal distribution.

Though other multivariate skew-normal distributions are introduced, as discussed in

Azzalini and Valle [1996], this dissertation focuses solely on the multivariate skew-normal distribution which is most relevant to the SUN distribution for we aim to introduce the SUN distribution more naturally and comprehensibly. According to Gupta et al. [2004], an  $N$ -dimensional random vector  $\boldsymbol{\theta}$  is considered multivariate skew-normal distributed if it exhibits the following density:

$$p(\boldsymbol{\theta}) = \frac{1}{\Phi_N(\mathbf{0}_N; I_N + D\Sigma D^\top)} \phi_N(\boldsymbol{\theta}; \boldsymbol{\mu}, \Sigma) \Phi_N(D(\boldsymbol{\theta} - \boldsymbol{\mu})), \quad (2.2)$$

where  $\boldsymbol{\mu}, \boldsymbol{\theta} \in \mathbb{R}^N$ ,  $\Sigma$  is positive definite,  $D$  is a  $N \times N$  matrix. It is worth noticing that when all elements in  $D$  is 0,  $p(\boldsymbol{\theta})$  in Eq. (2.2) becomes  $\phi_N(\boldsymbol{\theta}; \boldsymbol{\mu}_N, \Sigma)$ , thus, multivariate normal distribution is a special case of the multivariate skew-normal distribution. The distribution in Eq. (2.2) can be represented as:

$$\boldsymbol{\theta} \sim \text{SN}_N(\boldsymbol{\mu}, \Sigma, D)$$

### 2.2.1 Derivation of Multivariate Skew-Normal Distribution

We will now present the derivation of the multivariate skew-normal distribution, illustrating how it is derived from the simple multivariate normal distribution. Let's start by assuming we have a  $(2N)$ -dimensional multivariate normal distribution:

$$\begin{pmatrix} \boldsymbol{\theta}_1 \\ \boldsymbol{\theta}_2 \end{pmatrix} \sim \mathcal{N}_{2N} \left( \begin{pmatrix} \boldsymbol{\gamma} \\ \boldsymbol{\mu} \end{pmatrix}, \begin{pmatrix} I_N + D\Sigma D^\top & D\Sigma \\ \Sigma D^\top & \Sigma \end{pmatrix} \right),$$

where  $\boldsymbol{\theta}_1$  and  $\boldsymbol{\theta}_2$  are both  $N$ -dimensional multivariate normally distributed, parameters in  $\mathcal{N}_{2N}(\cdot)$  are their corresponding partitions. Then, from Gupta et al. [2004], we have

$$(\boldsymbol{\theta}_2 | \boldsymbol{\theta}_1 \geq \boldsymbol{\gamma}) \sim \text{SN}_N(\boldsymbol{\mu}, \Sigma, D).$$

### 2.2.2 Some Properties of Multivariate Skew-Normal Distribution

As an extension, multivariate skew-normal distribution still maintains some properties of multivariate normal distribution mentioned above. We only demonstrate these properties as proofs can be found in Gupta et al. [2004].

- If  $\boldsymbol{\theta}$  has the density in Eq. (2.2), its MGF will be

$$M(t) = \frac{\Phi_N(D\Sigma t; I_N + D\Sigma D^\top)}{\Phi_N(\mathbf{0}_N; I_N + D\Sigma D^\top)} \exp\left(\boldsymbol{\mu}^\top t + \frac{t^\top \Sigma t}{2}\right), \quad t \in \mathbb{R}^N.$$

- Closed under affine transformation. Assume  $\boldsymbol{\theta} \sim \text{SN}_N(\boldsymbol{\mu}, \Sigma, D)$ . Given a  $N \times N$

non-singular matrix  $B$  and a constant vector  $\mathbf{b} \in \mathbb{R}^N$ , then

$$B\theta + \mathbf{b} \sim \text{SN}_N(\mathbf{b} + B\mu; B\Sigma B^\top, DB^{-1}).$$

- The mean of  $\theta \sim \text{SN}_N(\mu, \Sigma, D)$  is given by

$$\mathbb{E}(\theta) = \mu + \frac{d\Phi_N(D\Sigma t; I_N + D\Sigma D^\top)}{\Phi_N(\mathbf{0}_N; I_N + D\Sigma D^\top)} \Big|_{t=0}.$$

## 2.3 The Unified Skew-Normal Distribution

It is worth noting that the multivariate skew-normal distribution introduced above has certain limitations. The derivation procedure outlined in Sec. 2.2.1 requires the partitioning of the multivariate normal distribution into two parts with the same dimensions. Additionally, it retains only a few properties of the multivariate normal distribution, as discussed in Sec. 2.2.2. In pursuit of a more general extension, Arellano-Valle and Azzalini [2006] propose the unified skew-normal (SUN) distribution. Let us now delve deeper into this distribution.

### 2.3.1 Derivation of Unified Skew-Normal Distribution

The derivation of SUN distribution begins with the consideration of the following  $(N+T)$ -dimensional multivariate normal distribution:

$$\begin{pmatrix} \theta \\ \tilde{\theta} \end{pmatrix} \sim \mathcal{N}_{N+T}(\mathbf{0}_{N+T}, \Omega^*), \quad \Omega^* := \begin{pmatrix} \bar{\Omega} & \Delta \\ \Delta^\top & \Gamma \end{pmatrix}, \quad (2.3)$$

where  $\tilde{\theta}$  denotes a  $T$ -dimensional random vector with  $\tilde{\theta} = (\theta_{N+1}, \dots, \theta_{N+T})^\top$ , and  $\Omega^*$  denotes the full-rank correlation matrix of  $\begin{pmatrix} \theta \\ \tilde{\theta} \end{pmatrix}$ . Let  $\omega \in \mathbb{R}^{N \times N}$  be a diagonal matrix with all elements in its diagonal being positive, and let  $\xi$  and  $\gamma$  be  $N$ -dimensional and  $T$ -dimensional constant vectors, respectively. Then,  $Z = \xi + \omega(\theta | \tilde{\theta} + \gamma > 0)^{(1)}$  follows a SUN distribution:

$$Z \sim \text{SUN}_{N,T}(\xi, \Omega, \Delta, \gamma, \Gamma), \quad (2.4)$$

and it can be characterized by the following density function at  $z$ :

$$\phi_N(z; \xi, \Omega) \frac{\Phi_T(\gamma + \Delta^\top \bar{\Omega}^{-1} \omega^{-1}(z - \xi); \Gamma - \Delta^\top \bar{\Omega}^{-1} \Delta)}{\Phi_T(\gamma; \Gamma)}, \quad (2.5)$$

where  $\Omega = \omega \bar{\Omega} \omega$ ,  $\phi_N(z; \xi, \Omega)$  represents the PDF of a  $N$ -dimensional Gaussian distribution at  $z$  with mean  $\xi$  and variance-covariance matrix  $\Omega$ .  $\Phi_T(\gamma + \Delta^\top \bar{\Omega}^{-1} \omega^{-1}(z - \xi); \Gamma - \Delta^\top \bar{\Omega}^{-1} \Delta)$

<sup>(1)</sup>  $\tilde{\theta} + \gamma > 0$  indicates that the inequality sign holds for each element of the  $T$  components.

(resp.  $\Phi_T(\gamma; \Gamma)$ ) stands for the CDF of a  $T$ -dimensional Gaussian distribution evaluated at  $\gamma + \Delta^\top \bar{\Omega}^{-1} \omega^{-1}(z - \xi)$  (resp.  $\gamma$ ) with mean  $\mathbf{0}_T$  and variance-covariance matrix  $\Gamma - \Delta^\top \bar{\Omega}^{-1} \Delta$  (resp.  $\Gamma$ ).

### 2.3.2 Some Properties of Unified Skew-Normal Distribution

Clearly, the SUN distribution offers more flexibility compared to the multivariate skew-normal distribution in Eq. (2.2), as shown in Eq. (2.3), where  $T$  can differ from  $N$ . Additionally, the multivariate skew-normal distribution introduced in Gupta and Miescke [1996], which has a density

$$p(\theta) = 2\phi_N(\theta; \Omega)\Phi(\alpha^\top \theta), \quad \text{with } \theta, \alpha \in \mathbb{R}^N,$$

is a special case of the SUN distribution in Eq. (2.5), with  $T = 1$ . When  $\Delta = \mathbf{0}$ , the density in Eq. (2.5) becomes  $\phi_N(z; \xi, \Omega)$ , which is the density of the multivariate normal distribution. Thus, SUN distribution is an extension of multivariate normal distribution. Furthermore, the SUN distribution retains many properties of the multivariate normal distribution. In the following, we will demonstrate these properties, the proofs of which can be found in Arellano-Valle and Azzalini [2006], Aziz [2011].

- The CDF of  $Z$  in Eq. (2.4) takes the form of

$$F_Z(z) := \Pr(Z \leq z) = \frac{\Phi_{N+T}(\tilde{z}; \tilde{\Omega})}{\Phi_T(\gamma; \Gamma)}, \quad \text{where } \tilde{z} = \begin{pmatrix} \frac{z-\xi}{\omega} \\ \gamma \end{pmatrix} \text{ and } \tilde{\Omega} = \begin{pmatrix} \bar{\Omega} & -\Delta \\ -\Delta^\top & \Gamma \end{pmatrix}. \quad (2.6)$$

- The MGF of  $Z$  in Eq. (2.4) takes the form of

$$M(t) = \exp\left(\xi^\top t + \frac{1}{2}t^\top \Omega t\right) + \frac{\Phi_T(\gamma + \Delta^\top \omega t; \Gamma)}{\Phi_T(\gamma; \Gamma)}, \quad \text{with } t \in \mathbb{R}^N.$$

Then the CGF of  $Z$  in Eq. (2.4) will be

$$K(t) = \xi^\top t + \frac{1}{2}t^\top \Omega t + \log \Phi_T(\gamma + \Delta^\top \omega t; \Gamma) - \log \Phi_T(\gamma; \Gamma).$$

Note that, when  $\Delta = \mathbf{0}$ , the MGF and CGF will be the same as in the multivariate normal case.

- The mean of  $Z$ , denoted as  $\mu_z$ , given in Eq. (2.4) takes the form of

$$\mu_z = \xi + \frac{\omega \Delta \nabla \Phi_T(\Gamma)}{\Phi_T(\gamma; \Gamma)}, \quad (\nabla \Phi_T(\Gamma))_j = \begin{cases} \phi(\gamma_j) & \text{if } T = 1, \\ \phi(\gamma_j) \Phi_{T-1}(\gamma_{-j} - \Gamma_{-j} \gamma_j; \tilde{\Gamma}_{-j}) & \text{if } T > 1. \end{cases} \quad (2.7)$$

Here,  $\phi(\gamma_j)$  is the PDF of the standard normal distribution evaluated at  $\gamma_j$ .  $(\nabla \Phi_T(\Gamma))_j$  denotes the  $j$ -th element of the  $T$ -dimensional gradient vector.  $\boldsymbol{\gamma}_{-j}$  denotes a vector derived from  $\boldsymbol{\gamma}$  by excluding its  $j$ -th element. The term  $\Gamma_{-j}$  represents the  $j$ -th column of the matrix  $\Gamma$  with its  $j$ -th element omitted.  $\tilde{\Gamma}_{-j} = \Gamma_{-j,-j} - \Gamma_{-j}\Gamma_{-j}^\top$ , where  $\Gamma_{-j,-j}$  is a  $(T-1) \times (T-1)$  matrix obtained by eliminating the  $j$ -th row and column from  $\Gamma$ .

- Closed under conditional distribution. Assume  $Z$  in Eq. (2.4) is partitioned as  $Z = \begin{pmatrix} Z_1 \\ Z_2 \end{pmatrix}$ , with size  $\begin{pmatrix} k \\ N-k \end{pmatrix}$ .  $\boldsymbol{\xi}$  is partitioned as  $\boldsymbol{\xi} = \begin{pmatrix} \boldsymbol{\xi}_1 \\ \boldsymbol{\xi}_2 \end{pmatrix}$ , with size  $\begin{pmatrix} k \\ N-k \end{pmatrix}$ . For notational simplicity, we denote  $\omega$  given below Eq. (2.5) as  $\omega = \text{diag}(\bar{\omega})$  and  $\bar{\omega}$  is partitioned as  $\bar{\omega} = \begin{pmatrix} \bar{\omega}_1 \\ \bar{\omega}_2 \end{pmatrix}$  with size  $\begin{pmatrix} k \\ N-k \end{pmatrix}$ . Additionally,  $\Delta$  is partitioned as  $\Delta = \begin{pmatrix} \Delta_1 \\ \Delta_2 \end{pmatrix}$  with size  $\begin{pmatrix} k \times T \\ (N-k) \times T \end{pmatrix}$ . We then denote  $\Omega_1^* = \begin{pmatrix} \Gamma & \Delta_1^\top \\ \Delta_1 & \bar{\Omega}_{11} \end{pmatrix}$ , with  $\bar{\Omega}_{11}$  given in the partition of  $\bar{\Omega} = \begin{pmatrix} \bar{\Omega}_{11} & \bar{\Omega}_{12} \\ \bar{\Omega}_{21} & \bar{\Omega}_{22} \end{pmatrix}$ , the size of which is  $\begin{pmatrix} k \times k & k \times (N-k) \\ (N-k) \times k & (N-k) \times (N-k) \end{pmatrix}$ . We also denote the partition of  $\Omega = \omega \bar{\Omega} \omega = \begin{pmatrix} \Omega_{11} & \Omega_{12} \\ \Omega_{21} & \Omega_{22} \end{pmatrix}$  with size  $\begin{pmatrix} k \times k & k \times (N-k) \\ (N-k) \times k & (N-k) \times (N-k) \end{pmatrix}$ . Then the distribution of  $(Z_1 | Z_2 = z)$  is

$$(Z_1 | Z_2 = z) \sim \text{SUN}_{k,T}(\boldsymbol{\xi}_{1:2}, \text{diag}(\bar{\omega}_1) \bar{\Omega}_{11:2} \text{diag}(\bar{\omega}_1), \Delta_{1:2}, \boldsymbol{\gamma}_{1:2}, \Gamma_{1:2}),$$

where  $\boldsymbol{\xi}_{1:2} = \boldsymbol{\xi}_1 + \Omega_{12}\Omega_{22}^{-1}(z - \boldsymbol{\xi}_2)$ ,  $\bar{\Omega}_{11:2} = \bar{\Omega}_{11} - \bar{\Omega}_{12}\bar{\Omega}_{22}^{-1}\bar{\Omega}_{21}$ ,  $\Delta_{1:2} = \Delta_1 - \bar{\Omega}_{12}\bar{\Omega}_{22}^{-1}\Delta_2$ ,  $\Gamma_{1:2} = \Gamma - \Delta_2^\top \bar{\Omega}_{22}^{-1} \Delta_2$ .

- Closed under marginalization. Supposed,  $Z$  in Eq. (2.4) is partitioned as in the case of the conditional distribution. Then the distribution of  $Z_1$  will be

$$Z_1 \sim \text{SUN}_{k,T}(\boldsymbol{\xi}_1, \Omega_{11}, \Delta_1, \boldsymbol{\gamma}, \Gamma).$$

- Closed under affine transformation. Given  $Z$  in Eq. (2.4) and  $b \in \mathbb{R}^d$  and  $D \in \mathbb{R}^{N \times d}$  with full rank, then we will have

$$b + D^\top Z \sim \text{SUN}_{d,T}(b + D^\top \boldsymbol{\xi}, D^\top \Omega D, \Delta_D, \boldsymbol{\gamma}, \Gamma), \quad (2.8)$$

where  $\Delta_D = \text{Diag}(D^\top \Omega D)^{-1/2} D^\top \omega \Delta$ , and  $\text{Diag}(\cdot)$  specifies a diagonal matrix formed by the diagonal elements of a square matrix within the bracket.

- Closed under summation of independent SUN distributions. To clearly state it, we firstly introduce the kronecker product of two matrix. Assume we have a  $m \times n$  matrix

$A$ , and  $p \times q$  matrix  $B$ , then  $A \otimes B = \begin{pmatrix} a_{11}B & a_{12}B \dots a_{1n}B \\ a_{21}B & a_{22}B \dots a_{2n}B \\ \vdots & \vdots \\ a_{m1}B & a_{m2}B \dots a_{mn}B \end{pmatrix}$ . After the introduction

of such a product, assume we have two SUN distributed random vectors, with  $Z_1 \sim \text{SUN}_{N,T_1}(\boldsymbol{\xi}_1, \Omega_1, \Delta_1, \boldsymbol{\gamma}_1, \Gamma_1)$ ,  $Z_2 \sim \text{SUN}_{N,T_2}(\boldsymbol{\xi}_2, \Omega_2, \Delta_2, \boldsymbol{\gamma}_2, \Gamma_2)$ ,  $\Omega_1 = \omega_1 \bar{\Omega}_1 \omega_1$ ,  $\Omega_2 = \omega_2 \bar{\Omega}_2 \omega_2$  and  $Z_1, Z_2$  are independent. Then  $Z_1 + Z_2$  is still SUN distributed with

$$Z_1 + Z_2 \sim \text{SUN}_{N,T^*}(\boldsymbol{\xi}^*, \Omega^*, \Delta^*, \boldsymbol{\gamma}^*, \Gamma^*),$$

where  $T^* = T_1 + T_2$ ,  $\boldsymbol{\xi}^* = \boldsymbol{\xi}_1 + \boldsymbol{\xi}_2$ ,  $\Omega^* = \Omega_1 + \Omega_2$ ,  $\Delta^* = (\omega_1 + \omega_2)^{-1}(\mathbf{1}_2^\top \otimes I_N)(\omega_1 \Delta_1 \otimes \omega_2 \Delta_2)$ ,  $\mathbf{1}_2$  being a 2-dimensional vector with all elements set to 1,  $\boldsymbol{\gamma}^* = \begin{pmatrix} \boldsymbol{\gamma}_1 \\ \boldsymbol{\gamma}_2 \end{pmatrix}$ ,  $\Gamma^* = \Gamma_1 \otimes \Gamma_2$ .

There are additional properties of the SUN distribution documented in Aziz [2011], albeit their correlation with this dissertation is limited. As observed earlier, the SUN distribution preserves all the properties of the multivariate normal distribution mentioned in Sec. 2.1.1. Given that the multivariate normal distribution is a special case of the SUN distribution, we can assert that the SUN distribution serves as a general extension of the multivariate normal distribution.

### 2.3.3 Applications of the Unified Skew-Normal Distribution

The PDF of the SUN distribution, as depicted in Eq. (2.5), is constructed by convolving a Gaussian density function with the CDF of a Gaussian distribution. Notably, this construction allows for flexibility in dimensionality, accommodating components with dimensions that may differ and exceed 1. This adaptability renders the SUN distribution, or its special case, the multivariate skew-normal distribution in Eq. (2.2), applicable across diverse fields, including but not limited to clinical trials [Azzalini and Bacchieri, 2010], productivity analysis [Colombi, 2013, Colombi et al., 2014], spatial data analysis [Allard and Naveau, 2007, Rimstad and Omre, 2014], time series models [Zarrin et al., 2019], and small area estimation [Diallo and Rao, 2018].

Of particular relevance to our framework is its role as a conjugate prior for various models, including:

- Probit model [Durante, 2019, Fasano et al., 2022].
- Multinomial probit models [Fasano and Durante, 2022].
- Tobit model [Anceschi et al., 2023].

- Thurston-Mosteller model, as explored in our work.

In the subsequent sections, we will demonstrate the utility of the SUN distribution as a conjugate prior for the Thurstone-Mosteller model. Additionally, we will propose our novel Bayesian active online ranking framework.

## 2.4 Chapter Summary

In this chapter, we introduced a generalization process from the multivariate normal distribution to the multivariate skew-normal distribution, culminating in the unified skew-normal distribution. We demonstrated how the SUN random vector is derived from the multivariate normal distribution and showed that both the multivariate normal distribution and the multivariate skew-normal distribution are special cases of the SUN distribution. Moreover, we highlighted properties of the multivariate normal distribution that also hold for SUN-distributed random vectors, underscoring the SUN distribution's role as a reasonable and more general extension of the multivariate normal distribution. Finally, we presented related works on the SUN distribution, showcasing its widely utilized applications and its relevance to the Thurstone-Mosteller model.



## Chapter 3 Conjugate Bayesian Framework for Thurstone-Mosteller Model

### 3.1 Introduction

Rank aggregation finds application in various domains such as web search and recommendation systems. Given the preference for pairwise compared labels in this field, we commence our exploration with pairwise comparison methods in this chapter. Initially, we present these methods from a frequentist perspective (Sec. 3.2), followed by a discussion on the Bayesian method proposed by Chen et al. [2016] (Sec. 3.3). Subsequently, we introduce our conjugate Bayesian ranking framework for Thurstone-Mosteller model based on the SUN distribution (Sec. 3.4). Finally, we illustrate the implementation of our conjugate Bayesian framework using Monte Carlo integration (Sec. 3.5) and discuss its convergence properties based on the Maximum Likelihood Estimator (Sec. 3.6).

### 3.2 Pairwise Comparison Methods

To introduce these methods, we first state basic setups. We assume there are  $N$  items labeled as  $1, 2, \dots, N$  to be ranked. Each item  $i$  ( $i = 1, \dots, N$ ) is linked to an underlying latent score  $\theta_i$ . A ranking  $\pi$  is defined as a mapping  $\pi : \{1, 2, \dots, N\} \rightarrow \{1, 2, \dots, N\}$ , i.e. a permutation of  $N$  items, and the ground-truth ranking, denoted as  $\pi^*$ , is established in accordance with the underlying scores  $\boldsymbol{\theta} = (\theta_1, \dots, \theta_N)^\top$ :

$$\pi^*(i) > \pi^*(j) \text{ if and only if } \theta_i > \theta_j. \quad (3.1)$$

To infer the ranking, pairwise comparison labels are collected through crowdsourcing platforms, where workers compare a pair of items such as  $(i, j)$ , and the corresponding comparison outcome  $Y_{ij}$  is recorded. A value of  $Y_{ij} = 1$  indicates a preference for item  $i$  over item  $j$ , while  $Y_{ij} = -1$  denotes the opposite preference.

After data collection, pairwise comparison methods are utilized. In this section, we outline several classical and widely employed methods as follows:

- **Thurstone-Mosteller (TM) Model** [Thurstone, 1927]: In the TM model,  $Y_{ij}$  follows

the distribution:

$$\Pr(Y_{ij} = 1|\boldsymbol{\theta}) = \Phi\left(\frac{\theta_i - \theta_j}{\sqrt{2}}\right), \quad \Pr(Y_{ij} = -1|\boldsymbol{\theta}) = \Phi\left(\frac{\theta_j - \theta_i}{\sqrt{2}}\right), \quad (3.2)$$

for all  $i, j = 1, \dots, N$  and  $i \neq j$ . After data collection,  $\boldsymbol{\theta}$  is estimated via maximum likelihood estimator (MLE). To clearly demonstrate this, we denote the MLE:

$$\begin{aligned}\hat{\boldsymbol{\theta}}_{\text{TM},T} &= \arg \max_{\boldsymbol{\theta} \in \mathbb{R}^N} \prod_{t=1}^T \Phi\left(\frac{\theta_{i_t} - \theta_{j_t}}{\sqrt{2}}\right) \\ &= \arg \max_{\boldsymbol{\theta} \in \mathbb{R}^N} \sum_{t=1}^T \log \left( \Phi\left(\frac{\theta_{i_t} - \theta_{j_t}}{\sqrt{2}}\right) \right),\end{aligned}\quad (3.3)$$

where the subscript  $T$  indicates the number of samples collected, and  $i_t$  is preferred to  $j_t$  in the  $t$ -th sample.

- **Bradley-Terry-Luce (BTL) Model** [Bradley and Terry, 1952, Luce, 2005]: In the BTL model,  $Y_{i,j}$  follows the distribution:

$$\Pr(Y_{ij} = 1|\boldsymbol{\theta}) = \frac{\theta_i}{\theta_i + \theta_j}, \quad \Pr(Y_{ij} = -1|\boldsymbol{\theta}) = \frac{\theta_j}{\theta_i + \theta_j}, \quad (3.4)$$

for all  $i, j = 1, \dots, N$  and  $i \neq j$ . After data collection,  $\boldsymbol{\theta}$  is also estimated via maximum likelihood estimation. If we have collected  $T$  samples, similar to TM setting, the MLE in BTL model can be expressed as:

$$\begin{aligned}\hat{\boldsymbol{\theta}}_{\text{BTL},T} &= \arg \max_{\boldsymbol{\theta} \in \mathbb{R}^N} \prod_{t=1}^T \frac{\theta_{i_t}}{\theta_{i_t} + \theta_{j_t}} \\ &= \arg \max_{\boldsymbol{\theta} \in \mathbb{R}^N} \sum_{t=1}^T \log \left( \frac{\theta_{i_t}}{\theta_{i_t} + \theta_{j_t}} \right),\end{aligned}$$

where the subscript  $T$  indicates the number of samples collected, and  $i_t$  is preferred to  $j_t$  in the  $t$ -th sample.

- **HodgeRank (Least Squares)** [Jiang et al., 2011]: This method considers a graph  $G = (V, E)$ , where  $V$  is the vertex set with  $|V| = N$ , representing the items, and  $E$  is the oriented edge set generated from the input data. Let  $Z$  be the  $N \times N$  matrix where  $Z(i, j)$  indicates the number of times item  $i$  is preferred over item  $j$  in the collected data. HodgeRank solves the least square problem:

$$\hat{\boldsymbol{\theta}} = \min_{\boldsymbol{\theta}} \|\mathbf{y} - D_0 \boldsymbol{\theta}\|_2^2,$$

where  $\mathbf{y} \in \mathbb{R}^T$  with  $T = \sum_{i,j=1}^N Z(i, j)$ , and  $D_0$  is a finite difference (coboundary) operator defined by  $D_0(i, j) = \theta_i - \theta_j$ .

- **Borda Count (Pairwise Variant)** [Ammar and Shah, 2011]: After data collection, the estimated score  $\hat{\theta}_i$  for item  $i$  is positively correlated to the number of times item  $i$  is preferred over others, calculated as:

$$\hat{\theta}_i = \frac{\# \text{ times item } i \text{ is preferred}}{\# \text{ times item } i \text{ is compared}}.$$

- **Rank Centrality [Negahban et al., 2016]**: This method assumes the BTL model for comparisons and models the comparison procedure as a Markov Chain. Specifically, this method employs an  $N \times N$  transition matrix, where  $P(i, j) \propto \frac{a_{ij}}{a_{ij} + a_{ji}}$ . Here,  $a_{ij} = \frac{\# \text{ times item } j \text{ is preferred over item } i}{\# \text{ times item } i \text{ is compared with item } j}$ . Intuitively, a higher value of  $P_{ij}$  implies that item  $i$  is more likely to be beaten by item  $j$  (i.e., the state at item  $i$  is more likely to transition to item  $j$ ). Finally, the Rank Centrality estimates item scores via the stationary distribution of the Markov Chain, which can be expressed as:

$$\hat{\theta} = \hat{\theta}P,$$

where  $P$  is the transition matrix of a Markov chain with its elements defined as described above.

There still exists a plethora of pairwise comparison methods, examples including Mallows models [Mallows, 1957, Tang, 2019], the Trueskill model [Herbrich et al., 2006], the Plackett-Luce model [Plackett, 1975, Azari Soufiani et al., 2013], SVM-based rank aggregation [Rajkumar and Agarwal, 2014a], the Generalized Method-of-Moments [Azari Soufiani et al., 2013], Spectral MLE [Chen and Suh, 2015], and the Divide-and-conquer rank algorithm [Chen et al., 2022], all these approaches are rooted in a frequentist perspective and tailored for batched data. In a Bayesian perspective, Chen et al. [2016] propose a Bayesian ranking framework, which we will explore further in the subsequent section.

### 3.3 Bayesian Ranking Framework

While there are other Bayesian methods for pairwise comparison data [Guo and Sanner, 2010, Priekule and Meisel, 2017], the decision to adopt the Bayesian framework, as outlined in Chen et al. [2016], is grounded in two fundamental considerations:

- Firstly, its inherent flexibility allows for adaptation not only to batched scenarios but also for seamless extension to active online ranking frameworks.
- Additionally, benefiting from the known closed form posterior, it has been shown to be more robust than other frequentist methods, as depicted in the experimental results

(Fig. 7.1 and 7.2).

This combination of flexibility and closed form nature underscores the effectiveness and robustness of the Bayesian approach in addressing ranking challenges.

We introduce this framework in a general context. Assuming there are  $N$  items to be ranked, each possessing latent scores  $\theta$ , the Bayesian framework defines the prior of  $\theta$  as

$$p_\alpha(\theta),$$

where  $\alpha$  represents the parameters of this prior. The likelihood function (comparison model) is denoted as  $f(\theta, i, j, y_{ij})$ . For instance, in the TM model, the likelihood function is expressed as:

$$f(\theta, i, j, y_{ij}) = \Phi\left(\frac{y_{ij}(\theta_i - \theta_j)}{\sqrt{2}}\right),$$

whereas in the BTL model, it is given by:

$$f(\theta, i, j, y_{ij}) = \begin{cases} \frac{\theta_i}{\theta_i + \theta_j} & \text{if } y_{ij} = 1, \\ \frac{\theta_j}{\theta_i + \theta_j} & \text{if } y_{ij} = -1. \end{cases}$$

After collecting  $T$  samples, the set of compared pairs is denoted as  $\mathcal{S}_T := \{(i_t, j_t)\}_{t=1}^T$ , and the outcomes as  $\mathcal{Y}_T(\mathcal{S}_T) := \{y_t\}_{t=1}^T$ , where  $y_t$  abbreviates  $Y_{i_t, j_t}$ . With this data defined, the posterior distribution of  $\theta$  can be expressed as

$$p(\theta | \mathcal{S}_T, \mathcal{Y}_T(\mathcal{S}_T), \alpha) = \frac{1}{B(\mathcal{S}_T, \mathcal{Y}_T(\mathcal{S}_T), \alpha)} \prod_{t=1}^T f(\theta, i_t, j_t, y_t) p_\alpha(\theta), \quad (3.5)$$

where  $B(\mathcal{S}_T, \mathcal{Y}_T(\mathcal{S}_T), \alpha)$  represents the normalization constant.

After deriving the posterior, this framework aims to maximize the expectation of a variant of Kendall's  $\tau$  rank correlation coefficient (abbreviated as Kendall's  $\tau$ ) [Kendall, 1938] over this posterior. We first introduce this coefficient as utilized in Chen et al. [2016]. Kendall's  $\tau$ , denoted as  $\tau(\pi, \pi^*)$ , can be expressed as:

$$\begin{aligned} \tau(\pi, \pi^*) &\equiv \frac{|\{(i, j) : i < j, (\pi(i) - \pi(j))(\pi^*(i) - \pi^*(j)) > 0\}|}{N(N-1)/2} \\ &= \frac{2}{N(N-1)} \sum_{i \neq j} \mathbf{1}_{\{\pi(i) > \pi(j)\}} \mathbf{1}_{\{\theta_i > \theta_j\}}, \end{aligned} \quad (3.6)$$

where  $\mathbf{1}_{\{\cdot\}}$  denotes the indicator function. The denominator,  $N(N-1)/2$ , represents the total number of possible pairs, while the numerator in  $\tau(\pi, \pi^*)$  counts the number of compared pairs in the proposed ranking  $\pi$  that match the ground-truth ranking  $\pi^*$ . In other papers such

as Xu et al. [2018a], Chen et al. [2022], Fan et al. [2022], Kendall's  $\tau$  may take the form:

$$\begin{aligned} \tau^0(\pi, \pi^*) &\equiv \frac{|\{(i, j) : i < j, (\pi(i) - \pi(j))(\pi^*(i) - \pi^*(j)) > 0\}|}{N(N-1)/2} \\ &\quad - \frac{|\{(i, j) : i < j, (\pi(i) - \pi(j))(\pi^*(i) - \pi^*(j)) < 0\}|}{N(N-1)/2}. \end{aligned} \quad (3.7)$$

Clearly,  $\tau(\pi, \pi^*)$  captures the essence of  $\tau^0(\pi, \pi^*)$  with  $\tau^0(\pi, \pi^*) = 2\tau(\pi, \pi^*) - 1$ , and maximizing the expectation of  $\tau(\pi, \pi^*)$  is essentially equivalent to maximizing that of  $\tau^0(\pi, \pi^*)$ .

With Kendall's  $\tau$  established, direct optimization of Eq. (3.6) becomes intractable due to the unknown ground-truth  $\theta$ . To address this challenge, Chen et al. [2016] propose a framework in which the estimated ranking  $\pi_T$  is determined by maximizing the following expression:

$$\pi_T \in \arg \max_{\pi} \mathbb{E}[\tau(\pi, \pi^*) | S_T, \mathcal{Y}_T(S_T), \alpha], \quad (3.8)$$

where the expectation is taken over the posterior distribution of  $\theta$ , i.e.,  $\theta \sim p(\theta | S_T, \mathcal{Y}_T(S_T), \alpha)$ ,  $\pi^*$  corresponds to the scores in Eq. (3.1), and  $\tau(\pi, \pi^*)$  is defined in Eq. (3.6). According to Chen et al. (2016), we have:

$$\pi_T \in \arg \max_{\pi} C_T(\pi),$$

where  $C_T(\pi)$  is defined as the summation of a series of probabilities:

$$C_T(\pi) \equiv \sum_{i \neq j} \mathbf{1}_{\{\pi(i) > \pi(j)\}} \text{Pred}_T(i > j).$$

Here, we denote the prediction probability of item  $i$  surpassing item  $j$ , based on the posterior distribution  $p(\theta | S_T, \mathcal{Y}_T(S_T), \alpha)$  and  $\tau(\pi, \pi^*)$ , as the posterior probability that  $\theta_i$  is greater than  $\theta_j$ :

$$\text{Pred}_T(i > j) := \Pr(\theta_i > \theta_j | S_T, \mathcal{Y}_T(S_T), \alpha) = \int_{\theta_i > \theta_j} p(\theta | S_t, \mathcal{Y}_t(S_t), \alpha) d\theta. \quad (3.9)$$

**Remark 3.1.** *The objective function in Eq. (3.8) can be generalized as follows:  $\pi_T \in \arg \max_{\pi} \mathbb{E}[f(\theta) | \theta \sim p(\theta | S_T, \mathcal{Y}_T(S_T), \alpha)]$ , where  $f(\theta)$  represents a ranking-related function, such as Kendall's  $\tau$  as depicted in Eq. (3.6). The choice of Kendall's  $\tau$  in this dissertation stems from its direct measurement of ranking accuracy and its widespread adoption in related research endeavors [Jiang et al., 2011, Xu et al., 2018a, Chen et al., 2022].*

Before proceeding further, it is pertinent to recognize that the optimization problem delineated in Eq. (3.8) can be construed as a *Minimum-Feedback-Arc-Set* (MFAS) problem [Jiang et al., 2011, Xu et al., 2013, Baharev et al., 2021], renowned for its potential NP-hard complexity. Returning to the directed graph  $G_d$  as elucidated in Eq. (3.32), we now expand

our perspective to encompass a weighted directed graph. In this augmentation,  $G_d$  evolves into:

$$G_d^W = (V, E_d, W_{E_d}),$$

where  $W$  represents the set of weights, denoted as

$$W_{E_d} = \{w(i, j) | (i, j) \in E_d\}. \quad (3.10)$$

Each weight  $w(i, j)$  encapsulates the magnitude of influence from item (vertex)  $i$  to  $j$  within the graph.

Specifically, within our Bayesian framework,  $G_d^W$  emerges as a complete weighted directed graph [Bapat et al., 2012]:

$$G_{d,c}^W = (V, V^2, W_{V^2}), \quad (3.11)$$

where  $V = \{1, \dots, N\}$ , and  $V^2$  is defined in Eq. (3.33). The weights  $w(i, j)$  in  $W_{V^2}$  are determined by  $\text{Pred}_T(i > j)$ , which is specified in Eq. (3.9). Additionally, another important concept is the tournament graph [Moon, 2015]:

$$G_{d,t}^W = (V, E_{d,t}, W_{E_{d,t}}), \quad (3.12)$$

where  $V$  remains the same as in  $G_{d,c}^W$ . The set  $E_{d,t}$  consists of either  $(i, j)$  or  $(j, i)$  for every possible compared pair in  $V^2$ . The associated weights  $W_{E_{d,t}}$  are defined as in Eq. (3.10). Before going to the MFAS problem, another important concept is *directed acyclic graph* [Byeon and Lee, 2023], which is defined below

**Definition 3.1.** A *directed acyclic graph* is defined as a graph devoid of any cycles. A cycle within a directed graph is delineated as a path (refer to Definition 3.3) that originates and terminates at the same vertex, with no recurrence of vertices in between, excluding the starting and ending vertex.

After introducing directed acyclic graphs, we can delve into the MFAS problem, which entails removing the smallest set of weighted edges to ensure the resulting graph is acyclic while minimizing the total weight of removed edges. Notably, in the complete weighted graph  $G_{d,c}^W$ , it is imperative to remove at least  $\frac{N(N-1)}{2}$  edges from  $V^2$ , as maintaining two edges with symmetric directions is infeasible. For instance, if both edge  $(i, j)$  and  $(j, i)$  exist in the edge set, a cycle is formed (the path (cycle) being  $i(i, j)j(j, i)i$ ), violating the acyclic property defined in Definition 3.1. Therefore, for any pair of vertices, only one edge  $(i, j)$  or  $(j, i)$  can

be present, resembling the structure of a tournament graph as defined in Eq. (3.12). Moreover, tournament graphs can be acyclic; for instance, if we have  $N$  vertices (items) and sort them according to a deterministic criterion denoted as  $\alpha_{\text{sort}} = (\alpha_1, \dots, \alpha_N)^\top$ , the corresponding edge set  $E_{\alpha_{\text{sort}}}$  is defined as  $\{(\alpha_k, \alpha_s) | s < k\}$ . This construction ensures the absence of cycles in the graph since there are no edges from vertices with lower subscripts to vertices with higher subscripts.

Then the goal function in Eq. (3.8) becomes reducing smallest set of edges in  $V^2$ , effectively transforming the complete weighted directed graph  $G_{d,t}^W$  into an acyclic tournament graph  $G_{d,t}^W$  with the maximized summation of weights constraint:

$$G_{d,t}^W \xrightarrow{\text{MFAS}} \max_{\sum_{(i,j) \in E_{d,t}} w(i,j)} G_{d,t}^W. \quad (3.13)$$

Unfortunately, the MFAS problem in Eq. (3.13) is known to be NP-hard [Baharev et al., 2021]. However, we demonstrate that, under mild and empirically observed conditions, addressing this challenge can be simplified to a sorting scheme.

**Remark 3.2.** *The problem posed in Eq. (3.13) can be likened to the linear ordering problem, aiming to discover an acyclic tournament graph with the maximal sum of weights. Notably, this challenge remains classified as NP-hard [Mishra and Sikdar, 2004, Martí and Reinelt, 2011, Baharev et al., 2021].*

### 3.4 Conjugate Bayesian for Thurstone-Mosteller Model

The work in Chen et al. [2016] has certain limitations, notably the lack of a known closed form for the posterior distribution. In this section, we will briefly introduce this framework based on the BTL model and subsequently discuss our conjugate framework for Thurstone-Mosteller Ranking.

The approach in Chen et al. [2016] assumes that  $\theta$  is drawn from the simplex:

$$\mathcal{D} = \left\{ \theta \in \mathbb{R}^N \middle| \sum_{i=1}^N \theta_i = 1, \theta_i > 0 \right\},$$

and follows a Dirichlet distributed prior:

$$\theta \sim \text{Dir}(\alpha^0) = \frac{1}{B(\alpha^0)} \prod_{i=1}^N \theta_i^{\alpha_i^0 - 1},$$

where  $\alpha^0 = (\alpha_1^0, \dots, \alpha_N^0)^\top$ , and  $B(\alpha^0)$  is the corresponding normalization constant. With  $T$  compared pairs collected, which follow the BTL model in Eq. (3.4), the posterior distribution

of  $\boldsymbol{\theta}$  takes the form:

$$p(\boldsymbol{\theta}|M^T, \boldsymbol{\alpha}^0) = \frac{1}{B(M^T, \boldsymbol{\alpha}^0)} \prod_{i \neq j} \left( \frac{\theta_i}{\theta_i + \theta_j} \right)^{M^T(i,j)} \prod_{i=1}^N \theta_i^{\alpha_i^{0,-1}},$$

where  $B(M^T, \boldsymbol{\alpha}^0)$  is the normalization constant, and  $M^T$  is an  $N \times N$  matrix collecting the compared data. Specifically, the  $(i, j)$ -th entry in  $M^T$ , denoted as  $M^T(i, j)$ , indicates how many times item  $i$  is preferred over item  $j$  in the past  $T$  comparisons.

However,  $p(\boldsymbol{\theta}|M^T, \boldsymbol{\alpha}^0)$  in Chen et al. [2016] lacks a closed-form solution due to its inherent complexity, making the derivation of  $\pi_T$  in Eq. (3.8) challenging. Researchers then resort to an approximated posterior via moment matching, which may, however, lead to significant estimation errors, as exemplified in Fig. 1.1. To overcome this challenge, we propose our conjugate framework based on the TM model.

Specifically, if we choose  $p_\alpha(\boldsymbol{\theta})$  in Eq. (3.5) as isotropic independent Gaussian distributions, i.e.,  $\theta_i \sim \mathcal{N}(\mu_i^0, (\sigma_i^0)^2)$ , the posterior distribution will be:

$$p(\boldsymbol{\theta}|\mathcal{S}_T, \mathcal{Y}_T(\mathcal{S}_T), \boldsymbol{\alpha} = (\boldsymbol{\mu}^0, \boldsymbol{\sigma}^0)) = \frac{\prod_{t=1}^T \Phi\left(\frac{(\theta_{i_t} - \theta_{j_t})y_t}{\sqrt{2}}\right) \prod_{i=1}^N \frac{1}{\sqrt{2\pi(\sigma_i^0)^2}} e^{-\frac{(\theta_i - \mu_i^0)^2}{2(\sigma_i^0)^2}}}{B(\mathcal{S}_T, \mathcal{Y}_T(\mathcal{S}_T), \boldsymbol{\mu}^0, \boldsymbol{\sigma}^0)},$$

where  $\boldsymbol{\mu}^0 = (\mu_1^0, \mu_2^0, \dots, \mu_N^0)^\top$ ,  $\boldsymbol{\sigma}^0 = (\sigma_1^0, \sigma_2^0, \dots, \sigma_N^0)^\top$ , and  $B(\mathcal{S}_T, \mathcal{Y}_T(\mathcal{S}_T), \boldsymbol{\mu}^0, \boldsymbol{\sigma}^0)$  represents the normalizing constant. In the absence of observations, we should have no preference among all the items, and we model it to have an i.i.d. standard normal prior:

$$\boldsymbol{\theta}_N \sim \mathcal{N}_N(\mathbf{0}_N, I_N), \text{Var}(\theta_i) = 1 \text{ for each } i. \quad (3.14)$$

**Remark 3.3.** *The assumption of a normal prior distribution for item scores aligns with the foundational principles of the Thurstone-Mosteller model. This model posits that the latent item scores are both independent and normally distributed. Under this framework, the probability of item  $i$  being preferred over item  $j$  is represented as  $\Pr(\theta_i > \theta_j) = \Pr(\theta_i - \theta_j > 0)$ . Given that the difference  $\theta_i - \theta_j$  follows a normal distribution, this probability calculation conforms to the Thurstone-Mosteller model as expressed in Equation (3.2).*

Then the posterior distribution becomes:

$$p(\boldsymbol{\theta}|\mathcal{S}_T, \mathcal{Y}_T(\mathcal{S}_T), \mathbf{0}_N, I_N) = \frac{\prod_{t=1}^T \Phi\left(\frac{(\theta_{i_t} - \theta_{j_t})y_t}{\sqrt{2}}\right) \prod_{i=1}^N \frac{1}{\sqrt{2\pi}} e^{-\frac{\theta_i^2}{2}}}{B(\mathcal{S}_T, \mathcal{Y}_T(\mathcal{S}_T), \mathbf{0}_N, I_N)}, \quad (3.15)$$

where  $B(\mathcal{S}_T, \mathcal{Y}_T(\mathcal{S}_T), \mathbf{0}_N, I_N)$  is the normalization constant, and we also denote

$$\tilde{\boldsymbol{\theta}} = D_T \boldsymbol{\theta} + \boldsymbol{\varepsilon}, \text{ where } \boldsymbol{\varepsilon} \sim \mathcal{N}_T(\mathbf{0}_T, I_T) \text{ is independent of } \boldsymbol{\theta}. \quad (3.16)$$

Here,  $D_T = \text{diag}(\mathbf{y}_T)X_T$ , where  $\text{diag}(\mathbf{a})$  specifies a diagonal matrix expanded by the vector  $\mathbf{a}$ . Here,  $X_T$  and  $\mathbf{y}_T$  represent the matrix form of  $\mathcal{S}_T$  and the vector form of  $\mathcal{Y}_T(\mathcal{S}_T)$ , respectively. Specifically,  $X_T \in \mathbb{R}^{T \times N}$  has its  $k$ -th row ( $k = 1, \dots, T$ ) defined according to the  $k$ -th comparison pair  $(i_k, j_k)$ : for  $l = 1, \dots, N$ ,  $X_T(k, l) \stackrel{\textcircled{1}}{=} \frac{1}{\sqrt{2}}$  if  $l = i_k$ ,  $= -\frac{1}{\sqrt{2}}$  if  $l = j_k$ , and  $= 0$  otherwise. Additionally,  $\mathbf{y}_T := (y_1, \dots, y_T)^\top$ . We can express the probability  $\Pr(\tilde{\theta}_t > 0 | \theta)$  as  $\Pr\left(\varepsilon_t > -y_t \frac{\theta_{i_t} - \theta_{j_t}}{\sqrt{2}} | \theta\right) = \Phi\left(\frac{y_t(\theta_{i_t} - \theta_{j_t})}{\sqrt{2}}\right)$ . Note that each element in  $\varepsilon$  is independent, then we can have

$$p(\theta | \tilde{\theta} > 0) \propto \Pr(\tilde{\theta} > 0 | \theta)p(\theta) = \prod_{t=1}^T \Phi\left(\frac{(\theta_{i_t} - \theta_{j_t})y_t}{\sqrt{2}}\right) \prod_{i=1}^N \frac{1}{\sqrt{2\pi}} e^{-\frac{\theta_i^2}{2}}.$$

Therefore, compared to Eq. (3.15), we find  $p(\theta | \mathcal{S}_T, \mathcal{Y}_T(\mathcal{S}_T), \mathbf{0}_N, I_N) = p(\theta | \tilde{\theta} > 0)$ . Furthermore, Eq. (3.16) implies  $(\tilde{\theta} | \theta) \sim \mathcal{N}_T(D_T\theta, I_T)$ . Since the derivation of the SUN variable above Eq. (2.5) is based on the correlation matrix, we first establish the following lemma.

**Lemma 3.1.** *Let  $\theta$  be defined as in Eq. (3.14), and  $\varepsilon \sim \mathcal{N}_T(\mathbf{0}_T, I_T)$  be independent of  $\theta$ . Consider a  $T \times N$  design matrix  $D_T$ , where  $D_T(k, l)$  equals  $a$  if  $l = i_k$ ,  $-a$  if  $l = j_k$ , and  $0$  otherwise, for  $k = 1, \dots, T$  and  $l = 1, \dots, N$ , with  $a \in \mathbb{R} - \{0\}$ ,  $i_k, j_k \in \{1, \dots, N\}$ . If  $\tilde{\theta} = D_T\theta + \varepsilon$ , then the distribution of  $p(\theta | \tilde{\theta} > 0)$  remains invariant whether derived from the variance-covariance matrix or the correlation matrix of the joint distribution  $\begin{pmatrix} \theta \\ \tilde{\theta} \end{pmatrix}$ .*

The proof of this Lemma can be found in Sec. 4.4. From Lemma 3.1,  $p(\theta | \tilde{\theta} > 0)$  can be derived from the joint distribution of  $\begin{pmatrix} \theta \\ \tilde{\theta} \end{pmatrix}$ , with mean and correlation matrix represented below:

$$\begin{pmatrix} \theta \\ \tilde{\theta} \end{pmatrix} \sim \mathcal{N}_{N+T} \left( \begin{pmatrix} \mathbf{0}_N \\ \mathbf{0}_T \end{pmatrix}, \begin{pmatrix} I_N & \Delta_T \\ \Delta_T^\top & \Gamma_T \end{pmatrix} \right), \quad (3.17)$$

where  $\Delta_T = D_T^\top s_T^{-1}$ ,  $\Gamma_T = s_T^{-1}(D_T D_T^\top + I_T)s_T^{-1}$ , in which  $s_T := \text{diag}(\sqrt{2}\mathbf{1}_T)$  ( $\mathbf{1}_T$  is a  $T$ -dimensional vector with all elements set to 1). With  $\xi = \mathbf{0}_N$ ,  $\gamma = \mathbf{0}_T$ ,  $\omega = I_N$ , based on the derivation of SUN variable above Eq. (2.5), we obtain:

$$(\theta | \mathcal{S}_T, \mathcal{Y}_T(\mathcal{S}_T), \mathbf{0}_N, I_N) \stackrel{d}{=} (\theta | \tilde{\theta} > 0) \sim \text{SUN}_{N,T}(\mathbf{0}_N, I_N, \Delta_T, \mathbf{0}_T, \Gamma_T). \quad (3.18)$$

According to Eq. (2.5), its density function can be expressed as:

$$p(\theta | \mathcal{S}_T, \mathcal{Y}_T(\mathcal{S}_T), \mathbf{0}_N, I_N) = \phi_N(\theta; \mathbf{0}_N, I_N) \frac{\Phi_T(\Delta_T^\top \theta; \Gamma_T - \Delta_T^\top \Delta_T)}{\Phi_T(\mathbf{0}_T; \Gamma_T)}. \quad (3.19)$$

<sup>①</sup>  $X(k, l)$  indicates the entry in the  $k$ -th row and  $l$ -th column of matrix  $X$ .

With the ground-truth posterior at hand, the objective used in Chen et al. [2016] within our framework becomes:

$$\pi_T \in \arg \max_{\pi} \mathbb{E}[\tau(\pi, \pi^*) | S_T, \mathcal{Y}_T(\mathcal{S}_T), \mathbf{0}_N, I_N], \quad (3.20)$$

where the expectation is taken over the posterior distribution of  $\boldsymbol{\theta}$ , i.e.,  $\boldsymbol{\theta} \sim p(\boldsymbol{\theta} | \mathcal{S}_T, \mathcal{Y}_T(\mathcal{S}_T), \mathbf{0}_N, I_N)$ ,  $\pi^*$  is in accordance with score  $\boldsymbol{\theta}$  in Eq. (3.1), and  $\tau(\pi, \pi^*)$  is given in Eq. (3.6). Additionally, we have:

$$\pi_T \in \arg \max_{\pi} C_T(\pi) \equiv \sum_{i \neq j} \mathbf{1}_{\{\pi(i) > \pi(j)\}} \text{Pred}_T(i > j), \quad (3.21)$$

where the prediction probability of item  $i$  surpassing item  $j$ , based on the posterior distribution in the TM setting, is defined as:

$$\text{Pred}_T(i > j) := \Pr(\theta_i > \theta_j | \mathcal{S}_T, \mathcal{Y}_T(\mathcal{S}_T), \mathbf{0}_N, I_N) = \int_{\theta_i > \theta_j} p(\boldsymbol{\theta} | \mathcal{S}_t, \mathcal{Y}_t(\mathcal{S}_t), \mathbf{0}_N, I_N) d\boldsymbol{\theta}. \quad (3.22)$$

Each pair in  $C_T(\pi)$  is uniquely assigned to either  $\text{Pred}_T(i > j)$  or  $\text{Pred}_T(j > i)$ , leading to the following upper bound for  $C_T(\pi)$ :

$$C_T(\pi) = \sum_{\pi(i) > \pi(j)} \text{Pred}_T(i > j) \leq \sum_{i=1}^N \sum_{j=i+1}^N \max(\text{Pred}_T(i > j), \text{Pred}_T(j > i)). \quad (3.23)$$

This upper bound can be achieved by a certain  $\pi$  if it exists and satisfies:  $\pi(i) > \pi(j)$  only if  $\text{Pred}_T(i > j) \geq \text{Pred}_T(j > i)$ , i.e.,  $\text{Pred}_T(i > j) \geq 0.5$ . To compute  $\text{Pred}_T(i > j)$ , we first define:  $\Delta_T(i, j)$  as a  $1 \times T$  matrix given by

$$\Delta_T(i, j) := \Delta_T(i, :) - \Delta_T(j, :). \quad (3.24)$$

Here  $\Delta_T(i, :)$  and  $\Delta_T(j, :)$  are respectively the  $i$ -th and  $j$ -th rows of  $\Delta_T$ . The computation of  $\text{Pred}_T(i > j)$  is detailed in the following proposition.

**Proposition 3.1.**  $\text{Pred}_T(i > j)$  defined in Eq. (3.22) can be expressed as:

$$\text{Pred}_T(i > j) = \frac{\Phi_{T+1}(\mathbf{0}_{T+1}; \tilde{\Omega}_{ij})}{\Phi_T(\mathbf{0}_T; \Gamma_T)}, \text{ where } \tilde{\Omega}_{ij} = \begin{pmatrix} 1 & \frac{\Delta_T(i, j)}{\sqrt{2}} \\ \frac{\Delta_T(i, j)^\top}{\sqrt{2}} & \Gamma_T \end{pmatrix}. \quad (3.25)$$

The proof of Proposition 3.1 can be found in Section 4.3. However, determining  $\pi_T$  in Eq. (3.21) via  $\{\text{Pred}_T(i > j)\}_{(i \neq j)}$  alone necessitates a well-defined ranking, implying the absence of a loop as defined below:

**Definition 3.2.** We say that a loop exists among  $i_1, \dots, i_K$  for some integer  $K \geq 3$  if, for each

$1 \leq r \leq K - 1$ ,  $\text{Pred}_T(i_r > i_{r+1}) \geq 0.5$ , with at least one occurrence of " $>$ " being satisfied, and additionally,  $\text{Pred}_T(i_K > i_1) > 0.5$ .

In the absence of loops, we can propose the estimated ranking with a simple iterative procedure, the core of which is

$$\text{find } s \in S \text{ such that } \text{Pred}_T(s > k) \geq 0.5 \text{ for all } k \in S \text{ and } k \neq s. \quad (3.26)$$

Here,  $S$  is the set of all candidate items, i.e.,  $S = \{1, 2, \dots, N\}$  initially. After picking  $s$  in each iteration,  $S$  will be updated as  $S = S - \{s\}$ . This criterion ensures that the earlier an item is picked, the higher rank it will have. The formal algorithm will be:

---

**Algorithm 1** Ranking Verification.

**Input**  $\{\text{Pred}_T(i > j)\}_{(i \neq j)}$ , where  $i, j \in \{1, \dots, N\}$ .

**Output** A ranking  $\pi$  if there is no loop, otherwise, **None**.

- 1: Set the candidate set  $S = \{1, 2, \dots, N\}$ .
  - 2: **while**  $|S| \geq 1$  **do**
  - 3:     **if** there exists  $s \in S$  such that  $\text{Pred}_T(s > k) \geq 0.5$  for all  $k \in S$  and  $k \neq s$ , or  $|S \cap \{s\}| = 1$ . **then**
  - 4:         Set  $\pi(s) = |S|$ , and remove  $s$  from  $S$ .
  - 5:     **else**
  - 6:         Break the loop and return **None**.
  - 7:     **end if**
  - 8: **end while**
- 

In the presence of such a loop, however,  $C_T(\pi)$  fails to reach its upper bound. In the worst case scenario, we would need to compare  $N!$  possible rankings to achieve the maximized  $C_T(\pi)$ , which is NP-hard. Fortunately, our empirical observations suggest that loops do not exist, and the proposed ranking based on Eq. (3.20) is, in fact, the sorting of the posterior mean of  $\boldsymbol{\theta}$ . This observation can be attributed to the always-satisfied sufficient condition in our empirical study, namely, the non-symmetric condition, which is introduced below:

**Condition 3.1.** If  $\Delta_T$  defined below Eq. (3.17) has  $\Delta_T(ij)^\top \neq \mathbf{0}_T$ , where  $\Delta_T(ij)$  is defined in Eq. (3.24), then we assume the following holds for all  $s \in (0, +\infty)$ :

$$\Phi_T\left(\frac{\Delta_T(ij)^\top s}{2}; \Gamma_T - \frac{\Delta_T(ij)^\top \Delta_T(ij)}{2}\right) \neq \Phi_T\left(\frac{-\Delta_T(ij)^\top s}{2}; \Gamma_T - \frac{\Delta_T(ij)^\top \Delta_T(ij)}{2}\right), \quad (3.27)$$

where  $\Gamma_T$  is obtained as shown below Eq. (3.17).

To empirically demonstrate this condition, we first introduce a univariate SUN-distributed random variable:

$$\theta_{ij} \sim A_{ij}^\top \boldsymbol{\theta}, \quad (3.28)$$

where  $A_{ij}$  is an  $N$ -dimensional vector with its  $i$ -th element set to 1,  $j$ -th element set to  $-1$ , and all other elements set to 0. Additionally,  $\theta$  follows the distribution given in Eq. (3.18). The  $x$ -axis represents the value of  $\theta_{ij}$ , while the  $y$ -axis represents its density.

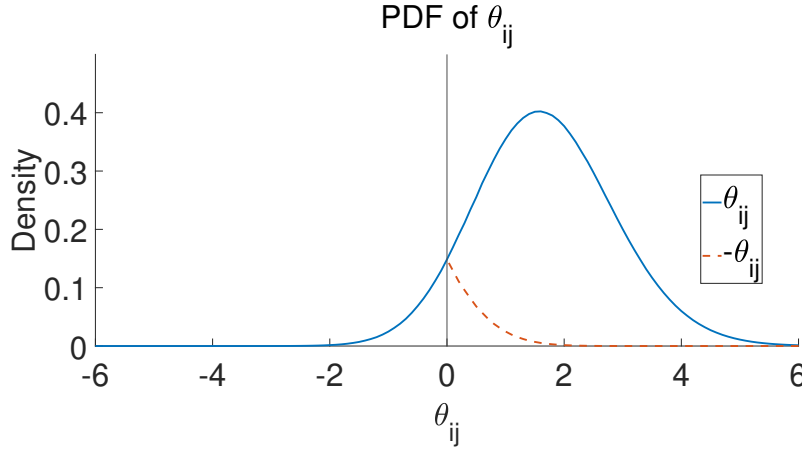


Figure 3.1 An empirical example of the non-symmetric condition.

The non-symmetric condition asserts that the PDF of  $\theta_{ij}$  will not yield identical values at points symmetric about the  $y$ -axis. We demonstrate one example of  $\theta_{ij}$  in our empirical study as shown in Fig. 3.1. The blue line represents the density of  $\theta_{ij}$ , while the orange line represents the density of  $-\theta_{ij}$ , with  $\theta_{ij} \in \{0, +\infty\}$ . The fact that the blue line and orange line do not intersect in  $\mathbb{R}^+$  demonstrates the satisfaction of the non-symmetric condition. This condition can be tested and is always satisfied in our empirical study. Under this condition, the following theorem guarantees the absence of loops, and we can propose our estimated ranking via the procedure in Eq. (3.26).

With the non-symmetric condition in 3.1 defined, we will have the following theorem, which states that the proposed ranking from Eq. (3.20) should be the sorting of the posterior mean of  $\theta$ .

**Theorem 3.1.** *If  $\theta$  follows the posterior distribution as described in Eq. (3.18), and Condition 3.1 is satisfied for all pairs, then the ranking  $\pi_{pos}$ , sorted by the posterior mean, i.e.  $\mathbb{E}[\theta | S_T, \mathcal{Y}_T(S_T), \mathbf{0}_N, I_N]$ , optimizes the expectation of Kendall's  $\tau$  as shown in Eq. (3.20).*

The proof of this theorem can be found in Sec. 4.2. This result implies that if the non-symmetric condition holds for all pairs, there are no loops in the ranking induced by  $\{\text{Pred}_T(i > j)\}_{(i \neq j)}$ , corresponding to the sorting of the posterior mean of  $\theta$ .

Although never encountered in our empirical study, the possibility of the presence of loops still exists. If a loop exists, determining the optimal ranking becomes NP-hard, as discussed in

---

**Algorithm 2** SUN Ranking

---

**Input** Observed data  $\mathcal{S}_T = \{(i_t, j_t)\}_{t=1}^T$ ,  $\mathcal{Y}_T(\mathcal{S}_T) = \{y_t\}_{t=1}^T$ .

**Output** Estimated Ranking  $\pi_{pos}$ .

- 1: Obtain the PDF of the posterior distribution in Eq. (3.19) from the observed data.
  - 2: Calculate  $\text{Pred}_T(i > j)$  with Eq. (3.25)  $\forall i < j$ . Set  $\text{Pred}_T(j > i) = 1 - \text{Pred}_T(i > j)$ .
  - 3: Run Algorighm 1 and check if there exists a loop.
  - 4: **if** return a ranking  $\pi$  **then**
  - 5:     Set  $\pi_{pos} = \pi$ .
  - 6: **else**
  - 7:     Obtain the posterior mean  $\mu_T$  using Eq. (3.29). Set  $\pi_{pos}$  based on the sorting of  $\mu_T$ .
  - 8: **end if**
- 

Chen et al. [2016]. In such cases, to ensure the completeness of our algorithm, we resort to the posterior mean, denoted as  $\mu_T$ , for estimation. Leveraging the sorting of  $\mu_T$  is optimal under the non-symmetric condition and widely applied in ranking scenarios, as demonstrated in Xu et al. [2018a], Chen et al. [2013]. We derive the form of its posterior mean from Eq. (2.7), with the distribution of  $\boldsymbol{\theta}$  given in Eq. (3.18).

$$\mu_T = \frac{\Delta_T \nabla \Phi_T(\Gamma_T)}{\Phi_T(\mathbf{0}_T; \Gamma_T)}, (\nabla \Phi_T(\Gamma))_j = \begin{cases} \phi(0) & \text{if } T = 1, \\ \phi(0) \Phi_{T-1}(\mathbf{0}_{T-1}, \Gamma_{-j,-j} - \Gamma_{-j} \Gamma_{-j}^\top) & \text{otherwise.} \end{cases} \quad (3.29)$$

Here  $\Gamma_{-j}$  (( $T - 1$ )-dimensional vector) represents the  $j$ -th column of the matrix  $\Gamma$  with its  $j$ -th element omitted.  $\tilde{\Gamma}_{-j} = \Gamma_{-j,-j} - \Gamma_{-j} \Gamma_{-j}^\top$ , where  $\Gamma_{-j,-j}$  is a  $(T - 1) \times (T - 1)$  matrix obtained by eliminating the  $j$ -th row and column from  $\Gamma$ .

We summarize our ranking estimation in Algorithm 2.

### 3.5 Monte Carlo Estimation of $\text{Pred}_T(i > j)$ and $\mu_T$

As the computation of  $\{\text{Pred}_T(i > j)\}_{(i \neq j)}$  with Eq. (3.25) requires to calculate  $(T + 1)$ -dimensional multivariate normal CDFs for  $N(N - 1)/2$  times, Algorithm 2 can be expensive when  $N$  is large. To address this issue, we implement Monte Carlo integration to compute  $\{\text{Pred}_T(i > j)\}_{(i \neq j)}$  or posterior mean. The key idea is based on the orthogonal decomposition of the SUN distribution into a multivariate normal distribution and a multivariate truncated normal distribution [Arellano-Valle and Azzalini, 2022].

Before proceeding further, we introduce the concept of a multivariate truncated normal distribution. Consider a random vector  $\boldsymbol{\theta} \sim \text{TN}(\boldsymbol{\mu}, \boldsymbol{\Sigma}, \mathbb{D}_c)$  with the density function given by

$$p(\boldsymbol{\theta}) = \frac{1}{B(\mathbb{D}_c)} \phi_N(\boldsymbol{\theta}; \boldsymbol{\mu}, \boldsymbol{\Sigma}), \quad \boldsymbol{\theta} \in \mathbb{D}_c, \quad (3.30)$$

where  $\mathbf{c} = (c_1, \dots, c_N)^\top$  represents the truncation values for  $\boldsymbol{\theta}$ ; we define the truncation of  $\boldsymbol{\theta}$  below  $\mathbf{c}$  as  $\boldsymbol{\theta} \in \mathbb{D}_{\mathbf{c}} = \{\boldsymbol{\theta} | \theta_i - c_i \geq 0 \text{ for } i = 1, \dots, N\}$ , and  $B(\mathbb{D}_{\boldsymbol{\theta}})$  is the corresponding normalization constant given by  $B(\mathbb{D}_{\boldsymbol{\theta}}) = \int_{\boldsymbol{\theta} \in \mathbb{D}_{\boldsymbol{\theta}}} \phi_N(\boldsymbol{\theta}; \boldsymbol{\mu}, \Sigma) d\boldsymbol{\theta}$ . This distribution is analogous to the multivariate normal distribution but truncated, restricting its domain to intervals, such as  $\theta_i \geq c_i$ , for each component of  $\boldsymbol{\theta}$ .

With the introduction of truncated normal distribution, we now turn to the following proposition.

**Proposition 3.2** (Eq. (6) in Arellano-Valle and Azzalini [2022]). *If the posterior distribution  $(\boldsymbol{\theta} | \mathcal{S}_T, \mathcal{Y}_T(\mathcal{S}_T), \mathbf{0}_N, \mathbf{I}_N)$  has the probability density function in Eq. (3.19), then it can be orthogonally decomposed into the following form:*

$$(\boldsymbol{\theta} | \mathcal{S}_T, \mathcal{Y}_T(\mathcal{S}_T), \mathbf{0}_N, \mathbf{I}_N) \stackrel{d}{=} \mathbf{V}_0 + D_T^\top (D_T D_T^\top + I_T)^{-1} s_T \mathbf{V}_1, \quad (\mathbf{V}_0 \perp \mathbf{V}_1) \quad (3.31)$$

where  $D_T$  and  $s_T$  are defined below Eq. (3.16) and Eq. (3.17) separately.  $\mathbf{V}_0$  follows a  $N$ -dimensional multivariate normal distribution with mean  $\mathbf{0}_N$  and variance-covariance matrix  $I_N - D_T^\top (D_T D_T^\top + I_T)^{-1} D_T$ .  $\mathbf{V}_1$  comes from a  $T$ -dimensional multivariate truncated normal distribution, with mean  $\mathbf{0}_T$ , variance-covariance matrix  $s_T^{-1} (D_T D_T^\top + I_T) s_T^{-1}$  and truncation below  $\mathbf{0}_T$ .

According to Eq. (3.31), we can approximate  $\text{Pred}_T(i > j)$  and  $\mu_T$  via Monte Carlo integration as summarized below:

---

**Algorithm 3** Monte Carlo Integration to estimate  $\text{Pred}_T(i > j)$  and  $\mu_T$

---

**Input** Observed data  $\mathcal{S}_T = \{(i_t, j_t)\}_{t=1}^T$ ,  $\mathcal{Y}_T(\mathcal{S}_T) = \{y_t\}_{t=1}^T$ , and the number of samples  $n$ .

**Output** Estimated  $\text{Pred}_T(i > j)$  and  $\mu_T$ .

- 1: Calculate  $D_T$  and  $s_T$ , introduced below Eq. (3.16) and Eq. (3.17) separately.
  - 2: Sample  $n$  independent samples  $v_0^{(1)}, \dots, v_0^{(n)}$  from an  $N$ -dimensional multivariate normal distribution with mean  $\mathbf{0}_N$  and variance-covariance matrix  $I_N - D_T^\top (D_T D_T^\top + I_T)^{-1} D_T$ .
  - 3: Sample  $n$  independent samples  $v_1^{(1)}, \dots, v_1^{(n)}$  from a  $T$ -dimensional multivariate truncated normal distribution with mean  $\mathbf{0}_T$ , variance-covariance matrix  $s_T^{-1} (D_T D_T^\top + I_T) s_T^{-1}$ , and truncation below  $\mathbf{0}_T$ .
  - 4: Obtain  $\boldsymbol{\theta}^{(1)}, \dots, \boldsymbol{\theta}^{(n)}$ , where  $\boldsymbol{\theta}^{(s)} = v_0^{(s)} + D_T^\top (D_T D_T^\top + I_T)^{-1} s_T v_1^{(s)}$ .
  - 5: For all  $i, j$  with  $i \neq j$ , estimate  $\text{Pred}_T(i > j) \approx \frac{1}{n} \sum_{s=1}^n \mathbf{1}_{\{\theta_i^{(s)} > \theta_j^{(s)}\}}$ .
  - 6: Estimate  $\mu_T \approx \frac{1}{n} \sum_{s=1}^n \boldsymbol{\theta}^{(s)}$ .
- 

We strongly advocate for the utilization of Monte Carlo integration in practical applications, especially considering the time-consuming nature of computing the multivariate normal CDF, as discussed in Durante [2019], Botev [2017].

### 3.6 Convergence of SUN Ranking Algorithm

In this section, we show the convergence of our SUN Ranking Algorithm with i.i.d. samples to the MLE. To demonstrate this clearly, let's recall the MLE of the TM model in Eq. (3.2), denoted as  $\hat{\theta}_{\text{TM},T}$  in Eq. (3.3). Before proceeding, it is crucial to note that the MLE may not always exist. Hence, we first delve into the conditions under which its existence can be guaranteed.

The TM comparison model hinges solely on the discrepancies between item scores, granting it the property of translational invariance as delineated in Eq. (3.2). With  $f(\boldsymbol{\theta}, i, j) = \Phi\left(\frac{\theta_i - \theta_j}{\sqrt{2}}\right)$ , it becomes apparent that for any pair of items  $i$  and  $j$ , the model's outcomes remain unaltered by translations of  $\boldsymbol{\theta}$  to  $\boldsymbol{\theta} + \mathbf{c}$ , where  $\mathbf{c} \in \mathbb{R}^N$  represents a constant vector, ensuring  $f(\boldsymbol{\theta}, i, j) = f(\boldsymbol{\theta} + \mathbf{c}, i, j)$ . Subsequently, a reference alternative  $\theta_r = 0$  is established for some  $r \in \{1, \dots, N\}$ . Consequently, the solution to the MLE problem, employing the TM likelihood function, demonstrates a unique and bounded nature under specific conditions, as illustrated in Noothigattu et al. [2020]. We briefly elucidate these conditions.

First and foremost, it is imperative to recognize that pairwise comparison data naturally lends itself to representation as a directed graph, denoted as

$$G_d = (V, E_d), \quad (3.32)$$

which is elucidated in the context of HodgeRank in Section 3.2. Here,  $V = \{1, 2, \dots, N\}$  signifies the set of vertices corresponding to items, while the set of directed edges, represented as

$$E_d = \{e_d^{(i,j)} = (i, j) \mid \#\{i > j\} > 0\},$$

captures the item relationships. Within  $E_d$ ,  $\#\{i > j\}$  quantifies the frequency with which item  $i$  is favored over item  $j$  in the observed data.

Next, we introduce the set of distinct pairs, denoted as

$$V^2 = \{(i, j) \mid i, j \in V, \text{ with } i \neq j\}, \quad (3.33)$$

which encompasses all possible item comparisons.

We now delve into definitions pertinent to connectivity [Bondy et al., 1976, Bender and Williamson, 2010].

**Definition 3.3.** A directed path in  $G_d$  is a sequence of alternating vertices and directed edges, exemplified by  $i_1 e_d^{(i_1, i_2)} i_2 \dots e_d^{(i_n, i_{n+1})} i_{n+1}$ , with  $n \geq 0$  and without repeated vertices.

Lastly, we present the definition of a strongly connected graph.

**Definition 3.4.**  *$G_d$  is strongly connected if every pair in  $V^2$  contains a directed path.*

With these foundational definitions established, we can now delineate the conditions requisite for the existence, boundedness, and uniqueness of the MLE in the TM model.

**Lemma 3.2.** *(Lemma 2.1, 2.2, and 2.3 in Noothigattu et al. [2020]) Given the comparison graph  $G_d$ , as delineated by Eq. (3.32), derived from pairwise comparison data, if it satisfies the condition of being strongly connected as per Definition 3.4, then there exists a unique and bounded Maximum Likelihood Estimator.*

**Remark 3.4.** *It is noteworthy that the space of MLE, denoted as  $\{\theta | \theta_r = 0\}$ , can equivalently be represented as  $\{\theta | \sum_{i=1}^N \theta_i = 1\}$ . The work Xu et al. [2018b] demonstrated that under such constraints, the loss function described in Eq. (3.3) is strictly convex, ensuring the existence of a unique MLE.*

Since we have established conditions for the bounded and unique MLE exists, as the number of samples  $T$  approaches  $+\infty$ , we assume the MLE is consistent to a fixed constant vector  $\theta_{TM}^*$  and is asymptotically normally distributed, i.e.,

$$\hat{\theta}_{TM,T} \xrightarrow{d} \mathcal{N}_N(\theta_{TM}^*, \Sigma_{TM}), \quad (3.34)$$

where  $\Sigma_{TM}$  is the asymptotic variance-covariance matrix, which will not influence our results. Then, we have the following convergence theorem based on MLE.

**Theorem 3.2.** *Suppose that*

- (a) *The data is generated by the Thurstone-Mosteller model as described in Eq. (3.2) with  $T$  i.i.d. samples.*
- (b) *The directed graph formed by the collected samples, as described in Eq. (3.32), is strongly connected, as per Definition 3.4.*
- (c) *The MLE  $\hat{\theta}_{TM,T}$  is asymptotically normally distributed  $\mathcal{N}_N(\theta_{TM}^*, \Sigma_{TM})$  as described in Eq. (3.34).*

*Then, as  $T$  tends to infinity, the estimated ranking  $\hat{\pi}_T$  induced by the posterior with respect to  $p(\theta | \mathcal{S}_T, \mathcal{Y}_T(\mathcal{S}_T), \mathbf{0}_N, I_N)$  as in Eq. (3.20), converges to the order induced by  $\theta_{TM}^*$ .*

The proof of this theorem can be found in Sec. 4.5, which essentially is a result of the Bernstein–von Mises Theorem. This theorem states that the proposed ranking from our SUN

Ranking algorithm converges to the sorting of the MLE as the number of i.i.d. drawn samples approaches infinity.

Although it may seem that our SUN Ranking algorithm merely yields the same result as MLE, practical applications demonstrate the utility of our approach. Our algorithm exhibits greater robustness than MLE when the comparison model does not match that of MLE, as shown in Fig. 7.1. Moreover, one advantage of our SUN-based framework over MLE lies in the online ranking (active sampling) scenario, where we have knowledge of the posterior distribution throughout the entire process. In contrast, the asymptotic distribution from MLE may not hold true at early steps in active sampling, as depicted in Example 1.1.

Although Theorem 3.1 relies on assumptions about MLE, our empirical study suggests that the convergent result can be achieved without such assumptions. As discussed in Bochkina and Green [2014], the Bernstein–von Mises theorem implies that for correctly specified regular finite-dimensional models with  $T$  independent observations, the posterior distribution can be approximated in a  $\frac{1}{\sqrt{T}}$  neighborhood of the true parameter value (for example, we can know the true parameter value in a simulated study) by a Gaussian distribution with variance determined by the Fisher information.

To illustrate this, we conduct a simulation experiment. We consider  $N = 5$  items to be ranked, with  $\theta_i \sim U(0, 10)$  for each  $i = 1, \dots, 5$ , and  $\pi^*$  defined according to  $\theta$ . We generate paired samples and outcomes following Eq. (3.2). We run 10 independent trials and plot the median curve of Kendall's  $\tau$  along with its error bar region whose lower bound is the 0.25th quantile and upper bound is the 0.75th quantile. As shown in Fig. 3.2, Kendall's  $\tau$  approaches 1 as  $T$  exceeds 60, indicating the recovery of  $\pi^*$ .

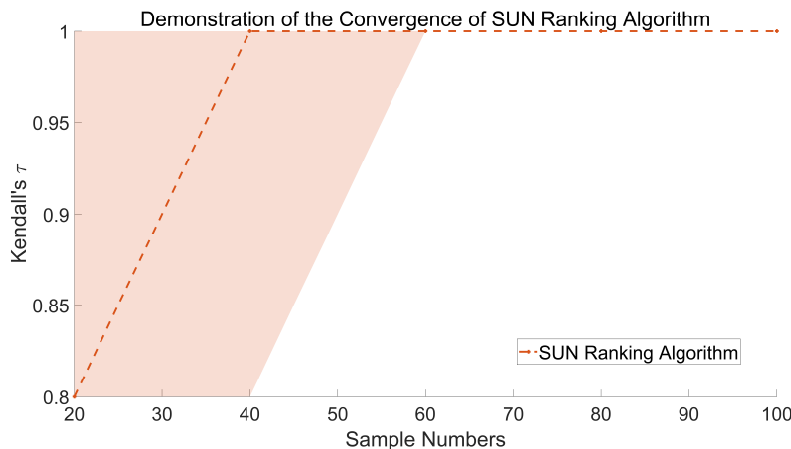


Figure 3.2 Convergence demonstration of SUN Ranking algorithm

### 3.7 Chapter Summary

In this chapter, we present our Bayesian conjugate framework for Thurstone-Mosteller ranking using the unified skew-normal distribution. We begin by discussing the ranking scenario, emphasizing the preference for pairwise comparison data over absolute scores. We provide an overview of various pairwise comparison methods for ranking from a frequentist perspective before delving into the Bayesian framework initially introduced by Chen et al. [2016].

Although well-formulated, the approach by Chen et al. [2016] suffers from a critical limitation: the lack of a known form for the ground-truth posterior. To address this challenge, we assume a Thurstone-Mosteller comparison model while employing an i.i.d. standard normal distribution as the prior. We demonstrate that under these assumptions, the posterior follows a unified skew-normal distribution. Leveraging the known form of the ground-truth posterior, we propose our SUN Ranking algorithm.

To clarify that the upper bound on the expectation of Kendall's  $\tau$  over the posterior can always be achieved in our empirical study, we introduce the sufficient condition known as the non-symmetric condition. With this condition, we establish that our proposed ranking corresponds to the sorting of the posterior mean of item scores. Additionally, we introduce the Monte Carlo integration method to alleviate computational burdens, particularly for large numbers of items.

Finally, we establish the convergence properties of our SUN Ranking algorithm based on the assumption of consistency of the Maximum Likelihood Estimator.

## Chapter 4 Proofs of the Conjugate Bayesian Framework

In this chapter, we present the proofs of lemmas, propositions, and theorems introduced earlier. By consolidating these proofs into a dedicated chapter, we aim to facilitate a seamless reading experience for our audience. While the proofs primarily entail computations based on the SUN distribution, they are not inherently challenging but rather meticulous in nature.

### 4.1 Preliminaries

In this section, we first provide details of several computations that will be utilized in the subsequent sections. This includes the moment-generating function of  $\theta_{ij}$ , which is described in Eq. (3.28), and the mean of  $\theta_{ij}$ .

According to the definition of the moment-generating function,  $M_T^{ij}(t)$  of  $\theta_{ij}$ , which is distributed as  $\text{SUN}_{1,T} \left( 0, 2, \frac{\Delta_T(ij)}{\sqrt{2}}, \mathbf{0}_T, \Gamma_T \right)$ , is defined as:

$$\begin{aligned} M_T^{ij}(t) &:= \int e^{t\theta_{ij}} \phi_1(\theta_{ij}; 0, 2) \frac{\Phi_T \left( \frac{\Delta_T(ij)^\top}{2} \theta_{ij}; \Gamma_T - \frac{\Delta_T(ij)^\top \Delta_T(ij)}{2} \right)}{\Phi_T(\mathbf{0}_T; \Gamma_T)} d\theta_{ij} \\ &= \int \frac{1}{\sqrt{2\pi}\sqrt{2}} e^{-\frac{\theta_{ij}^2}{4}} e^{t\theta_{ij}} \frac{\Phi_T \left( \frac{\Delta_T(ij)^\top}{2} \theta_{ij}; \Gamma_T - \frac{\Delta_T(ij)^\top \Delta_T(ij)}{2} \right)}{\Phi_T(\mathbf{0}_T; \Gamma_T)} d\theta_{ij} \\ &= e^{t^2} \int \frac{1}{\sqrt{2\pi}\sqrt{2}} e^{-\frac{(\theta_{ij}-2t)^2}{4}} \frac{\Phi_T \left( \frac{\Delta_T(ij)^\top}{2} \theta_{ij}; \Gamma_T - \frac{\Delta_T(ij)^\top \Delta_T(ij)}{2} \right)}{\Phi_T(\mathbf{0}_T; \Gamma_T)} d\theta_{ij} \\ &= e^{t^2} \int \phi_1(\theta_{ij}; 2t, 2) \frac{\Phi_T \left( \frac{\Delta_T(ij)^\top}{2} \theta_{ij}; \Gamma_T - \frac{\Delta_T(ij)^\top \Delta_T(ij)}{2} \right)}{\Phi_T(\mathbf{0}_T; \Gamma_T)} d\theta_{ij}, \end{aligned} \quad (4.1)$$

where  $\phi_1(x; \mu, \sigma)$  denotes the PDF of normal distribution  $\mathcal{N}(\mu, \sigma)$  at  $x$ . From Lemma 2.4.1 in Aziz [2011], the above integration becomes:

$$e^{t^2} \frac{\Phi_T \left( \frac{\Delta_T(ij)^\top}{2} \times 2t; \Gamma_T - \frac{\Delta_T(ij)^\top \Delta_T(ij)}{2} + \frac{\Delta_T(ij)^\top}{2} \times 2 \times \frac{\Delta_T(ij)}{2} \right)}{\Phi_T(\mathbf{0}_T; \Gamma_T)}. \quad (4.2)$$

Simplify the equation, we will get the moment generating function:

$$M_T^{ij}(t) = e^{t^2} \frac{\Phi_T(\Delta_T(ij)^\top t; \Gamma_T)}{\Phi_T(\mathbf{0}_T; \Gamma_T)}. \quad (4.3)$$

From the moment generating function, its cumulant generating function  $K_T^{ij}(t)$  will be

$$K_T^{ij}(t) = t^2 + \log \Phi_T(\Delta_T(ij)^\top t; \Gamma_T) - \log \Phi_T(\mathbf{0}_T; \Gamma_T) \quad (4.4)$$

Then the mean of  $\theta_{ij}$  will be

$$\mathbb{E}[\theta_{ij}] = \frac{dK_T^{ij}(t)}{dt} \Big|_{t=0} = \frac{\Delta_T(ij)\nabla\Phi_T(\Gamma_T)}{\Phi_T(\mathbf{0}_T; \Gamma_T)} = \mathbb{E}[\theta_i - \theta_j] \quad (4.5)$$

where  $\nabla\Phi_T(\Gamma_T)$  is given in Eq. (3.29), and  $\boldsymbol{\theta} \sim \text{SUN}_{N,T}(\mathbf{0}_N, I_N, \Delta_T, \mathbf{0}_T, \Gamma_T)$  with its PDF given in Eq. (3.19).

## 4.2 Proof of Theorem 3.1 for the Estimated Ranking

In this section, we first provide an outline of the proof for Theorem 3.1, with the necessary lemmas presented in this or subsequent sections.

Before proceeding further, it is important to note that if  $\Delta_T(ij) = \mathbf{0}_T$ , as indicated by Eq. (3.25), we necessarily have  $\text{Pred}_T(i > j) = \text{Pred}_T(j > i) = 0.5$ . When  $\Delta_T(ij) = \Delta_T(i, :) - \Delta_T(j, :) = \mathbf{0}_T$ , it implies that the comparison outcome of item  $i$  and item  $j$  is identical across the collected  $T$  samples. Consequently, in such instances, we treat them as having the same ranking, as evidenced by  $\text{Pred}_T(i > k) = \text{Pred}_T(j > k)$  for any other item  $k$  where  $k \neq i, j$ . Therefore, in the context of this theorem, we exclusively consider pairs where  $\Delta_T(ij) \neq \mathbf{0}_T$ .

The proof of Theorem 3.1 centers around the distribution of  $\theta_{ij}$ , as introduced in Eq. (3.28). This variable represents a linear transformation of the posterior distribution of  $\boldsymbol{\theta}$ , as described in Eq. (3.19), with  $\theta_{ij} \sim A_{ij}^\top \boldsymbol{\theta}$ . Here is the proof sketch:

1. Leveraging the properties of the SUN distribution outlined in Sec. 2.3.2, it is established that  $\theta_{ij}$  follows a univariate SUN distribution.
2. Considering  $A_{ij}$  as an  $N$ -dimensional vector with the  $i$ -th element being 1, the  $j$ -th element being  $-1$ , and all other elements being 0, we prove that  $\mathbb{E}[\theta_i - \theta_j] = \mathbb{E}[\theta_{ij}]$  in Sec. 4.1.
3. Furthermore, under Condition 3.1, it is demonstrated in Lemma 4.3 and Lemma 4.4 that  $\mathbb{E}[\theta_i - \theta_j]$  exhibits either a strictly positive or strictly negative expectation.
4. Lemma 4.4 shows that when Condition 3.1 is satisfied,  $\mathbb{E}[\theta_i - \theta_j] > 0$  will lead to  $\text{Pred}_T(i > j) > 0.5 > \text{Pred}_T(j > i)$ .
5. Consequently, when Condition 3.1 holds true for all feasible pairs, the sorting of posterior means attains the upper bound of  $C_T(\pi)$  as delineated in Eq. (3.23).
6. Finally, the satisfaction of Condition 3.1 across all pairs ensures that the sorting of posterior means maximizes the expectation of Kendall's  $\tau$  over the posterior distribution.

After providing the proof outline, we then turn to the detailed proof of Theorem 3.1.

*Proof of Theorem 3.1.* Note that

$$\begin{aligned} \mathbb{E}[\theta_i - \theta_j] &\stackrel{(1)}{=} \mathbb{E}[\theta_{ij}] \stackrel{(2)}{=} \int_{\theta_{ij} > 0} \theta_{ij} \times \phi_1(\theta_{ij}; 0, 2) \left( \frac{\Phi_T \left( \frac{\Delta_T(ij)^\top}{2} \theta_{ij}; \Gamma_T - \frac{\Delta_T(ij)^\top \Delta_T(ij)}{2} \right)}{\Phi_T(\mathbf{0}_T; \Gamma_T)} \right. \\ &\quad \left. - \frac{\Phi_T \left( \frac{-\Delta_T(ij)^\top}{2} \theta_{ij}; \Gamma_T - \frac{\Delta_T(ij)^\top \Delta_T(ij)}{2} \right)}{\Phi_T(\mathbf{0}_T; \Gamma_T)} \right) d\theta_{ij}, \end{aligned}$$

where  $\theta_{ij}$  is described in Eq. (3.28), and “(1)” is given in Eq. (4.5) and “(2)” is due to the distribution of  $\theta_{ij}$  given above Eq. (4.1). With Condition 3.1 for a pair  $(i, j)$  with  $i \neq j$  and Lemma 4.3, we observe either  $\mathbb{E}[\theta_i - \theta_j] > 0$  or  $\mathbb{E}[\theta_i - \theta_j] < 0$ , as the integrand is always positive or negative over its interval. Thus,  $\mathbb{E}[\theta_i - \theta_j] \neq 0$  for all  $(i, j)$  pairs.

By Lemma 4.4, if the posterior mean of item  $i$  is larger than that of item  $j$ , then  $\text{Pred}_T(i > j) > 0.5$ . Since  $\text{Pred}_T(i > j) + \text{Pred}_T(j > i) = 1$ , we conclude  $\text{Pred}_T(i > j) > \text{Pred}_T(j > i)$ . Recalling  $\pi_{pos}$  denotes the ranking sorted via the posterior mean, and  $\pi_{pos}(i) > \pi_{pos}(j)$  implies  $\text{Pred}_T(i > j) > 0.5$ . Thus,  $\pi_{pos} \in \arg \max_{\pi} C_T(\pi)$  based on Eq. (3.23), and this fact will end our proof. ■

Now that we have outlined the structure, we will delve into providing comprehensive proofs for the required lemmas. It is noteworthy that certain proofs may rely on references to lemmas introduced in other sections, a point we will explicitly underscore within the proofs.

From the proof in Sec. 4.3, such as Eq. (4.33),  $\Phi(M(\theta_i - \theta_j))$  can be interpreted as a likelihood function within our SUN distribution framework. This interpretation arises from the observation that when a SUN-distributed prior meets such a likelihood, the resulting posterior is also SUN. Therefore, we can view  $M$  as a tuning parameter, representing the probability of observing a new sample where item  $i$  outperforms item  $j$  under such a scalar. Notably, when  $M = \frac{1}{\sqrt{2}}$ , this likelihood function reduces to the TM model as defined in Eq. (3.2).

Given the convergent equation presented in Eq. (4.31), we denote the integration in Eq. (4.30) as:

$$\text{Pred}_T(i > j, M) \equiv \int \Phi(M(\theta_i - \theta_j)) p(\boldsymbol{\theta} | \mathcal{S}_T, \mathcal{Y}_T(\mathcal{S}_T), \mathbf{0}_N, I_N) d\boldsymbol{\theta}, \quad M \in (0, +\infty], \quad (4.6)$$

for the sake of notational consistency. This definition aligns with that of  $\text{Pred}_T(i > j)$  in Eq. (3.22), as Lemma 4.5 establishes

$$\text{Pred}_T(i > j, +\infty) = \text{Pred}_T(i > j). \quad (4.7)$$

With  $\text{Pred}_T(i > j, M)$  defined in Eq. (4.6), we proceed to propose a Lemma asserting that

$\text{Pred}_T(i > j, M)$  can also be expressed as an integration with respect to a univariate random variable.

**Lemma 4.1.** *The quantity  $\text{Pred}_T(i > j, M)$  defined in Eq. (4.6) can be expressed as*

$$\text{Pred}_T(i > j, M) = \int \Phi(M\theta_{ij}) p(\theta_{ij}) d\theta_{ij}, \quad (4.8)$$

where  $\theta_{ij}$  represents a univariate SUN-distributed random variable introduced in Eq. (3.28).

*Proof of Lemma 4.1.* When  $M \in (0, +\infty)$  Recall that  $\boldsymbol{\theta} \sim \text{SUN}_{N,T}(\mathbf{0}_N, I_N, \Delta_T, \mathbf{0}_T, \Gamma_T)$ , as shown in Eq. (3.18), according to Eq. (2.8), the distribution of  $\theta_{ij}$  will be

$$\text{SUN}_{N,1}\left(\mathbf{0}_N + A_{ij}^\top \mathbf{0}_N, A_{ij}^\top I_N A_{ij}, \Delta_{A_{ij}}, \mathbf{0}_T, \Gamma_T\right), \quad (4.9)$$

where

$$\Delta_{A_{ij}} = \text{diag}(A_{ij}^\top I_N A_{ij})^{-\frac{1}{2}} A_{ij}^\top I_N \Delta_T = \frac{\Delta_T(ij)}{\sqrt{2}},$$

with  $\Delta_T(ij)$  defined in Eq. (3.24) and  $A_{ij}$  given in Eq. (3.28). Simplify the expression in Eq. (4.9), we will have

$$\theta_{ij} \sim \text{SUN}_{N,1}\left(\mathbf{0}_N, 2, \frac{\Delta_T(ij)}{\sqrt{2}}, \mathbf{0}_T, \Gamma_T\right). \quad (4.10)$$

Then the integration in Eq. (4.8) can be expressed as

$$\int \Phi(M\theta_{ij}) \phi_1(\theta_{ij}; 0, 2) \frac{\Phi_T\left(\frac{\Delta_T(ij)^\top}{2} \theta_{ij}; \Gamma_T - \frac{\Delta_T(ij)^\top \Delta_T(ij)}{2}\right)}{\Phi_T(\mathbf{0}_T; \Gamma_T)} d\theta_{ij}, \quad (4.11)$$

where  $\phi_1(\theta_{ij}; 0, 2)$  is a univariate normal distribution at  $\theta_{ij}$ , with mean 0 and variance 2. To obtain the corresponding result in the above equation we first note that

$$(4.11) = \int \phi_1(\theta_{ij}; 0, 2) \frac{\Phi_{T+1}\left(\left(\frac{\Delta_T(ij)}{2}, M\right)^\top \theta_{ij}; \begin{pmatrix} \Gamma_T - \frac{\Delta_T(ij)^\top \Delta_T(ij)}{2} & \mathbf{0}_T \\ \mathbf{0}_T^\top & 1 \end{pmatrix}\right)}{\Phi_T(\mathbf{0}_T; \Gamma_T)} d\theta_{ij}. \quad (4.12)$$

Before proceeding, let us revisit the term  $\Delta_T(ij)$ , defined as a  $1 \times T$  matrix in Eq. (3.24). The absolute maximum value of  $\Delta_T(ij)$  can be attained through its  $t$ -th element if item  $i$  outperforms item  $j$  in the  $t$ -th comparison. This maximum value is  $\frac{1}{2} - (-\frac{1}{2}) = 1$ . Moreover, for  $M > 0$ , it follows that  $\frac{M\Delta_T(ij)}{\sqrt{2M^2+1}} = \frac{\Delta_T(ij)}{\sqrt{2+\frac{1}{M^2}}}$ , and each element in  $\frac{\Delta_T(ij)}{\sqrt{2+\frac{1}{M^2}}}$  is less than  $\frac{1}{\sqrt{2}}$ .

Subsequently, we assume a  $(T + 2)$ -dimensional multivariate normal distribution with mean and correlation matrix represented as follows:

$$\begin{pmatrix} \theta_{ij} \\ \tilde{\theta}'_{\text{new}} \end{pmatrix} \sim \mathcal{N}_{T+2} \left( \begin{pmatrix} \mathbf{0} \\ \mathbf{0}_{T+1} \end{pmatrix}, \begin{pmatrix} 1 & \left( \frac{\Delta_T(ij)}{\sqrt{2}}, \frac{\sqrt{2}M}{\sqrt{2M^2+1}} \right) \\ \left( \frac{\Delta_T(ij)}{\sqrt{2}}, \frac{\sqrt{2}M}{\sqrt{2M^2+1}} \right)^T & \begin{pmatrix} \Gamma_T & \frac{M\Delta_T(ij)^T}{\sqrt{2M^2+1}} \\ \frac{M\Delta_T(ij)}{\sqrt{2M^2+1}} & 1 \end{pmatrix} \end{pmatrix} \right),$$

where  $\tilde{\theta}'_{\text{new}}$  is a  $(T + 1)$ -dimensional multivariate normal random vector with its parameters introduced above and the term  $\frac{\sqrt{2}M}{\sqrt{2M^2+1}} = \frac{\sqrt{2}}{\sqrt{2+\frac{1}{M^2}}} < 1$  when  $M \in (0, +\infty)$ .

From the derivation of SUN distribution above Eq. (2.5), we have

$$\sqrt{2}(\theta_{ij} | \tilde{\theta}'_{\text{new}} > 0) \sim \text{SUN}_{1,T+1}(0, 2, \Delta', \mathbf{0}_{T+1}, \Gamma'),$$

where

$$\Delta' = \left( \frac{\Delta_T(ij)}{\sqrt{2}}, \frac{\sqrt{2}M}{\sqrt{2M^2+1}} \right), \text{ and } \Gamma' = \begin{pmatrix} \Gamma_T & \frac{M\Delta_T(ij)^T}{\sqrt{2M^2+1}} \\ \frac{M\Delta_T(ij)}{\sqrt{2M^2+1}} & 1 \end{pmatrix}. \quad (4.13)$$

From Eq. (2.5), the probability density function of  $\sqrt{2}(\theta_{ij} | \tilde{\theta}'_{\text{new}} > 0)$  will be

$$\begin{aligned} & \phi_1(\theta_{ij}; 0, 2) \frac{\Phi_T \left( \frac{1}{\sqrt{2}}(\Delta')^\top \theta_{ij}; \Gamma' - (\Delta')^\top \Delta' \right)}{\Phi_{T+1}(\mathbf{0}_{T+1}; \Gamma')} \\ &= \phi_1(\theta_{ij}; 0, 2) \\ & \times \frac{\Phi_{T+1} \left( \left( \frac{\Delta_T(ij)}{2}, \frac{M}{\sqrt{2M^2+1}} \right)^\top \theta_{ij}; \begin{pmatrix} \Gamma_T & \frac{M\Delta_T(ij)^T}{\sqrt{2M^2+1}} \\ \frac{M\Delta_T(ij)}{\sqrt{2M^2+1}} & 1 \end{pmatrix} - \left( \frac{\Delta_T(ij)^\top}{\sqrt{2}} \right) \left( \frac{\Delta_T(ij)}{\sqrt{2}}, \frac{\sqrt{2}M}{\sqrt{2M^2+1}} \right) \right)}{\Phi_{T+1}(\mathbf{0}_{T+1}; \Gamma')} \\ &= \phi_1(\theta_{ij}; 0, 2) \frac{\Phi_{T+1} \left( \left( \frac{\Delta_T(ij)}{2}, \frac{M}{\sqrt{2M^2+1}} \right)^\top \theta_{ij}; \begin{pmatrix} \Gamma_T - \frac{\Delta_T(ij)^\top \Delta_T(ij)}{2} & \mathbf{0}_T \\ \mathbf{0}_T^\top & \frac{1}{2M^2+1} \end{pmatrix} \right)}{\Phi_{T+1}(\mathbf{0}_{T+1}; \Gamma')} \\ &= \phi_1(\theta_{ij}; 0, 2) \frac{\Phi_{T+1} \left( \left( \frac{\Delta_T(ij)}{2}, M \right)^\top \theta_{ij}; \begin{pmatrix} \Gamma_T - \frac{\Delta_T(ij)^\top \Delta_T(ij)}{2} & \mathbf{0}_T \\ \mathbf{0}_T^\top & 1 \end{pmatrix} \right)}{\Phi_{T+1}(\mathbf{0}_{T+1}; \Gamma')}, \end{aligned}$$

the kernel of which is the same with the kernel in the integration in Eq. (4.12). Then we can have

$$\int \phi_1(\theta_{ij}; 0, 2) \Phi_{T+1} \left( \left( \frac{\Delta_T(ij)}{2}, M \right)^\top \theta_{ij}; \begin{pmatrix} \Gamma_T - \frac{\Delta_T(ij)^\top \Delta_T(ij)}{2} & \mathbf{0}_T \\ \mathbf{0}_T^\top & 1 \end{pmatrix} \right) d\theta_{ij} = \Phi_{T+1}(\mathbf{0}_{T+1}; \Gamma'),$$

where  $\Phi_{T+1}(\mathbf{0}_{T+1}; \Gamma')$  is the normalization constant of  $\text{SUN}_{1,T+1}(0, 2, \Delta', \mathbf{0}_{T+1}, \Gamma')$ . Then we

can have

$$(4.12) = \frac{\Phi_{T+1}(\mathbf{0}_{T+1}; \Gamma')}{\Phi_T(\mathbf{0}_T; \Gamma_T)} = \frac{\Phi_{T+1}\left(\mathbf{0}_{T+1}; \begin{pmatrix} \Gamma_T & \frac{M\Delta_T(ij)^\top}{\sqrt{2M^2+1}} \\ \frac{M\Delta_T(ij)}{\sqrt{2M^2+1}} & 1 \end{pmatrix}\right)}{\Phi_T(\mathbf{0}_T; \Gamma_T)} = (4.11).$$

From Eq. (4.38), we know that

$$\text{Pred}_T(i > j, M) = \frac{\Phi_{T+1}\left(\mathbf{0}_{T+1}; \begin{pmatrix} \Gamma_T & \frac{M\Delta_T(ij)^\top}{\sqrt{2M^2+1}} \\ \frac{M\Delta_T(ij)}{\sqrt{2M^2+1}} & 1 \end{pmatrix}\right)}{\Phi_T(\mathbf{0}_T; \Gamma_T)} = (4.11),$$

which ends our proof for  $M \in (0, +\infty)$ .

For  $M = \infty$ , note that

$$\begin{aligned} \lim_{M \rightarrow +\infty} \text{Pred}_T(i > j, M) &= \lim_{M \rightarrow +\infty} \int \Phi(M\theta_{ij}) p(\theta_{ij}) d\theta_{ij} \\ &\stackrel{(1)}{=} \int \lim_{M \rightarrow +\infty} \Phi(M\theta_{ij}) p(\theta_{ij}) d\theta_{ij} \\ &\stackrel{(2)}{=} \int_{\mathbf{1}_{\{\theta_{ij} > 0\}}} p(\theta_{ij}) d\theta_{ij} = \Pr(\theta_{ij} > 0), \end{aligned}$$

where “(1)” is due to the dominated convergence theorem, and “(2)” is due to the converged function of  $\Phi(M\theta_{ij})$  when  $M \rightarrow \infty$  as depicted below Eq. (4.32). Given the distribution of  $\theta_{ij}$  in Eq. (4.10) and the CDF function of SUN distribution in Eq. (2.6) in Sec. 2.3, we have that

$$\begin{aligned} \text{Pr}(\theta_{ij} > 0) &= 1 - \text{Pr}(\theta_{ij} \leq 0) = 1 - \frac{\Phi_{T+1}\left(\mathbf{0}_{T+1}; \begin{pmatrix} 1 & \frac{-\Delta_T(ij)}{\sqrt{2}} \\ \frac{-\Delta_T(ij)^\top}{\sqrt{2}} & \Gamma_T \end{pmatrix}\right)}{\Phi_T(\mathbf{0}_T; \Gamma_T)} \\ &= \frac{\Phi_{T+1}\left(\mathbf{0}_{T+1}; \begin{pmatrix} 1 & \frac{\Delta_T(ij)}{\sqrt{2}} \\ \frac{\Delta_T(ij)^\top}{\sqrt{2}} & \Gamma_T \end{pmatrix}\right)}{\Phi_T(\mathbf{0}_T; \Gamma_T)} = \text{Pred}_T(i > j), \end{aligned}$$

which ends our proof. ■

Now, we establish Lemma 4.2, which lays the foundation for the condition of loop absence by connecting the posterior mean and  $\text{Pred}_T(i > j)$ . We begin by stating this lemma.

**Lemma 4.2.** *If  $\boldsymbol{\theta}$  follows the posterior distribution as described in Eq. (3.19), and  $\mathbb{E}[\theta_i - \theta_j] > 0$ , then there exists a specific value  $M_0 > 0$  such that  $\text{Pred}_T(i > j, M_0) > 0.5$ , where  $\text{Pred}_T(i > j, M)$  is defined in Eq. (4.6).*

*Proof of Lemma 4.2.* From the definition of  $\text{Pred}_T(i > j, M)$  in Eq. (4.6) and Lemma 4.1,

$\text{Pred}_T(i > j, M)$  will take the form:

$$\begin{aligned}\text{Pred}_T(i > j, M) &= \int \Phi(M(\theta_i - \theta_j)) p(\theta | \mathcal{S}_T, \mathcal{Y}_T(\mathcal{S}_T), \mathbf{0}_N, I_N) d\theta \\ &= \int \Phi(M\theta_{ij}) p(\theta_{ij}) d\theta_{ij} \\ &= \int \Phi(M\theta_{ij}) \phi_1(\theta_{ij}; 0, 2) \frac{\Phi_T\left(\frac{\Delta_T(ij)^\top}{2}\theta_{ij}; \Gamma_T - \frac{\Delta_T(ij)^\top \Delta_T(ij)}{2}\right)}{\Phi_T(\mathbf{0}_T; \Gamma_T)} d\theta_{ij}.\end{aligned}\quad (4.14)$$

Here,  $\theta_{ij}$  is a univariate random variable the distribution of which is described in Eq. (3.28).

Since  $M$  is a tuning parameter, to delve deeper, we take derivatives of  $\text{Pred}_T(i > j, M)$  with respect to  $M$ :

$$\begin{aligned}\frac{d\text{Pred}_T(i > j, M)}{dM} &= \int \theta_{ij} \phi_1(M\theta_{ij}; 0, 1) \phi_1(\theta_{ij}; 0, 2) \\ &\quad \times \frac{\Phi_T\left(\frac{\Delta_T(ij)^\top}{2}\theta_{ij}; \Gamma_T - \frac{\Delta_T(ij)^\top \Delta_T(ij)}{2}\right)}{\Phi_T(\mathbf{0}_T; \Gamma_T)} d\theta_{ij}\end{aligned}\quad (4.15)$$

Note that Eq. (4.15) is proportional to the expectation of a random variable, denoted as  $Y$ , whose probability density function takes the form:

$$\frac{1}{C_Y} \phi_1(MY; 0, 1) \phi_1(Y; 0, 2) \Phi_T\left(\frac{\Delta_T(ij)^\top}{2}Y; \Gamma_T - \frac{\Delta_T(ij)^\top \Delta_T(ij)}{2}\right). \quad (4.16)$$

Here,  $C_Y$  is a normalization constant. The moment generating function of  $Y$  is:

$$\begin{aligned}&\int \frac{1}{C_Y} e^{tY} \phi_1(MY; 0, 1) \phi_1(Y; 0, 2) \Phi_T\left(\frac{\Delta_T(ij)^\top}{2}Y; \Gamma_T - \frac{\Delta_T(ij)^\top \Delta_T(ij)}{2}\right) dY \\ &= \int \frac{1}{C'_Y} e^{tY} e^{\frac{-M^2 Y^2}{2}} e^{\frac{-Y^2}{4}} \Phi_T\left(\frac{\Delta_T(ij)^\top}{2}Y; \Gamma_T - \frac{\Delta_T(ij)^\top \Delta_T(ij)}{2}\right) dY \\ &= \int \frac{1}{C'_Y} e^{-\frac{(2M^2+1)Y^2-4tY}{4}} \Phi_T\left(\frac{\Delta_T(ij)^\top}{2}Y; \Gamma_T - \frac{\Delta_T(ij)^\top \Delta_T(ij)}{2}\right) dY \\ &= \int \frac{1}{C'_Y} e^{\frac{t^2}{2M^2+1}} e^{-\frac{(2M^2+1)(Y-\frac{2t}{2M^2+1})^2}{4}} \Phi_T\left(\frac{\Delta_T(ij)^\top}{2}Y; \Gamma_T - \frac{\Delta_T(ij)^\top \Delta_T(ij)}{2}\right) dY \\ &= \frac{1}{C''_Y} e^{\frac{t^2}{2M^2+1}} \int \phi_1\left(Y; \frac{2t}{2M^2+1}, \frac{2}{2M^2+1}\right) \Phi_T\left(\frac{\Delta_T(ij)^\top}{2}Y; \Gamma_T - \frac{\Delta_T(ij)^\top \Delta_T(ij)}{2}\right) dY,\end{aligned}\quad (4.17)$$

where  $C'_Y$  and  $C''_Y$  are constants that do not affect the results. The integration part in Eq. (4.17),

from Lemma 2.4.1 in Aziz [2011], will be:

$$\begin{aligned}
 & \int \phi_1 \left( Y; \frac{2t}{2M^2+1}, \frac{2}{2M^2+1} \right) \Phi_T \left( \frac{\Delta_T(ij)^\top}{2} Y; \Gamma_T - \frac{\Delta_T(ij)^\top \Delta_T(ij)}{2} \right) dY \\
 &= \Phi_T \left( \frac{\Delta_T(ij)^\top}{2} \cdot \frac{2t}{2M^2+1}; \Gamma_T - \frac{\Delta_T(ij)^\top \Delta_T(ij)}{2} + \frac{\Delta_T(ij)^\top}{2} \frac{2}{2M^2+1} \frac{\Delta_T(ij)}{2} \right) \quad (4.18) \\
 &= \Phi_T \left( \frac{\Delta_T(ij)^\top}{2M^2+1} t; \Gamma_T - \frac{M^2}{2M^2+1} \Delta_T(ij)^\top \Delta_T(ij) \right).
 \end{aligned}$$

So, the moment generating function takes the form:

$$\frac{1}{C_Y''} e^{\frac{t^2}{2M^2+1}} \Phi_T \left( \frac{\Delta_T(ij)^\top}{2M^2+1} t; \Gamma_T - \frac{M^2}{2M^2+1} \Delta_T(ij)^\top \Delta_T(ij) \right). \quad (4.19)$$

Then the cumulant generating function of  $Y$  will be:

$$K_Y(t) = \log C_Y'' + \frac{t^2}{2M^2+1} + \log \Phi_T \left( \frac{\Delta_T(ij)^\top}{2M^2+1} t; \Gamma_T - \frac{M^2}{2M^2+1} \Delta_T(ij)^\top \Delta_T(ij) \right). \quad (4.20)$$

Therefore, the expectation of  $Y$  derived from the cumulant generating function is shown in the next equation:

$$\begin{aligned}
 \frac{dK_Y(t)}{dt} \Big|_{t=0} &= \mathbb{E}[Y] = \frac{1}{\Phi_T \left( \mathbf{0}_T; \Gamma_T - \frac{M^2}{2M^2+1} \Delta_T(ij)^\top \Delta_T(ij) \right)} \\
 &\quad \times \frac{d\Phi_T \left( \frac{\Delta_T(ij)^\top}{2M^2+1} t; \Gamma_T - \frac{M^2}{2M^2+1} \Delta_T(ij)^\top \Delta_T(ij) \right)}{dt} \Big|_{t=0}. \quad (4.21)
 \end{aligned}$$

Note that when  $M = 0$ :

$$\begin{aligned}
 \mathbb{E}[Y] &= \frac{1}{\Phi_T(\mathbf{0}_T; \Gamma_T)} \frac{d\Phi_T(\Delta_T(ij)^\top t; \Gamma_T)}{dt} \Big|_{t=0} \\
 &= \frac{\Delta_T(ij)}{\Phi_T(\mathbf{0}_T; \Gamma_T)} \nabla \Phi_T(\Gamma_T),
 \end{aligned}$$

which is actually the value of  $\mathbb{E}[\theta_i - \theta_j]$  as depicted in Eq.(3.29). As we already know that  $\mathbb{E}[\theta_i - \theta_j]$  is larger than 0, and this fact will lead to:

$$\frac{d\text{Pred}_T(i > j, M)}{dM} \Big|_{M=0} > 0 \quad (4.22)$$

Note that  $\text{Pred}_T(i > j, 0) = 0.5$ , so there exists a certain  $M_0 > 0$ , which will ensure  $\text{Pred}_T(i > j, M_0) > 0.5$ . ■

Now, with Lemma 4.2 established, we proceed to Lemma 4.3, which is derived from the non-symmetric condition in Eq. (3.27).

**Lemma 4.3.** If the non-symmetric condition holds for a pair  $(i, j)$ , then for  $s \in (0, +\infty)$ , either

$$\Phi_T \left( \frac{\Delta_T(ij)^\top}{2} s; \Gamma_T - \frac{\Delta_T(ij)^\top \Delta_T(ij)}{2} \right) < \Phi_T \left( \frac{-\Delta_T(ij)^\top}{2} s; \Gamma_T - \frac{\Delta_T(ij)^\top \Delta_T(ij)}{2} \right), \quad (4.23)$$

or

$$\Phi_T \left( \frac{\Delta_T(ij)^\top}{2} s; \Gamma_T - \frac{\Delta_T(ij)^\top \Delta_T(ij)}{2} \right) > \Phi_T \left( \frac{-\Delta_T(ij)^\top}{2} s; \Gamma_T - \frac{\Delta_T(ij)^\top \Delta_T(ij)}{2} \right). \quad (4.24)$$

*Proof of Lemma 4.3.* Given  $\Delta_T(ij)$ , for notational simplicity, we denote

$$g(s) := \Phi_T \left( \frac{\Delta_T(ij)^\top}{2} s; \Gamma_T - \frac{\Delta_T(ij)^\top \Delta_T(ij)}{2} \right).$$

We can obtain the derivative of  $g(s)$  with respect to  $s$  (for details of  $\frac{dg(s)}{s}$ , please refer to Section 2 in Arellano-Valle and Azzalini [2022]), and based on this fact  $g(s)$  is continuous with respect to  $s$ . We also denote

$$\begin{aligned} f(s) &= \Phi_T \left( \frac{\Delta_T(ij)^\top}{2} s; \Gamma_T - \frac{\Delta_T(ij)^\top \Delta_T(ij)}{2} \right) - \Phi_T \left( \frac{-\Delta_T(ij)^\top}{2} s; \Gamma_T - \frac{\Delta_T(ij)^\top \Delta_T(ij)}{2} \right) \\ &= g(s) - g(-s). \end{aligned}$$

Note that  $f(0) = 0$ , and  $\lim_{s \rightarrow +\infty} f(s) = 0$ . Recall the non-symmetric condition in Eq. (3.27), we will have  $f(s) \neq 0$  when  $s \in (0, +\infty)$  since  $f(s)$  is continuous. In other words we will have either  $f(s) > 0$  or  $f(s) < 0$  when  $s \in (0, +\infty)$ , which corresponds to Eq. (4.23) and Eq. (4.24). ■

In the subsequent part of this section, we delve into the proof of Lemma 4.4. This lemma asserts the equivalence between the ranking provided by  $\text{Pred}_T(i > j)$  and that derived from the posterior mean  $\mathbb{E}[\theta_i - \theta_j]$ , where  $\boldsymbol{\theta}$  follows the distribution described in Eq. (3.18).

**Lemma 4.4.** If  $\boldsymbol{\theta}$  follows the posterior distribution as described in Eq. (3.18), then for any pair  $(i, j)$  that satisfies Condition 3.1, we have  $\text{sign}(\mathbb{E}[\theta_i - \theta_j]) = \text{sign}(\text{Pred}_T(i > j) - 0.5)$ .

*Proof of Lemma 4.4.* If Condition 3.1 is satisfied with  $\mathbb{E}[\theta_i - \theta_j] \neq 0$ , we can only consider the case when  $\mathbb{E}[\theta_i - \theta_j] > 0$  since when  $\mathbb{E}[\theta_i - \theta_j] < 0$  the proof is similar. From 4.1 we know that the expectation  $\mathbb{E}[\theta_i - \theta_j] > 0$  has the same value with the expectation of  $\theta_{ij}$  which is described in Eq. (3.28). With the known PDF of  $\theta_{ij}$ ,  $\mathbb{E}[\theta_i - \theta_j] = \mathbb{E}[\theta_{ij}]$  takes the form of:

$$\begin{aligned} &\int_{\theta_{ij} > 0} \phi_1(\theta_{ij}; 0, 2) \frac{\Phi_T \left( \frac{\Delta_T(ij)^\top}{2} \theta_{ij}; \Gamma_T - \frac{\Delta_T(ij)^\top \Delta_T(ij)}{2} \right)}{\Phi_T(\mathbf{0}_T; \Gamma_T)} \theta_{ij} d\theta_{ij} \\ &+ \int_{\theta_{ij} < 0} \phi_1(\theta_{ij}; 0, 2) \frac{\Phi_T \left( \frac{\Delta_T(ij)^\top}{2} \theta_{ij}; \Gamma_T - \frac{\Delta_T(ij)^\top \Delta_T(ij)}{2} \right)}{\Phi_T(\mathbf{0}_T; \Gamma_T)} \theta_{ij} d\theta_{ij} > 0. \end{aligned} \quad (4.25)$$

Then we will have:

$$\int_{\theta_{ij}>0} \phi_1(\theta_{ij}; 0, 2) \theta_{ij} \left( \frac{\Phi_T \left( \frac{\Delta_T(ij)^\top}{2} \theta_{ij}; \Gamma_T - \frac{\Delta_T(ij)^\top \Delta_T(ij)}{2} \right)}{\Phi_T(\mathbf{0}_T; \Gamma_T)} - \frac{\Phi_T \left( \frac{-\Delta_T(ij)^\top}{2} \theta_{ij}; \Gamma_T - \frac{\Delta_T(ij)^\top \Delta_T(ij)}{2} \right)}{\Phi_T(\mathbf{0}_T; \Gamma_T)} \right) d\theta_{ij} > 0. \quad (4.26)$$

From Lemma 4.3, and given the fact that  $\phi_1(\theta_{ij}; 0, 2) > 0$  when  $\theta_{ij} \in (0, +\infty)$ , we will have

$$\Phi_T \left( \frac{\Delta_T(ij)^\top}{2} \theta_{ij}; \Gamma_T - \frac{\Delta_T(ij)^\top \Delta_T(ij)}{2} \right) > \Phi_T \left( \frac{-\Delta_T(ij)^\top}{2} \theta_{ij}; \Gamma_T - \frac{\Delta_T(ij)^\top \Delta_T(ij)}{2} \right). \quad (4.27)$$

Recall that in Lemma 4.2, since  $\mathbb{E}[\theta_i - \theta_j] > 0$ , we will have  $\frac{d\text{Pred}_T(i > j, M)}{dM} \Big|_{M=0} > 0$ .

For the definition of derivative, we have

$$\frac{\text{Pred}_T(i > j, 0 + M_0) - \text{Pred}_T(i > j, 0)}{M_0} > 0,$$

for  $M_0 \in (0, \delta)$ , where  $(0, \delta)$  denotes a small neighborhood greater than 0 with a fixed tiny value  $\delta$ .

When  $M < M_0$ , since  $\text{Pred}_T(i > j, 0) = 0.5$ , from the definition of derivative mentioned above, for any  $M < M_0$ , we have  $\text{Pred}_T(i > j, M) > \text{Pred}_T(i > j, 0) = 0.5$ .

As for  $M > M_0$ , we can have:

$$\begin{aligned} & \text{Pred}_T(i > j, M) - \text{Pred}_T(i > j, M_0) \\ &= \int \Phi(M(\theta_i - \theta_j)) - \Phi(M_0(\theta_i - \theta_j)) p(\boldsymbol{\theta} | \mathcal{S}_T, \mathcal{Y}_T(\mathcal{S}_T), \mathbf{0}_N, I_N) d\boldsymbol{\theta} \\ &\stackrel{(1)}{=} \int [\Phi(M\theta_{ij}) - \Phi(M_0\theta_{ij})] p(\theta_{ij}) d\theta_{ij} \\ &= \int [(\Phi(M\theta_{ij}) - 0.5) - (\Phi(M_0\theta_{ij}) - 0.5)] p(\theta_{ij}) d\theta_{ij} \\ &= \int_{\theta_{ij}>0} [(\Phi(M\theta_{ij}) - 0.5) - (\Phi(M_0\theta_{ij}) - 0.5)] p(\theta_{ij}) d\theta_{ij} \\ &\quad + \int_{\theta_{ij}<0} [(\Phi(M\theta_{ij}) - 0.5) - (\Phi(M_0\theta_{ij}) - 0.5)] p(\theta_{ij}) d\theta_{ij} \\ &\stackrel{(2)}{=} \int_{\theta_{ij}>0} [(\Phi(M\theta_{ij}) - 0.5) - (\Phi(M_0\theta_{ij}) - 0.5)] p(\theta_{ij}) d\theta_{ij} \\ &\quad - \int_{\theta_{ij}>0} [(\Phi(-M\theta_{ij}) - 0.5) - (\Phi(-M_0\theta_{ij}) - 0.5)] p(-\theta_{ij}) d\theta_{ij}, \end{aligned} \quad (4.28)$$

where “(1)” in Eq. (4.28) is due to Lemma 4.1 with the distribution of  $\theta_{ij}$  also described in this Lemma, and “(2)” in Eq. (4.28) is due to that  $\Phi(M\theta_{ij}) - 0.5$  is an odds function with respect

to  $\theta_{ij}$ . For notational simplicity, we denote

$$f_M(\theta_{ij}) := \Phi(M\theta_{ij}) - 0.5,$$

then we will have

$$\begin{aligned} (4.28) &= \int_{\theta_{ij}>0} f_M(\theta_{ij}) [p(\theta_{ij}) - p(-\theta_{ij})] d\theta_{ij} - \int_{\theta_{ij}>0} f_{M_0}(\theta_{ij}) [p(\theta_{ij}) - p(-\theta_{ij})] d\theta_{ij} \\ &\stackrel{(3)}{=} \int_{\theta_{ij}>0} [f_M(\theta_{ij}) - f_{M_0}(\theta_{ij})] \phi_1(\theta_{ij}; 0, 2) \left( \frac{\Phi_T\left(\frac{\Delta_T(ij)^\top}{2}\theta_{ij}; \Gamma_T - \frac{\Delta_T(ij)^\top\Delta_T(ij)}{2}\right)}{\Phi_T(\mathbf{0}_T; \Gamma_T)} \right. \\ &\quad \left. - \frac{\Phi_T\left(\frac{-\Delta_T(ij)^\top}{2}\theta_{ij}; \Gamma_T - \frac{\Delta_T(ij)^\top\Delta_T(ij)}{2}\right)}{\Phi_T(\mathbf{0}_T; \Gamma_T)} \right) d\theta_{ij} > 0, \end{aligned} \quad (4.29)$$

where “ $>$ ” in the right hand side of equation “(3)” is based on Eq. (4.27) and  $f_M(\theta_{ij}) - f_{M_0}(\theta_{ij}) = \Phi(M\theta_{ij}) - \Phi(M_0\theta_{ij}) > 0$ , for  $\theta_{ij} \in (0, +\infty)$ , which makes elements in the integration in Eq. (4.29) is positive, resulting in  $\text{Pred}_T(i > j, M) - \text{Pred}_T(i > j, M_0) > 0$ . From Lemma 4.5, when  $M > M_0$ , we have that

$$\text{Pred}_T(i > j) = \lim_{M \rightarrow +\infty} \text{Pred}_T(i > j, M) \geq \text{Pred}_T(i > j, M_0) > 0.5,$$

which ends our proof. ■

Finally, we can give the proof of the theorem at the beginning of this section. This theorem ensures the absence of loops, which is always observed in our empirical study.

### 4.3 Proof of Proposition 3.1 for the CDF form of $\text{Pred}_T(i > j)$

In this section, we begin by exploring the expectation of the TM model for item  $i$  being preferred over item  $j$  with a tuning parameter  $M > 0$ . This expectation is computed over the posterior distribution given in Eq. (3.19). The resulting expression is as follows:

$$\int \Phi(M(\theta_i - \theta_j)) p(\boldsymbol{\theta} | \mathcal{S}_T, \mathcal{Y}_T(\mathcal{S}_T), \mathbf{0}_N, I_N) d\boldsymbol{\theta}. \quad (4.30)$$

The following lemma states the relationship between Eq. (4.30), and  $\text{Pred}_T(i > j)$ .

**Lemma 4.5.** *As  $M \rightarrow +\infty$ , the integration in Eq. (4.30) will converge to  $\text{Pred}_T(i > j)$  which is defined in Eq. (3.22), i.e. we have*

$$\lim_{M \rightarrow +\infty} \int \Phi(M(\theta_i - \theta_j)) p(\boldsymbol{\theta} | \mathcal{S}_T, \mathcal{Y}_T(\mathcal{S}_T), \mathbf{0}_N, I_N) d\boldsymbol{\theta} = \text{Pred}_T(i > j). \quad (4.31)$$

*Proof of Lemma 4.5.* According to the dominated convergence theorem and the fact that  $|\Phi(M(\theta_i - \theta_j))| \leq 1$ , we have

$$\begin{aligned}
 & \lim_{M \rightarrow +\infty} \int \Phi(M(\theta_i - \theta_j)) p(\theta | \mathcal{S}_T, \mathcal{Y}_T(\mathcal{S}_T), \mathbf{0}_N, I_N) d\theta \\
 &= \int \lim_{M \rightarrow +\infty} \Phi(M(\theta_i - \theta_j)) p(\theta | \mathcal{S}_T, \mathcal{Y}_T(\mathcal{S}_T), \mathbf{0}_N, I_N) d\theta \\
 &= \mathbb{E} \left[ \lim_{M \rightarrow +\infty} \Phi(M(\theta_i - \theta_j)) | \mathcal{S}_T, \mathcal{Y}_T(\mathcal{S}_T), \mathbf{0}_N, I_N \right] \\
 &\stackrel{(1)}{=} \mathbb{E}[\mathbf{1}_{\{\theta_i - \theta_j > 0\}} | \mathcal{S}_T, \mathcal{Y}_T(\mathcal{S}_T), \mathbf{0}_N, I_N] \\
 &= \Pr(\theta_i > \theta_j | \mathcal{S}_T, \mathcal{Y}_T(\mathcal{S}_T), \mathbf{0}_N, I_N) = \text{Pred}_T(i > j),
 \end{aligned} \tag{4.32}$$

where “(1)” is due to that

$$\lim_{M \rightarrow \infty} \Phi(M(\theta_i - \theta_j)) = \begin{cases} 1 & \text{if } \theta_i - \theta_j > 0, \\ 0.5 & \text{if } \theta_i - \theta_j = 0, \\ 0 & \text{otherwise,} \end{cases}$$

which ends our proof. ■

With the above lemma established, we can prove Proposition 3.1.

*Proof of Proposition 3.1.* Expanding the form of the posterior distribution as shown in Eq. (3.19), the integration in Eq. (4.30) can be represented as:

$$\begin{aligned}
 (4.30) &= \int \Phi(M(\theta_i - \theta_j)) \phi_N(\boldsymbol{\theta}; \mathbf{0}_N, I_N) \frac{\Phi_T(\Delta_T^\top \boldsymbol{\theta}; \Gamma_T - \Delta_T^\top \Delta_T)}{\Phi_T(\mathbf{0}_T; \Gamma_T)} d\boldsymbol{\theta} \\
 &= \int \phi_N(\boldsymbol{\theta}; \mathbf{0}_N, I_N) \frac{\Phi_{T+1}\left(\begin{pmatrix} \Delta_T^\top \boldsymbol{\theta} \\ D_{ij}^\top \boldsymbol{\theta} \end{pmatrix}; \Omega_{\text{new}}\right)}{\Phi_T(\mathbf{0}_T; \Gamma_T)} d\boldsymbol{\theta},
 \end{aligned} \tag{4.33}$$

where  $D_{ij}$  is an  $N$ -dimensional vector with its  $i$ -th element set to  $M$ ,  $j$ -th element set to  $-M$ , and other elements set to 0. Besides,  $\Omega_{\text{new}}$  is given by

$$\Omega_{\text{new}} = \begin{pmatrix} \Gamma_T - \Delta_T^\top \Delta_T & \mathbf{0}_T \\ \mathbf{0}_T^\top & 1 \end{pmatrix}.$$

Recall the derivation of  $\Gamma_T$  and  $\Delta_T$  below Eq. (3.17), we have

$$\Gamma_T - \Delta_T^\top \Delta_T = s_T^{-1} s_T^{-1},$$

with  $s_T$  also defined below Eq. (3.17). Then we have

$$\Phi_{T+1} \left( \begin{pmatrix} \Delta_T^\top \boldsymbol{\theta} \\ D_{ij}^\top \boldsymbol{\theta} \end{pmatrix}; \Omega_{\text{new}} \right) = \Phi_{T+1} \left( \begin{pmatrix} \Delta_T^\top \boldsymbol{\theta} \\ D_{ij}^\top \boldsymbol{\theta} \end{pmatrix}; \begin{pmatrix} s_T^{-1} s_T^{-1} & \mathbf{0}_T \\ \mathbf{0}_T^\top & 1 \end{pmatrix} \right), \quad (4.34)$$

which is a multivariate normal CDF with a diagonal variance-covariance matrix. Given that a univariate normal CDF with mean 0, variance  $b$ , and evaluated at  $a$  satisfies:  $\Phi(a; b) = \Phi(\frac{a}{\sqrt{b}})$ , we will have

$$(4.34) = \Phi_{T+1} \left( \begin{pmatrix} D_T \boldsymbol{\theta} \\ D_{ij}^\top \boldsymbol{\theta} \end{pmatrix}; \begin{pmatrix} I_T & \mathbf{0}_T \\ \mathbf{0}_T^\top & 1 \end{pmatrix} \right) = \Phi_{T+1} \left( (D_{\text{new}}^{\{D_T, (i, j)\}}) \boldsymbol{\theta}; I_{T+1} \right), \quad (4.35)$$

where  $D_{\text{new}}^{\{D_T, (i, j)\}} \in \mathbb{R}^{(T+1) \times N}$ , and the first  $T$  rows of  $D_{\text{new}}^{\{D_T, (i, j)\}}$  is  $D_T$ , with the  $(T+1)$ -th row of  $D_{\text{new}}^{\{D_T, (i, j)\}}$  being  $D_{ij}^\top$ .

Imitating the derivation of SUN distribution in Eq. (3.18), we denote,

$$\tilde{\boldsymbol{\theta}}_{\text{new}} = D_{\text{new}}^{\{D_T, (i, j)\}} \boldsymbol{\theta} + \varepsilon_{\text{new}}, \text{ where } \varepsilon_{\text{new}} \sim \mathcal{N}_{T+1}(\mathbf{0}_{T+1}, I_{T+1}) \text{ is independent of } \boldsymbol{\theta}.$$

Then we have

$$\Pr(\tilde{\boldsymbol{\theta}}_{\text{new}} > 0 | \boldsymbol{\theta}) = \Pr(\varepsilon_{\text{new}} > -D_{\text{new}}^{\{D_T, (i, j)\}} \boldsymbol{\theta} | \boldsymbol{\theta}) = \prod_{t=1}^{T+1} \Phi \left( D_{\text{new}}^{\{D_T, (i, j)\}}(t, :) \boldsymbol{\theta} \right) = (4.35)$$

where  $D_{\text{new}}^{\{D_T, (i, j)\}}(t, :)$  is the  $t$ -th row of  $D_{\text{new}}^{\{D_T, (i, j)\}}$ .

Equipped with the above equation we can also have

$$\begin{aligned} p(\boldsymbol{\theta} | \tilde{\boldsymbol{\theta}}_{\text{new}} > 0) &\propto \Pr(\tilde{\boldsymbol{\theta}}_{\text{new}} > 0 | \boldsymbol{\theta}) p(\boldsymbol{\theta}) = \prod_{t=1}^{T+1} \Phi \left( D_{\text{new}}^{\{D_T, (i, j)\}}(t, :) \boldsymbol{\theta} \right) \phi_N(\boldsymbol{\theta}; \mathbf{0}_N, I_N) \\ &= \Phi_{T+1} \left( (D_{\text{new}}^{\{D_T, (i, j)\}}) \boldsymbol{\theta}; I_{T+1} \right) \phi_N(\boldsymbol{\theta}; \mathbf{0}_N, I_N) \\ &\stackrel{(1)}{=} \Phi_{T+1} \left( \begin{pmatrix} \Delta_T^\top \boldsymbol{\theta} \\ D_{ij}^\top \boldsymbol{\theta} \end{pmatrix}; \begin{pmatrix} s_T^{-1} s_T^{-1} & \mathbf{0}_T \\ \mathbf{0}_T^\top & 1 \end{pmatrix} \right) \phi_N(\boldsymbol{\theta}; \mathbf{0}_N, I_N) \\ &\stackrel{(2)}{=} \Phi_{T+1} \left( \begin{pmatrix} D_T \boldsymbol{\theta} \\ D_{ij}^\top \boldsymbol{\theta} \end{pmatrix}; \Omega_{\text{new}} \right) \phi_N(\boldsymbol{\theta}; \mathbf{0}_N, I_N) \\ &\stackrel{(3)}{=} \Phi(M(\theta_i - \theta_j)) \phi_N(\boldsymbol{\theta}; \mathbf{0}_N, I_N) \Phi_T(\Delta_T^\top \boldsymbol{\theta}; \Gamma_T - \Delta_T^\top \Delta_T), \end{aligned} \quad (4.36)$$

which is the kernel of the integration in Eq. (4.33). In Eq. (4.36), “(1)” is a consequence of Eq. (4.35) and Eq. (4.34), “(2)” arises from Eq. (4.34), and “(3)” is a result of Eq. (4.33).

Recalling that

$$\tilde{\boldsymbol{\theta}}_{\text{new}} = D_{\text{new}}^{\{D_T, (i, j)\}} \boldsymbol{\theta} + \varepsilon_{\text{new}},$$

we firstly have the  $(N + T + 1)$ -dimensional multivariate normal distribution of  $\begin{pmatrix} \boldsymbol{\theta} \\ \tilde{\boldsymbol{\theta}}_{\text{new}} \end{pmatrix}$  with mean and correlation matrix represented below:

$$\begin{pmatrix} \boldsymbol{\theta} \\ \tilde{\boldsymbol{\theta}}_{\text{new}} \end{pmatrix} \sim \mathcal{N}_{N+T+1} \left( \begin{pmatrix} \mathbf{0}_N \\ \mathbf{0}_{T+1} \end{pmatrix}, \begin{pmatrix} I_N & \Delta_{\text{new}}^{\{\Delta_T, (i, j)\}} \\ (\Delta_{\text{new}}^{\{\Delta_T, (i, j)\}})^\top & \Gamma_{\text{new}}^{\{\Gamma_T, (i, j)\}} \end{pmatrix} \right), \quad (4.37)$$

parameters of which are defined as following. We first denote

$$s_{\text{new}}^{\{s_T, (i, j)\}} := \begin{pmatrix} s_T & \mathbf{0}_T \\ \mathbf{0}_T^\top & \sqrt{2M^2 + 1} \end{pmatrix},$$

and then we have

$$\begin{aligned} \Delta_{\text{new}}^{\{\Delta_T, (i, j)\}} &= (D_{\text{new}}^{\{D_T, (i, j)\}})^\top (s_{\text{new}}^{\{s_T, (i, j)\}})^{-1} \\ &= (D_T^\top, D_{ij}) \begin{pmatrix} s_T^{-1} & \mathbf{0}_T \\ \mathbf{0}_T^\top & \frac{1}{\sqrt{2M^2 + 1}} \end{pmatrix} \\ &= \left( D_T^\top s_T^{-1}, \frac{D_{ij}}{\sqrt{2M^2 + 1}} \right) \end{aligned}$$

Then  $\Gamma_{\text{new}}^{\{\Gamma_T, (i, j)\}}$  can be represented as:

$$\begin{aligned} \Gamma_{\text{new}}^{\{\Gamma_T, (i, j)\}} &= \begin{pmatrix} s_T^{-1} & \mathbf{0}_T \\ \mathbf{0}_T^\top & \frac{1}{\sqrt{2M^2 + 1}} \end{pmatrix} \left( D_{\text{new}}^{\{D_T, (i, j)\}} \left( D_{\text{new}}^{\{D_T, (i, j)\}} \right)^\top + I_{T+1} \right) \begin{pmatrix} s_T^{-1} & \mathbf{0}_T \\ \mathbf{0}_T^\top & \frac{1}{\sqrt{2M^2 + 1}} \end{pmatrix} \\ &= \begin{pmatrix} s_T^{-1} & \mathbf{0}_T \\ \mathbf{0}_T^\top & \frac{1}{\sqrt{2M^2 + 1}} \end{pmatrix} \left( \begin{pmatrix} D_T \\ D_{ij}^\top \end{pmatrix} \left( D_T^\top, D_{ij} \right) + I_{T+1} \right) \begin{pmatrix} s_T^{-1} & \mathbf{0}_T \\ \mathbf{0}_T^\top & \frac{1}{\sqrt{2M^2 + 1}} \end{pmatrix} \\ &= \begin{pmatrix} s_T^{-1} & \mathbf{0}_T \\ \mathbf{0}_T^\top & \frac{1}{\sqrt{2M^2 + 1}} \end{pmatrix} \begin{pmatrix} D_T D_T^\top + I_T & D_T D_{ij} \\ D_{ij}^\top D_T & D_{ij}^\top D_{ij} + 1 \end{pmatrix} \begin{pmatrix} s_T^{-1} & \mathbf{0}_T \\ \mathbf{0}_T^\top & \frac{1}{\sqrt{2M^2 + 1}} \end{pmatrix} \\ &= \begin{pmatrix} s_T^{-1} (D_T D_T^\top + I_T) s_T^{-1} & \frac{s_T^{-1} D_T D_{ij}}{\sqrt{2M^2 + 1}} \\ \frac{D_{ij}^\top D_T s_T^{-1}}{\sqrt{2M^2 + 1}} & \frac{D_{ij}^\top D_{ij} + 1}{2M^2 + 1} \end{pmatrix} = \begin{pmatrix} \Gamma_T & \frac{M \Delta_T (ij)^\top}{\sqrt{2M^2 + 1}} \\ \frac{M \Delta_T (ij)}{\sqrt{2M^2 + 1}} & 1 \end{pmatrix}, \end{aligned}$$

recalling  $\Gamma_T$  defined below Eq. (3.17) and  $\Delta_T (ij)$  defined in Eq. (3.24). From Lemma 3.1 and the derivation of SUN variable above Eq. (2.5), we have

$$p(\boldsymbol{\theta} | \tilde{\boldsymbol{\theta}}_{\text{new}} > 0) \sim \text{SUN}_{N, T+1} \left( \mathbf{0}_N, I_N, \Delta_{\text{new}}^{\{\Delta_T, (i, j)\}}, \mathbf{0}_{T+1}, \Gamma_{\text{new}}^{\{\Gamma_T, (i, j)\}} \right).$$

From Eq. (4.36), the result of the integration

$$\int \Phi(M(\theta_i - \theta_j)) \phi_N(\boldsymbol{\theta}; \mathbf{0}_N, I_N) \Phi_T(\Delta_T^\top \boldsymbol{\theta}; \Gamma_T - \Delta_T^\top \Delta_T) d\boldsymbol{\theta}$$

corresponds to the normalization constant of  $p(\boldsymbol{\theta} | \tilde{\boldsymbol{\theta}}_{\text{new}} > 0)$ , which is

$$\Phi_{T+1} \left( \mathbf{0}_{T+1}; \Gamma_{\text{new}}^{\{\Gamma_T, (i,j)\}} \right).$$

Then the integration result in Eq. (4.33) will be

$$(4.33) = \frac{\Phi_{T+1} \left( \mathbf{0}_{T+1}; \Gamma_{\text{new}}^{\{\Gamma_T, (i,j)\}} \right)}{\Phi_T (\mathbf{0}_T; \Gamma_T)} = \frac{\Phi_{T+1} \left( \mathbf{0}_{T+1}; \begin{pmatrix} \Gamma_T & \frac{M\Delta_T(i,j)^\top}{\sqrt{2M^2+1}} \\ \frac{M\Delta_T(i,j)}{\sqrt{2M^2+1}} & 1 \end{pmatrix} \right)}{\Phi_T (\mathbf{0}_T; \Gamma_T)}. \quad (4.38)$$

From Plackett [1954], we know that the multivariate normal CDF is continuous with respect to the correlation term in the variance-covariance matrix. Equipped with Lemma 4.5, we will have

$$(4.33) \rightarrow \frac{\Phi_{T+1} \left( \mathbf{0}_{T+1}; \begin{pmatrix} \Gamma_T & \frac{\Delta_T(i,j)^\top}{\sqrt{2}} \\ \frac{\Delta_T(i,j)}{\sqrt{2}} & 1 \end{pmatrix} \right)}{\Phi_T (\mathbf{0}_T; \Gamma_T)} = \text{Pred}_T(i > j) \text{ as } M \rightarrow +\infty,$$

which ends our proof. ■

#### 4.4 Proof of Lemma 3.1 for the Derivation of SUN Distribution

*Proof of Lemma 3.1.* From Eq. (3.14) and  $\tilde{\boldsymbol{\theta}} = D_T \boldsymbol{\theta} + \boldsymbol{\varepsilon}$ , the joint distribution of  $\begin{pmatrix} \boldsymbol{\theta} \\ \tilde{\boldsymbol{\theta}} \end{pmatrix}$  is given by

$$\begin{pmatrix} \boldsymbol{\theta} \\ \tilde{\boldsymbol{\theta}} \end{pmatrix} \sim \mathcal{N}_{N+T} \left( \begin{pmatrix} \mathbf{0}_N \\ \mathbf{0}_T \end{pmatrix}, \begin{pmatrix} I_N & D_T^\top \\ D_T & D_T D_T^\top + I_T \end{pmatrix} \right).$$

According to properties of the multivariate normal distribution, the conditional distribution  $p(\tilde{\boldsymbol{\theta}} | \boldsymbol{\theta})$  takes the form

$$p(\tilde{\boldsymbol{\theta}} | \boldsymbol{\theta}) \sim \mathcal{N}_T(D_T \boldsymbol{\theta}, I_T).$$

Thus,  $\Pr(\tilde{\boldsymbol{\theta}} > 0 | \boldsymbol{\theta})$  is given by

$$\Pr(\tilde{\boldsymbol{\theta}} > 0 | \boldsymbol{\theta}) = \Phi_T(D_T \boldsymbol{\theta}, I_T) = \Phi_T(s_T^{-1} D_T \boldsymbol{\theta}, s_T^{-1}), \quad (4.39)$$

where

$$\begin{aligned} s_T &= \text{diag} \left( (D_T(1,:)) D_T(1,:)^\top + 1)^{\frac{1}{2}}, \dots, (D_T(T,:)) D_T(T,:)^\top + 1)^{\frac{1}{2}} \right) \\ &= \text{diag} \left( (a^2 + 1)^{\frac{1}{2}}, \dots, (a^2 + 1)^{\frac{1}{2}} \right), \end{aligned}$$

with  $D_T(i,:)$  representing the  $i$ -th row of  $D_T$  for  $i = 1, \dots, T$ .

On the other hand, the joint distribution of  $\begin{pmatrix} \theta \\ \tilde{\theta} \end{pmatrix}$ , with the correlation matrix form, is

$$\begin{pmatrix} \theta \\ \tilde{\theta} \end{pmatrix} \sim \mathcal{N}_{N+T} \left( \begin{pmatrix} \mathbf{0}_N \\ \mathbf{0}_T \end{pmatrix}, \begin{pmatrix} I_N & \Delta_T \\ \Delta_T^\top & \Gamma_T \end{pmatrix} \right),$$

where  $\Delta_T = D_T^\top s_T^{-1}$ ,  $\Gamma_T = s_T^{-1}(D_T D_T^\top + I_T)s_T^{-1}$ . In this scenario,

$$p(\tilde{\theta}|\theta) \sim \mathcal{N}_T (\Delta_T^\top \theta, \Gamma_T - \Delta_T^\top \Delta_T) = \mathcal{N}_T (s_T^{-1} D_T \theta, s_T^{-1} s_T^{-1}).$$

Hence, from the above equation, we also obtain

$$\Pr(\tilde{\theta} > 0 | \theta) = \Phi_T (s_T^{-1} D_T \theta, s_T^{-1} s_T^{-1}),$$

which is identical to Eq. (4.39). Since the distribution of  $p(\theta | \tilde{\theta} > 0)$  is given by

$$p(\theta | \tilde{\theta} > 0) \propto \Pr(\tilde{\theta} > 0 | \theta) p(\theta) = \Phi_T (s_T^{-1} D_T \theta, s_T^{-1} s_T^{-1}) p(\theta), \quad (4.40)$$

we conclude the proof. ■

## 4.5 Proof of Theorem 3.2 on Convergence Property

In this section we give the proof of lemma and theorem for the convergence property of our SUN Ranking framework, which shows the completeness of our algorithm. We firstly introduce the following lemma:

**Lemma 4.6.** *If  $(x, y)$  is a joint distribution of a bivariate normal distribution with parameters given by:*

$$\begin{pmatrix} x \\ y \end{pmatrix} \sim \mathcal{N}_2 \left( \begin{pmatrix} \mu_x \\ \mu_y \end{pmatrix}, \begin{pmatrix} \sigma_x^2 & \sigma_{xy} \\ \sigma_{xy} & \sigma_y^2 \end{pmatrix} \right). \quad (4.41)$$

*Then the integration in the following will become:*

$$\int \int \Phi(M(x-y); b) \phi_2 \left( \begin{pmatrix} x \\ y \end{pmatrix}; \begin{pmatrix} \mu_x \\ \mu_y \end{pmatrix}, \begin{pmatrix} \sigma_x^2 & \sigma_{xy} \\ \sigma_{xy} & \sigma_y^2 \end{pmatrix} \right) dx dy = \Phi \left( \frac{M(\mu_x - \mu_y)}{\sqrt{b + M^2(\sigma_x^2 + \sigma_y^2 - 2\sigma_{xy})}} \right) \quad (4.42)$$

*Where  $M$  is a positive real constant,  $\phi_2 \left( \begin{pmatrix} x \\ y \end{pmatrix}; \begin{pmatrix} \mu_x \\ \mu_y \end{pmatrix}, \begin{pmatrix} \sigma_x^2 & \sigma_{xy} \\ \sigma_{xy} & \sigma_y^2 \end{pmatrix} \right)$  is the probability density function of  $(x, y)$ ,  $\Phi(a; b)$  is the CDF of a univariate normal distribution evaluated at  $a$  with mean 0, and variance  $b$ .*

We give the proof of the Lemma 4.6.

*Proof of Lemma 4.6.* From Lemma 2.4.1 in Aziz [2011], Eq. (4.42) will become:

$$\begin{aligned}
 & \Phi \left( M(\mu_x - \mu_y); b + (M, -M) \begin{pmatrix} \sigma_x^2 & \sigma_{xy} \\ \sigma_{xy} & \sigma_y^2 \end{pmatrix} \begin{pmatrix} M \\ -M \end{pmatrix} \right) \\
 &= \Phi \left( M(\mu_x - \mu_y); b + M^2(\sigma_x^2 + \sigma_y^2 - 2\sigma_{xy}) \right) \\
 &= \Phi \left( \frac{M(\mu_x - \mu_y)}{\sqrt{b + M^2(\sigma_x^2 + \sigma_y^2 - 2\sigma_{xy})}} \right),
 \end{aligned} \tag{4.43}$$

which ends our proof. ■

With the above lemma is settled, then we will give the proof of the core theorem in the convergence of our framework.

*Proof of Theorem 3.2.* Before going further, note that from Lemma 4.6, if we have a  $N$ -dimensional multivariate normal distribution

$$\mathbf{x} \sim \mathcal{N}_N(\boldsymbol{\mu}, \Sigma),$$

with

$$\boldsymbol{\mu} = \begin{pmatrix} \mu_1 \\ \mu_2 \\ \vdots \\ \mu_N \end{pmatrix}, \text{ and } \Sigma = \begin{pmatrix} \sigma_{11} & \sigma_{12} & \dots & \sigma_{1N} \\ \sigma_{21} & \sigma_{22} & \dots & \sigma_{2N} \\ \dots & \dots & \dots & \dots \\ \sigma_{N1} & \sigma_{N2} & \dots & \sigma_{NN} \end{pmatrix}.$$

the integration involving only two elements, for example  $\theta_i$  and  $\theta_j$ , will be

$$\int \Phi(M(x_i - x_j)) \phi_N(\mathbf{x}; \boldsymbol{\mu}, \Sigma) d\mathbf{x} = \Phi \left( \frac{M(x_i - x_j)}{\sqrt{M^2(\sigma_{ii}^2 + \sigma_{jj}^2 - 2\sigma_{ij})}} \right). \tag{4.44}$$

The above result is due to that, we first obtain the marginal distribution of  $(x_i, x_j)^\top$ , and then utilize Lemma 4.6.

Now, let's turn to our theorem. From Bernstein-von Mises theorem Van der Vaart [2000], when  $T$  becomes extremely large, the posterior distribution of  $\boldsymbol{\theta}$  will converges to a multivariate normal distribution as shown below:

$$p(\boldsymbol{\theta} | \mathcal{S}_T, \mathcal{Y}_T(\mathcal{S}_T), \mathbf{0}_N, I_N) \xrightarrow{d} \mathcal{N}_N \left( \hat{\boldsymbol{\theta}}_{\text{TM}, T}, \frac{\mathcal{I}(\boldsymbol{\theta}^*)^{-1}}{T} \right), \tag{4.45}$$

where  $\mathcal{I}(\boldsymbol{\theta}^*)$  is the Fisher information matrix Ly et al. [2017] evaluated at the true population parameter value  $\boldsymbol{\theta}^*$ .

On the other hand, based on Lemma 3.2, as  $T$  goes to extremely large, as assumed in our theorem,  $\hat{\theta}_T$  will also converge to a multivariate Gaussian distribution:

$$\hat{\theta}_{\text{TM},T} \xrightarrow{d} \mathcal{N}_N(\theta_{\text{TM}}^*, \Sigma_{\text{TM}}), \quad (4.46)$$

where  $\Sigma_{\text{TM}}$  is the variance-covariance matrix, which will not influence our results. When  $M \in (0, +\infty)$ , the expectation of the prediction probability in (4.6) will be carried out in normal distributions:

$$\begin{aligned} \text{Pred}_T(i > j, M) &= \mathbb{E} [\mathbb{E} [\Phi(M(\theta_i - \theta_j)) | \hat{\theta}_{\text{TM},T}]] , \quad \theta \sim p(\theta | \mathcal{S}_T, \mathcal{Y}_T(\mathcal{S}_T), \mathbf{0}_N, I_N) \\ &\rightarrow \mathbb{E}_{\hat{\theta}_{\text{TM},T}} \left[ \Phi \left( \frac{M(\hat{\theta}_{\text{TM},Ti} - \hat{\theta}_{\text{TM},Tj})}{\sqrt{1 + M^2(\sigma_{T,ii}^2 + \sigma_{T,jj}^2 - 2\sigma_{T,ij})}} \right) \right], \text{ as } T \rightarrow +\infty \\ &\rightarrow \Phi \left( \frac{M(\theta_{\text{TM},i}^* - \theta_{\text{TM},j}^*)}{\sqrt{1 + M^2(\sigma_{T,ii}^2 + \sigma_{T,jj}^2 + \sigma_{ii}^2 + \sigma_{jj}^2 - 2\sigma_{T,ij} - 2\sigma_{ij})}} \right), \text{ as } T \rightarrow +\infty, \end{aligned} \quad (4.47)$$

where  $\hat{\theta}_{\text{TM},Ti}$  and  $\hat{\theta}_{\text{TM},Tj}$  indicate the  $i$ -th and  $j$ -th elements of  $\hat{\theta}_{\text{TM}}$  respectively.  $\sigma_{T,ij}^2$  represents the  $i$ -th row and  $j$ -th column entry of the variance-covariance matrix  $\frac{\mathcal{I}(\theta^*)^{-1}}{T}$ , where  $\sigma_{ij}$  denotes the  $i$ -th row and  $j$ -th column entry of the variance-covariance matrix  $\Sigma$ . Furthermore,  $\theta_{\text{TM},i}^*$  and  $\theta_{\text{TM},j}^*$  denote the  $i$ -th and  $j$ -th element of  $\theta_{\text{TM}}^*$  respectively.

The first equation in Eq. (4.47) is due to the property of conditional expectation.

The first  $\rightarrow$  in Eq. (4.47) is due to that the posterior distribution  $p(\theta | \mathcal{S}_T, \mathcal{Y}_T(\mathcal{S}_T), \mathbf{0}_N, I_N)$  will converge in distribution to a multivariate normal distribution with parameters shown in Eq. (4.45), and since  $\Phi(\cdot)$  is bounded continuous function, from Theorem 1.9 in Shao [2003], the expectation of  $\Phi(\cdot)$  over the posterior distribution will also converges to the expectation of  $\Phi(\cdot)$  over the corresponding multivariate normal distribution. Taking lemma 4.6 and Eq. (4.44) into consideration, will comes the result in the right hand side of the first  $\rightarrow$ .

The derivation of the second  $\rightarrow$  is similar. Note that the distribution of the MLE  $\hat{\theta}_{\text{TM},T}$  will also converge in distribution to a multivariate distribution given in Eq. (4.46), since  $\Phi(\cdot)$  is bounded continuous function from theorem 1.9 in Shao [2003], lemma 4.6 and Eq. (4.44) we will also have the result in the right hand side of the second  $\rightarrow$ .

As for  $M$  approaches  $+\infty$ , from Lemma 4.5 we will have:

$$\text{Pred}_T(i > j) = \lim_{M \rightarrow +\infty} \text{Pred}_T(i > j, M)$$

$$\begin{aligned}
 & \rightarrow \lim_{M \rightarrow +\infty} \Phi \left( \frac{M(\theta_{\text{TM},i}^* - \theta_{\text{TM},j}^*)}{\sqrt{1 + M^2 (\sigma_{T,ii}^2 + \sigma_{T,jj}^2 + \sigma_{ii}^2 + \sigma_{jj}^2 - 2\sigma_{T,ij}^* - 2\sigma_{ij})}} \right), \text{ as } T \rightarrow +\infty \\
 & = \Phi \left( \frac{\theta_{\text{TM},i}^* - \theta_{\text{TM},j}^*}{\sqrt{\sigma_{T,ii}^2 + \sigma_{T,jj}^2 + \sigma_{ii}^2 + \sigma_{jj}^2 - 2\sigma_{T,ij}^* - 2\sigma_{ij}}} \right).
 \end{aligned}$$

Then, when  $T \rightarrow +\infty$ ,  $\text{Pred}_T(i > j) > 0.5$  if and only if  $\theta_{\text{TM},i}^* > \theta_{\text{TM},j}^*$ , and the proposed ranking from Algorithm 2 equals the sorting of the ground-truth score  $\theta^*$ .  $\blacksquare$



## Chapter 5 Conjugate Bayesian Active Online Ranking

### 5.1 Introduction

Although we have successfully established our SUN Ranking algorithm in previous sections, challenges persist. Despite the availability of numerous crowd-sourcing platforms, such as MTurk<sup>①</sup>, data collection can encounter obstacles in practical scenarios. Task requesters often face constraints such as budgetary and time limitations. Traditional methods involving hiring a number of professors to label data are invariably time-consuming and financially burdensome.

Consequently, recent efforts have focused on active sampling methods on crowd-sourcing platforms, many of which are grounded in the Bayesian framework. However, these methods still exhibit certain deficiencies, which we will elucidate in Sec. 5.2. Subsequently, we will introduce our Bayesian Online Ranking framework, i.e., the SUN Active Ranking algorithm (Sec. 5.3 and 5.4), as a solution to these challenges. Finally, we will demonstrate the interesting properties of our SUN Active Ranking algorithm in Sec. 5.5.

### 5.2 Previous Online Ranking Frameworks and Their Defects

In this section, we will introduce previous works in detail.

- **MLE-based method for the TM model:** The work by Pfeiffer et al. [2012] is grounded in MLE. It employs the TM model as the likelihood function and approximates the item scores using MLE. Additionally, Pfeiffer et al. [2012] leverages the asymptotically multivariate normal distribution to select the next pair for comparison. Specifically, it chooses the next pair to maximize the Expected Information Gain (EIG), where this expectation is computed over the asymptotic distribution. The information gain in EIG quantifies the Kullback-Leibler (KL) divergence Kullback and Leibler [1951] between the multivariate normal distribution at a given state and the corresponding asymptotic distribution after sampling the pair.
- **MLE-based method for the BTL model:** Similarly, Li et al. [2018] also employ MLE in their work. They use the BTL model as the likelihood function. Moreover, the posterior distribution is approximated via the asymptotically multivariate normal

---

<sup>①</sup> <https://www.mturk.com/>

distribution. They, too, select the next pair by maximizing the EIG.

- **Moment matching method for the TM model:** Chen et al. [2013] utilizes the TM model for comparison. After sampling, it employs another normal distribution to approximate the posterior distribution via moment matching. Specifically, the normal distribution is adjusted to have the same first and second moments as the target distribution. After moment matching, the normal distribution is treated as the new prior, and this process is iterated throughout. Furthermore, it selects the next pair by maximizing the EIG.
- **Moment matching method for the BTL model:** Chen et al. [2016] utilizes the BTL model for comparison with a Dirichlet distributed prior. It also employs the moment matching method. After sampling one comparison, the posterior, derived from one sample and the prior, is approximated by another Dirichlet distribution through moment matching. This approximation procedure is iterated throughout. Additionally, it selects the next pair by maximizing the expectation of Kendall’s  $\tau$  over the posterior, as detailed in previous sections.
- **Message Passing method:** Mikhailiuk et al. [2021] employs the TM model for comparison. They utilize the message passing method to approximate the posterior distribution, which should be the SUN distribution as demonstrated in our work. Additionally, they select the next pair by maximizing the EIG.
- **Regression-based method:** Xu et al. [2018a] extend the Hodgerank algorithm from a batched method to an online ranking method. They also utilize the TM setting, where the scores of items are assumed to be normally distributed. To transform the framework into conjugation, they employ ridge regression as the goal function and use the density of the normal distribution as the likelihood to achieve conjugation. Furthermore, they select the next pair through the maximization of the EIG.

There are many Bayesian online ranking frameworks, and several examples are mentioned above detailedly, but they still exhibit certain deficiencies. For instance, Pfeiffer et al. [2012] and Li et al. [2018] utilize the asymptotic distribution of the Maximum Likelihood Estimator for active sampling. However, these methods may encounter substantial errors, particularly at the beginning of the sampling process, especially when the sample size is small. Additionally, Mikhailiuk et al. [2021] approximates the posterior using the message-passing method, but the approximation target may deviate from the ground-truth posterior distribution as the method iterates. Xu et al. [2018a] estimate the ranking through ridge regression. However, the

inherent bias in ridge regression introduces estimation errors in item scores. Notably, Chen et al. [2013] introduce the Crowd-BT method under the Bradley-Terry-Luce model, optimizing EIG based on the approximated posterior via moment matching. Furthermore, Chen et al. [2016] extend this approach to optimize the expectation of Kendall’s  $\tau$  correlation coefficient over the approximated posterior distribution via moment matching. However, both of these works employing moment matching methods may suffer from accumulated estimation errors over time due to potential deviations of the target distribution for approximation from the ground-truth posterior as the sample size increases.

In contrast, our framework leverages the known form of the ground-truth posterior, the SUN distribution, generated from the classical TM model with a Gaussian prior. Thanks to the closed-form, our active sampling strategy relies on the ground-truth posterior throughout the entire process, enhancing both theoretical robustness and estimation accuracy. For the approximated version of our approach, we ensure that the target distribution for approximation remains consistent with the ground-truth posterior throughout the entire process, guaranteeing dependable approximation performance.

### 5.3 Bayesian Markov Decision Process

In this section, we will briefly introduce our active online ranking framework, which is originated from Chen et al. [2016] but enjoys known form posterior. In previous sections, we considered the static ranking problem over  $T$  samples, which are provided beforehand. However, such an offline setting ignores the impact of the data collection process, which can affect the effectiveness of collected samples in recovering the true ranking. This issue is particularly pertinent in scenarios involving crowdsourcing, often constrained by a limited budget. In such cases, there is a desire to dynamically collect the most impactful pairs concerning Kendall’s  $\tau$ .

To determine the optimal sampling process, we in this section extend our Bayesian ranking method to the active learning setting. Similar to the batched scenario, we consider  $N$  items to be ranked under the TM model in Eq. (3.2), and the prior remains i.i.d. standard normal. With a sampling budget of at most  $T$  samples, the primary objective of our active learning algorithm is to determine a sequence of sampling pairs  $\mathcal{S}_T$  to maximize the expectation of Kendall’s  $\tau$  over the posterior given  $\mathcal{S}_T$  and  $\mathcal{Y}_T(\mathcal{S}_T)$  (with  $\mathcal{S}_0 = \emptyset$  and  $\mathcal{Y}_0(\mathcal{S}_0) = \emptyset$ ):

$$\max_{\mathcal{S}_T} \mathbb{E}^{\mathcal{S}_T} \left( U(\mathcal{S}_T, \mathcal{Y}_T(\mathcal{S}_T)) \middle| \mathbf{0}_N, I_N \right), \quad (5.1)$$

where  $U(\mathcal{S}_T, \mathcal{Y}_T(\mathcal{S}_T)) := C_T\left(\pi_T^{\{\mathcal{S}_T, \mathcal{Y}_T(\mathcal{S}_T)\}}\right)$  with  $C_T(\cdot)$  defined in Eq. (3.21) and  $\pi_T^{\{\mathcal{S}_T, \mathcal{Y}_T(\mathcal{S}_T)\}} \in \arg \max_{\pi} C_T(\pi)$ , indicating its dependence on  $\mathcal{S}_T$  and  $\mathcal{Y}_T(\mathcal{S}_T)$ .  $\mathbb{E}^{\mathcal{S}_T}$  denotes the expectation over the sample path  $\mathcal{S}_T$  and the corresponding outcomes. Eq. (5.1) was introduced by Chen et al. [Chen et al., 2016], which formulated the objective into a Bayesian Markov Decision Process. Specifically, Eq. (5.1) can be equivalently written as:

$$\max_{\mathcal{S}_T} \mathbb{E}^{\mathcal{S}_T} \left( U(\mathcal{S}_0, \mathcal{Y}_0(\mathcal{S}_0)) + \sum_{t=0}^{T-1} \mathcal{I}(\mathcal{S}_t, \mathcal{Y}_t(\mathcal{S}_t), (i_{t+1}, j_{t+1}, y_{t+1})) \mid \mathbf{0}_N, I_N \right),$$

where  $\mathcal{I}(\mathcal{S}_t, \mathcal{Y}_t(\mathcal{S}_t), (i_{t+1}, j_{t+1}, y_{t+1})) := U(\mathcal{S}_{t+1}, \mathcal{Y}_{t+1}(\mathcal{S}_{t+1})) - U(\mathcal{S}_t, \mathcal{Y}_t(\mathcal{S}_t))$ , and a newly collected sample at stage  $t+1$  is denoted as  $(i_{t+1}, j_{t+1}, y_{t+1})$ , such that  $\mathcal{S}_{t+1} = \mathcal{S}_t \cup \{(i_{t+1}, j_{t+1})\}$  and  $\mathcal{Y}_{t+1}(\mathcal{S}_{t+1}) = \mathcal{Y}_t(\mathcal{S}_t) \cup \{y_{t+1}\}$ . However, directly solving Eq. (5.1) can be intractable since the space of  $\{\mathcal{S}_t, \mathcal{Y}_t(\mathcal{S}_t)\}$  grows exponentially in  $t$ , making the precise resolution challenging through traditional methods like value or policy iteration, as detailed in Chen et al. [2016]. To address this issue, we propose the knowledge gradient (KG) policy in the subsequent section.

## 5.4 Knowledge Gradient Policy and SUN Active Ranking

In this section, we employ the KG policy [Frazier et al., 2008, Powell, 2010] to address the optimization problem defined in Eq. (5.1). It is worth noting that the KG policy within our framework distinguishes itself from Chen et al. [2013, 2016], by consistently utilizing the ground-truth posterior distribution throughout the entire process. This is in contrast to policies in Chen et al. [2013, 2016] that rely on an approximated posterior distribution, potentially leading to significant estimation errors, as illustrated in Example 1.1. These errors hinder the accuracy of the estimated ranking in practice, as demonstrated in experimental evaluation chapter.

Now, let us delve into our procedure. At the  $t$ -th stage, assuming we have gathered  $\mathcal{S}_t$  and their corresponding outcomes  $\mathcal{Y}_t(\mathcal{S}_t)$ , the KG policy within our framework selects the next pair to maximize the expected increment of the expectation of Kendall's  $\tau$  based on the accumulated data and the prior distribution, which can be expressed as:

$$\begin{aligned} (i_{t+1}, j_{t+1})_{KG} &\in \arg \max_{(i,j)} \mathbb{E} [\mathcal{I}(\mathcal{S}_t, \mathcal{Y}_t(\mathcal{S}_t), (i, j, Y_{ij})) \mid \mathcal{S}_t, \mathcal{Y}_t(\mathcal{S}_t), \mathbf{0}_N, I_N] \\ &= \arg \max_{(i,j)} \mathbb{E} \left[ C_{t+1} \left( \pi_{t+1}^{\{\mathcal{S}_t, \mathcal{Y}_t(\mathcal{S}_t), (i, j, Y_{ij})\}} \right) \middle| \mathcal{S}_t, \mathcal{Y}_t(\mathcal{S}_t), \mathbf{0}_N, I_N \right] \\ &\quad - C_t \left( \pi_t^{\{\mathcal{S}_t, \mathcal{Y}_t(\mathcal{S}_t)\}} \right). \end{aligned} \tag{5.2}$$

The second equation in Eq. (5.2) is due to the tower property of conditional expectation.

Expanding the expectation over  $Y_{ij}$  in Eq. (5.2) and given that  $C_t \left( \pi_t^{\{S_t, Y_t(S_t)\}} \right)$  is fixed at  $t$ -th stage with respect to any newly sampled pair  $(i, j)$ , we obtain

$$(i_{t+1}, j_{t+1})_{KG} \in \arg \max_{(i,j)} \left[ \Pr(Y_{ij} = 1 | S_t, Y_t(S_t), \mathbf{0}_N, I_N) C_{t+1} \left( \pi_{t+1}^{\{S_t, Y_t(S_t), (i,j, Y_{ij}=1)\}} \right) + \Pr(Y_{ij} = -1 | S_t, Y_t(S_t), \mathbf{0}_N, I_N) C_{t+1} \left( \pi_{t+1}^{\{S_t, Y_t(S_t), (i,j, Y_{ij}=-1)\}} \right) \right], \quad (5.3)$$

where  $\Pr(Y_{ij} = \pm 1 | S_t, Y_t(S_t), \mathbf{0}_N, I_N)$  represents the probabilities of observing  $Y_{ij} = \pm 1$ , given the current data  $S_t$ ,  $Y_t(S_t)$  and the prior distribution. To implement the KG policy in Eq. (5.3), we need to compute these probabilities. According to Corollary 2 in Durante [2019], we have

$$\Pr(Y_{ij} = \pm 1 | S_t, Y_t(S_t), \mathbf{0}_N, I_N) = \frac{\Phi_{t+1} \left( \mathbf{0}_{t+1}; \Gamma_{t+1}^{\{S_t, Y_t(S_t), (i,j, Y_{ij}=\pm 1)\}} \right)}{\Phi_t \left( \mathbf{0}_t; \Gamma_t^{\{S_t, Y_t(S_t)\}} \right)}. \quad (5.4)$$

Here, the elements within the braces of  $\Gamma_t^{\{\cdot\}}$  or  $\Gamma_{t+1}^{\{\cdot\}}$  represent the collected data from which the variance-covariance matrix  $\Gamma$  is derived, as illustrated below Eq. (3.17). To avoid any ambiguity, we state that  $\Phi_t \left( \mathbf{0}_t; \Gamma_t^{\{S_t, Y_t(S_t)\}} \right) = 1$  when  $t = 0$ . The derivation of Eq. (5.4) is provided in Section 5.6.

It is worth noting that obtaining  $\pi_t^{\{S_t, Y_t(S_t)\}}$  can be computationally expensive due to potential loops. From an alternative perspective, in active sampling, proposing the estimated ranking after each sampling isn't necessary. Thus, utilizing the KG policy on the upper bound of  $C_t(\cdot)$  is advantageous, as a larger upper bound may propose a superior ranking (based on Eq. (3.21)) and alleviate potential computational burden. Moreover, loops never occur in our empirical study, making this approach reasonable. The KG policy on the upper bound will be:

$$(i_{t+1}, j_{t+1})_{KG} \approx \arg \max_{(i,j)} \left[ \Pr(Y_{ij} = 1 | S_t, Y_t(S_t), \mathbf{0}_N, I_N) \max_{\pi} C_{t+1}^{\{S_t, Y_t(S_t), (i,j, Y_{ij}=1)\}} (\pi) + \Pr(Y_{ij} = -1 | S_t, Y_t(S_t), \mathbf{0}_N, I_N) \max_{\pi} C_{t+1}^{\{S_t, Y_t(S_t), (i,j, Y_{ij}=-1)\}} (\pi) \right], \quad (5.5)$$

where  $C_{t+1}^{\{S_t, Y_t(S_t), (i,j, Y_{ij}=\pm 1)\}} (\pi)$  indicates  $C_{t+1}(\pi)$  from Eq. (3.21), with the posterior generated from  $S_t, Y_t(S_t), (i, j, Y_{ij} = \pm 1)$ , under an i.i.d. standard normal prior. The upper bound given in Eq. (3.23) can be easily obtained given the known form of the posterior.

After collecting all the data, we can propose the estimated ranking using Algorithm 2, and our SUN Active Ranking algorithm is summarized in Algorithm 4:

**Algorithm 4** SUN Active Ranking

---

**Input** The budget  $T$  for sampling.  
**Output** Estimated ranking  $\pi_{pos}^{\{\mathcal{S}_T, \mathcal{Y}_T(\mathcal{S}_T)\}}$ .

- 1: Initialize  $\mathcal{S}_0 = \emptyset$  and  $\mathcal{Y}_0(\mathcal{S}_0) = \emptyset$ .
- 2: **for**  $t = 0$  to  $T - 1$  **do**
- 3:   Obtain data  $\mathcal{S}_t \cup \{(i, j)\}$  and  $\mathcal{Y}_t(\mathcal{S}_t) \cup \{Y_{ij} = \pm 1\}$  for all possible pairs  $(i, j)$ .
- 4:   Calculate probabilities using parameters generated from inputted data in Eq. (5.4).
- 5:   Obtain  $\text{Pred}_{t+1}(i > j)$  via Monte Carlo Integration in Algorithm 3.
- 6:   Select  $(i_{t+1}, j_{t+1})$  via KG policy on upper bound in Eq. (5.5).
- 7:   Record outcome  $y_{t+1}$ .
- 8:   Renew data:  $\mathcal{S}_{t+1} = \mathcal{S}_t \cup \{(i_{t+1}, j_{t+1})\}$ ,  $\mathcal{Y}_{t+1}(\mathcal{S}_{t+1}) = \mathcal{Y}_t(\mathcal{S}_t) \cup \{y_{t+1}\}$ .
- 9: **end for**
- 10: Estimate ranking  $\pi_{pos}^{\{\mathcal{S}_T, \mathcal{Y}_T(\mathcal{S}_T)\}}$  using Algorithm 2.

---

## 5.5 Interesting Properties of SUN Active Ranking

In this section, we demonstrate that the KG policy in Eq. (5.3) can be simplified, especially when loops are absent. To illustrate this simplification, we first denote the prediction probability based on the collected data  $\mathcal{S}_t$  and  $\mathcal{Y}_t(\mathcal{S}_t)$  as:

$$\text{Pred}_t^{\{\mathcal{S}_t, \mathcal{Y}_t(\mathcal{S}_t)\}}(i > j) = \int_{\theta_i > \theta_j} p(\boldsymbol{\theta} | \mathcal{S}_t, \mathcal{Y}_t(\mathcal{S}_t), \mathbf{0}_N, I_N) d\boldsymbol{\theta}. \quad (5.6)$$

We then propose the following proposition:

**Proposition 5.1.** *If we have collected  $\mathcal{S}_t$  and  $\mathcal{Y}_t(\mathcal{S}_t)$ , for any two items  $i$  and  $j$  with  $i \neq j$ , the prediction probability  $\text{Pred}_t^{\{\mathcal{S}_t, \mathcal{Y}_t(\mathcal{S}_t)\}}(i > j)$  can be expressed as a form incorporating newly sampled data, for example,  $(i_{t+1}, j_{t+1}, y_{t+1})$ :*

$$\begin{aligned} \text{Pred}_t^{\{\mathcal{S}_t, \mathcal{Y}_t(\mathcal{S}_t)\}}(i > j) &= \Pr(y_{t+1} = 1 | \mathcal{S}_t, \mathcal{Y}_t(\mathcal{S}_t), \mathbf{0}_N, I_N) \text{Pred}_{t+1}^{\{\mathcal{S}_t, \mathcal{Y}_t(\mathcal{S}_t), (i_{t+1}, j_{t+1}, y_{t+1}=1)\}}(i > j) \\ &\quad + \Pr(y_{t+1} = -1 | \mathcal{S}_t, \mathcal{Y}_t(\mathcal{S}_t), \mathbf{0}_N, I_N) \text{Pred}_{t+1}^{\{\mathcal{S}_t, \mathcal{Y}_t(\mathcal{S}_t), (i_{t+1}, j_{t+1}, y_{t+1}=-1)\}}(i > j). \end{aligned} \quad (5.7)$$

The proof of this proposition can be found in Sec. 5.6. From the proposition above, we can deduce the following corollary, the proof of which can be found in Sec. 5.6.

**Corollary 5.1.** *For  $t = 0, 1, \dots, T - 1$ ,  $C_t \left( \pi_t^{\{\mathcal{S}_t, \mathcal{Y}_t(\mathcal{S}_t)\}} \right)$  can be represented as:*

$$C_t \left( \pi_t^{\{S_t, Y_t(S_t)\}} \right) = \sum_{\pi_t^{\{S_t, Y_t(S_t)\}}(i) > \pi_t^{\{S_t, Y_t(S_t)\}}(j)} \frac{\Phi_{t+2} \left( \mathbf{0}_{t+2}; \tilde{\Omega}_{ij}^{\{S_t, Y_t(S_t), (i_{t+1}, j_{t+1}, y_{t+1}=1)\}} \right)}{\Phi_t \left( \mathbf{0}_t; \Gamma_t^{\{S_t, Y_t(S_t)\}} \right)} \\ + \sum_{\pi_t^{\{S_t, Y_t(S_t)\}}(i) > \pi_t^{\{S_t, Y_t(S_t)\}}(j)} \frac{\Phi_{t+2} \left( \mathbf{0}_{t+2}; \tilde{\Omega}_{ij}^{\{S_t, Y_t(S_t), (i_{t+1}, j_{t+1}, y_{t+1}=-1)\}} \right)}{\Phi_t \left( \mathbf{0}_t; \Gamma_t^{\{S_t, Y_t(S_t)\}} \right)}, \quad (5.8)$$

where  $\tilde{\Omega}_{ij}^{\{\cdot\}}$  is the same as in Eq. (3.25) with the corresponding  $\Delta_{t+1}(ij)$  and  $\Gamma_{t+1}$  generated from the collected data in the braces, and  $\Phi_t \left( \mathbf{0}_t; \Gamma_t^{\{S_t, Y_t(S_t)\}} \right)$  is set to 1 when  $t = 0$ .

We denote  $\tilde{\Omega}_{ji}^{\{\cdot\}}$  as having a similar form with  $\tilde{\Omega}_{ij}^{\{\cdot\}}$  with the only difference being the substitution of  $\Delta_{t+1}(ij)$  with  $\Delta_{t+1}(ji)$ . If we denote the Increased CDF as:

$$IC_{(i,j,s)}(S_t, Y_t(S_t), (i_{t+1}, j_{t+1})) = \Phi_{t+2} \left( \mathbf{0}_{t+2}; \tilde{\Omega}_{ij}^{\{S_t, Y_t(S_t), (i_{t+1}, j_{t+1}, y_{t+1}=s)\}} \right) - \Phi_{t+2} \left( \mathbf{0}_{t+2}; \tilde{\Omega}_{ji}^{\{S_t, Y_t(S_t), (i_{t+1}, j_{t+1}, y_{t+1}=s)\}} \right), \quad (5.9)$$

where  $s = \pm 1$ . Then from Eq. (5.8)(5.9), the KG policy can be simplified:

**Corollary 5.2.** *The KG policy in Eq. (5.3) can be simplified as the following equation:*

$$(i, j) = \operatorname{argmax}_{(i_{t+1}, j_{t+1})} \sum_{s=\pm 1} \sum_{\substack{\pi_t^{\{S_t, Y_t(S_t), (i_{t+1}, j_{t+1}, y_{t+1}=s)\}}(i) \\ > \pi_t^{\{S_t, Y_t(S_t), (i_{t+1}, j_{t+1}, y_{t+1}=s)\}}(j) \\ \text{and } \pi_t^{\{S_t, Y_t(S_t)\}}(i) < \pi_t^{\{S_t, Y_t(S_t)\}}(j)}} IC_{(i,j,s)}(S_t, Y_t(S_t), (i_{t+1}, j_{t+1})). \quad (5.10)$$

The proof of the above corollary can be found in Sec. 5.6. Note that Corollary 5.2 does not depend on whether loops are present or absent. Following a new observation, for instance,  $(i_{t+1}, j_{t+1}, y_{t+1})$ , the proposed rank between any pair  $(i, j)$  can either change or remain unchanged (i.e., the sign that is  $\operatorname{sign}(\pi_t^{\{S_t, Y_t(S_t)\}}(i) - \pi_t^{\{S_t, Y_t(S_t)\}}(j))$  can be equal to or unequal to the sign that is  $\operatorname{sign}(\pi_{t+1}^{\{S_t, Y_t(S_t), (i_{t+1}, j_{t+1}, y_{t+1})\}}(i) - \pi_{t+1}^{\{S_t, Y_t(S_t), (i_{t+1}, j_{t+1}, y_{t+1})\}}(j))$ ). As illustrated in Chapter 3, without loops, the estimated ranking is essentially the sorting of the posterior mean. Thus, we only need to consider the changed rank in the sorting of the posterior mean after a new sample as depicted in Eq. (5.10). Empirically, one can substitute Eq. (5.10) for Eq. (5.5) if needed.

## 5.6 Proofs in This Chapter

In this section, we provide a detailed proofs in this chapter. Firstly, we propose the computation details for the transitional probabilities in Eq. (5.4).

We only provide the computation details for  $s = 1$ , as the one for  $s = -1$  is similar. As  $\mathcal{S}_t$  contains collected pairs and  $\mathcal{Y}_t(\mathcal{S}_t)$  records the comparison labels, we rewrite Eq. (5.4) when  $s = 1$

$$\begin{aligned}\Pr(Y_{i_{t+1}j_{t+1}} = 1 | \mathcal{S}_t, \mathcal{Y}_t(\mathcal{S}_t), \mathbf{0}_N, I_N) &= \Pr(y_{t+1} = 1 | \mathcal{S}_t, \mathcal{Y}_t(\mathcal{S}_t), (i_{t+1}, j_{t+1}), \mathbf{0}_N, I_N) \\ &= \Pr(y_{t+1} = 1 | X_t, Y_t, x_{t+1}, \mathbf{0}_N, I_N),\end{aligned}\quad (5.11)$$

where  $Y_t = (y_1, \dots, y_t)^\top$  denotes the label vector and  $X_t \in \mathbb{R}^{t \times N}$  represents the pairwise comparison matrix for  $\mathcal{S}_t$ , such that for each sample  $(i_k, j_k)$ , the  $k$ -th row of  $X_t$  has  $X_t(k, l) = \frac{1}{\sqrt{2}}$  if  $l = i_k$ ,  $= -\frac{1}{\sqrt{2}}$  if  $l = j_k$ , and  $= 0$  otherwise.  $x_{t+1}$  is a  $N$ -dimensional vector with its  $i_{t+1}$ -th element set to  $\frac{1}{\sqrt{2}}$ ,  $j_{t+1}$ -th element set to  $\frac{-1}{\sqrt{2}}$ , and other elements set to 0. According to Eq. (3.2) and the fact that the prior distribution of  $\theta$  is  $\mathcal{N}_N(\mathbf{0}, I_N)$ , we can apply Corollary 2 in Durante [2019] and obtain that

$$\Pr(y_{t+1} = 1 | X_t, Y_t, x_{t+1}, \mathbf{0}_N, I_N) = \frac{\Phi_{t+1}(\mathbf{0}_{t+1}; \Gamma_{t+1})}{\Phi_t(\mathbf{0}_t; \Gamma_t)},$$

where  $\Gamma_t := s_t^{-1}(D_t I_N D_t^\top + I_t) s_t^{-1}$ , with  $s_t = [(x_1^\top x_1 + 1)^{1/2}, \dots, (x_t^\top x_t + 1)^{1/2}]$  and  $D_t = \text{diag}(y_t)X_t$  for each  $t$ , which is the same with parameters of SUN distribution derived below Eq. (3.17). We thus obtain Eq. (5.4).

We then turn to Proposition 5.1 in the active learning framework. Note that the KG policy in Eq. (5.3) requires too many prediction probabilities (multivariate normal CDFs) to compute in each iteration, causing a significant computational burden. We aim to alleviate this by simplifying the KG policy. Specifically, the proposition states that if the proposed ranking for a pair remains unchanged after a certain sample, the prediction probability involving this pair will be canceled out in Eq. (5.3). Consequently, we can exclude the unchanged pair from consideration when executing the KG policy in Eq. (5.3) and obtain the simplified version of the KG policy in Eq. (5.5).

*Proof of Proposition 5.1.* From Eq. (3.25), the prediction probability equals:

$$\text{Pred}_{t+1}^{\{\mathcal{S}_t, \mathcal{Y}_t(\mathcal{S}_t), (i_{t+1}, j_{t+1}, y_{t+1})\}}(i > j) = \frac{\Phi_{t+2}\left(\mathbf{0}_{t+2}; \tilde{\Omega}_{ij}^{\{\mathcal{S}_t, \mathcal{Y}_t(\mathcal{S}_t), (i_{t+1}, j_{t+1}, y_{t+1})\}}\right)}{\Phi_{t+1}\left(\mathbf{0}_{t+1}; \Gamma_{t+1}^{\{\mathcal{S}_t, \mathcal{Y}_t(\mathcal{S}_t), (i_{t+1}, j_{t+1}, y_{t+1})\}}\right)}, \quad (5.12)$$

where  $\Gamma_{t+1}^{\{\mathcal{S}_t, \mathcal{Y}_t(\mathcal{S}_t), (i_{t+1}, j_{t+1}, y_{t+1})\}}$  represents the corresponding  $\Gamma_{t+1}$  generated from the collected data, which is actually  $\mathcal{S}_t, \mathcal{Y}_t(\mathcal{S}_t), (i_{t+1}, j_{t+1}, y_{t+1})$ , as shown below Eq. (3.17).  $\tilde{\Omega}_{ij}^{\{\mathcal{S}_t, \mathcal{Y}_t(\mathcal{S}_t), (i_{t+1}, j_{t+1}, y_{t+1})\}}$

is the same with its corresponding one in Eq. (3.25), and it takes the form of:

$$\tilde{\Omega}_{ij}^{\{S_t, Y_t(S_t), (i_{t+1}, j_{t+1}, y_{t+1})\}} = \begin{pmatrix} 1 & \frac{\Delta_{t+1}^{\{S_t, Y_t(S_t), (i_{t+1}, j_{t+1}, y_{t+1})\}}(ij)}{\sqrt{2}} \\ \frac{(\Delta_{t+1}^{\{S_t, Y_t(S_t), (i_{t+1}, j_{t+1}, y_{t+1})\}}(ij))^\top}{\sqrt{2}} & \Gamma_{t+1}^{\{S_t, Y_t(S_t), (i_{t+1}, j_{t+1}, y_{t+1})\}} \end{pmatrix}, \quad (5.13)$$

where  $\Delta_{t+1}^{\{S_t, Y_t(S_t), (i_{t+1}, j_{t+1}, y_{t+1})\}}(ij)$  represents a row vector obtained by subtracting the  $j$ -th row from the  $i$ -th row of  $\Delta_{t+1}^{\{S_t, Y_t(S_t), (i_{t+1}, j_{t+1}, y_{t+1})\}}$ .  $\Delta_{t+1}^{\{S_t, Y_t(S_t), (i_{t+1}, j_{t+1}, y_{t+1})\}}$  corresponds to  $\Delta_{t+1}$ , generated from the collected data  $S_t, Y_t(S_t), (i_{t+1}, j_{t+1}, y_{t+1})$ , as shown below Eq. (3.17).

From Eq. (5.4) and (5.12), the right hand side of Eq. (5.7) is:

$$\begin{aligned} & \sum_{y_{t+1}=\pm 1} \Pr(y_{t+1} | S_t, Y_t(S_t), \mathbf{0}_N, I_N) \text{Pred}_{t+1}^{\{S_t, Y_t(S_t), (i_{t+1}, j_{t+1}, y_{t+1})\}}(i > j) \\ &= \frac{\Phi_{t+1}(\mathbf{0}_{t+1}; \Gamma_{t+1}^{\{S_t, Y_t(S_t), (i_{t+1}, j_{t+1}, y_{t+1}=1)\}})}{\Phi_t(\mathbf{0}_t; \Gamma_t^{\{S_t, Y_t(S_t)\}})} \frac{\Phi_{t+2}(\mathbf{0}_{t+2}; \tilde{\Omega}_{ij}^{\{S_t, Y_t(S_t), (i_{t+1}, j_{t+1}, y_{t+1}=1)\}})}{\Phi_{t+1}(\mathbf{0}_{t+1}; \Gamma_{t+1}^{\{S_t, Y_t(S_t), (i_{t+1}, j_{t+1}, y_{t+1}=1)\}})} \\ &+ \frac{\Phi_{t+1}(\mathbf{0}_{t+1}; \Gamma_{t+1}^{\{S_t, Y_t, (i_{t+1}, j_{t+1}, y_{t+1}=-1)\}})}{\Phi_t(\mathbf{0}_t; \Gamma_t^{\{S_t, Y_t(S_t)\}})} \frac{\Phi_{t+2}(\mathbf{0}_{t+2}; \tilde{\Omega}_{ij}^{\{S_t, Y_t(S_t), (i_{t+1}, j_{t+1}, y_{t+1}=-1)\}})}{\Phi_{t+1}(\mathbf{0}_{t+1}; \Gamma_{t+1}^{\{S_t, Y_t, (i_{t+1}, j_{t+1}, y_{t+1}=-1)\}})} \\ &= \frac{\Phi_{t+2}(\mathbf{0}_{t+2}; \tilde{\Omega}_{ij}^{\{S_t, Y_t(S_t), (i_{t+1}, j_{t+1}, y_{t+1}=1)\}})}{\Phi_t(\mathbf{0}_t; \Gamma_t^{\{S_t, Y_t(S_t)\}})} + \frac{\Phi_{t+2}(\mathbf{0}_{t+2}; \tilde{\Omega}_{ij}^{\{S_t, Y_t(S_t), (i_{t+1}, j_{t+1}, y_{t+1}=-1)\}})}{\Phi_t(\mathbf{0}_t; \Gamma_t^{\{S_t, Y_t(S_t)\}})}. \end{aligned} \quad (5.14)$$

Note that when  $y_{t+1} = 1$ :

$$\Gamma_{t+1}^{\{S_t, Y_t, (i_{t+1}, j_{t+1}, y_{t+1}=1)\}} = \begin{pmatrix} \Gamma_t^{\{S_t, Y_t(S_t)\}} & (\Gamma_1^{\{(i_{t+1}, j_{t+1}, y_{t+1}=1)\}})^\top \\ \Gamma_1^{\{(i_{t+1}, j_{t+1}, y_{t+1}=1)\}} & 1 \end{pmatrix}, \quad (5.15)$$

where  $\Gamma_1^{\{(i_{t+1}, j_{t+1}, y_{t+1}=1)\}}$  represents the corresponding correlation vector (row vector) between the newly observed data  $(i_{t+1}, j_{t+1}, y_{t+1} = 1)$  and the previously collected data  $S_t$  and  $Y_t(S_t)$ , as computed in  $\Gamma_{t+1}$  below Eq. (3.17). On the other hand, when  $y_{t+1} = -1$ , the computation yields:

$$\begin{aligned} \Gamma_{t+1}^{\{S_t, Y_t, (i_{t+1}, j_{t+1}, y_{t+1}=-1)\}} &= \begin{pmatrix} \Gamma_t^{\{S_t, Y_t(S_t)\}} & (\Gamma_1^{\{i_{t+1}, j_{t+1}, y_{t+1}=-1\}})^\top \\ \Gamma_1^{\{i_{t+1}, j_{t+1}, y_{t+1}=-1\}} & 1 \end{pmatrix} \\ &= \begin{pmatrix} \Gamma_t^{\{S_t, Y_t(S_t)\}} & -(\Gamma_1^{\{i_{t+1}, j_{t+1}, y_{t+1}=-1\}})^\top \\ -\Gamma_1^{\{i_{t+1}, j_{t+1}, y_{t+1}=-1\}} & 1 \end{pmatrix}, \end{aligned} \quad (5.16)$$

where  $\Gamma_1^{\{i_{t+1}, j_{t+1}, y_{t+1}=-1\}}$  denotes the corresponding correlation vector (row vector) between

$(i_{t+1}, j_{t+1}, y_{t+1} = -1)$  and the previously collected data  $\mathcal{S}_t, \mathcal{Y}_t(\mathcal{S}_t)$ , as computed in  $\Gamma_{t+1}$  below Eq. (3.17). Then, from Eq. (5.13), (5.15) and (5.16), we will have:

$$\tilde{\Omega}_{ij}^{\{\mathcal{S}_t, \mathcal{Y}_t(\mathcal{S}_t), (i_{t+1}, j_{t+1}, y_{t+1}=1)\}} = \begin{pmatrix} 1 & \frac{\Delta_{t+1}^{\{\mathcal{S}_t, \mathcal{Y}_t(\mathcal{S}_t), (i_{t+1}, j_{t+1}, y_{t+1}=1)\}}(ij)}{\sqrt{2}} \\ \frac{\left(\Delta_{t+1}^{\{\mathcal{S}_t, \mathcal{Y}_t(\mathcal{S}_t), (i_{t+1}, j_{t+1}, y_{t+1}=1)\}}(ij)\right)^T}{\sqrt{2}} & \begin{pmatrix} \Gamma_t^{\{\mathcal{S}_t, \mathcal{Y}_t(\mathcal{S}_t)\}} & \left(\Gamma_1^{\{(i_{t+1}, j_{t+1}, y_{t+1}=1)\}}\right)^T \\ \Gamma_1^{\{(i_{t+1}, j_{t+1}, y_{t+1}=1)\}} & 1 \end{pmatrix} \end{pmatrix}, \quad (5.17)$$

$$\begin{aligned} \tilde{\Omega}_{ij}^{\{\mathcal{S}_t, \mathcal{Y}_t(\mathcal{S}_t), (i_{t+1}, j_{t+1}, y_{t+1}=-1)\}} \\ = \begin{pmatrix} 1 & \frac{\Delta_{t+1}^{\{\mathcal{S}_t, \mathcal{Y}_t(\mathcal{S}_t), (i_{t+1}, j_{t+1}, y_{t+1}=-1)\}}(ij)}{\sqrt{2}} \\ \frac{\left(\Delta_{t+1}^{\{\mathcal{S}_t, \mathcal{Y}_t(\mathcal{S}_t), (i_{t+1}, j_{t+1}, y_{t+1}=-1)\}}(ij)\right)^T}{\sqrt{2}} & \begin{pmatrix} \Gamma_t^{\{\mathcal{S}_t, \mathcal{Y}_t(\mathcal{S}_t)\}} & \left(\Gamma_1^{\{(i_{t+1}, j_{t+1}, y_{t+1}=-1)\}}\right)^T \\ \Gamma_1^{\{(i_{t+1}, j_{t+1}, y_{t+1}=-1)\}} & 1 \end{pmatrix} \end{pmatrix} \\ = \begin{pmatrix} 1 & \frac{\Delta_{t+1}^{\{\mathcal{S}_t, \mathcal{Y}_t(\mathcal{S}_t), (i_{t+1}, j_{t+1}, y_{t+1}=-1)\}}(ij)}{\sqrt{2}} \\ \frac{\left(\Delta_{t+1}^{\{\mathcal{S}_t, \mathcal{Y}_t(\mathcal{S}_t), (i_{t+1}, j_{t+1}, y_{t+1}=-1)\}}(ij)\right)^T}{\sqrt{2}} & \begin{pmatrix} \Gamma_t^{\{\mathcal{S}_t, \mathcal{Y}_t(\mathcal{S}_t)\}} & -\left(\Gamma_1^{\{(i_{t+1}, j_{t+1}, y_{t+1}=1)\}}\right)^T \\ -\Gamma_1^{\{(i_{t+1}, j_{t+1}, y_{t+1}=1)\}} & 1 \end{pmatrix} \end{pmatrix}. \end{aligned} \quad (5.18)$$

We then denote the  $k$ -th element ( $k \in \{1, 2, \dots, t+1\}$ ) of the vector  $\Delta_{t+1}^{\{\mathcal{S}_t, \mathcal{Y}_t(\mathcal{S}_t), (i_{t+1}, j_{t+1}, y_{t+1}=1)\}}(ij)$  as  $\Delta_{t+1}^{\{\mathcal{S}_t, \mathcal{Y}_t(\mathcal{S}_t), (i_{t+1}, j_{t+1}, y_{t+1}=1)\}}(ij)_k$ . From the computation of  $\Delta_T$  below Eq. (3.17) and the definition of  $\Delta_T(ij)$  in Eq. (3.24), one can easily determine that

$$\Delta_{t+1}^{\{\mathcal{S}_t, \mathcal{Y}_t(\mathcal{S}_t), (i_{t+1}, j_{t+1}, y_{t+1}=1)\}}(ij)_{t+1} = -\Delta_{t+1}^{\{\mathcal{S}_t, \mathcal{Y}_t(\mathcal{S}_t), (i_{t+1}, j_{t+1}, y_{t+1}=-1)\}}(ij)_{t+1} \quad (5.19)$$

From Eq. (5.17), (5.18) and (5.19), we have:

$$\begin{aligned} \Phi_{t+2} \left( \mathbf{0}_{t+2}; \tilde{\Omega}_{ij}^{\{\mathcal{S}_t, \mathcal{Y}_t(\mathcal{S}_t), (i_{t+1}, j_{t+1}, y_{t+1}=1)\}} \right) + \Phi_{t+2} \left( \mathbf{0}_{t+2}; \tilde{\Omega}_{ij}^{\{\mathcal{S}_t, \mathcal{Y}_t(\mathcal{S}_t), (i_{t+1}, j_{t+1}, y_{t+1}=-1)\}} \right) \\ = \Phi_{t+1} \left( \mathbf{0}_{t+1}; \tilde{\Omega}_{ij}^{\{\mathcal{S}_t, \mathcal{Y}_t(\mathcal{S}_t)\}} \right), \end{aligned} \quad (5.20)$$

where  $\tilde{\Omega}_{ij}^{\{\mathcal{S}_t, \mathcal{Y}_t(\mathcal{S}_t)\}}$  takes the form of:

$$\tilde{\Omega}_{ij}^{\{\mathcal{S}_t, \mathcal{Y}_t(\mathcal{S}_t)\}} = \begin{pmatrix} 1 & \frac{\Delta_t^{\{\mathcal{S}_t, \mathcal{Y}_t(\mathcal{S}_t)\}}(ij)}{\sqrt{2}} \\ \frac{\left(\Delta_t^{\{\mathcal{S}_t, \mathcal{Y}_t(\mathcal{S}_t)\}}(ij)\right)^T}{\sqrt{2}} & \Gamma_t^{\{\mathcal{S}_t, \mathcal{Y}_t(\mathcal{S}_t)\}} \end{pmatrix}$$

The equation in (5.20) arises from the correlation of the  $(t+2)$ -th row or column in the correlation matrix  $\tilde{\Omega}_{ij}^{\{\mathcal{S}_t, \mathcal{Y}_t(\mathcal{S}_t), (i_{t+1}, j_{t+1}, y_{t+1}=1)\}}$ , exhibiting an opposite sign compared to the corresponding portion in the correlation matrix  $\tilde{\Omega}_{ij}^{\{\mathcal{S}_t, \mathcal{Y}_t(\mathcal{S}_t), (i_{t+1}, j_{t+1}, y_{t+1}=-1)\}}$ .

Then, on the left-hand side of Eq. (5.7), leveraging Eq. (3.25) and (5.20), we obtain:

$$\begin{aligned}
 \text{Pred}_t^{\{\mathcal{S}_t, \mathcal{Y}_t(\mathcal{S}_t)\}}(i > j) &= \frac{\Phi_{t+1}(\mathbf{0}_{t+1}; \tilde{\Omega}_{ij}^{\{\mathcal{S}_t, \mathcal{Y}_t(\mathcal{S}_t)\}})}{\Phi_t(\mathbf{0}_t; \Gamma_t^{\{\mathcal{S}_t, \mathcal{Y}_t(\mathcal{S}_t)\}})} \\
 &= \frac{\Phi_{t+2}(\mathbf{0}_{t+2}; \tilde{\Omega}_{ij}^{\{\mathcal{S}_t, \mathcal{Y}_t(\mathcal{S}_t), (i_{t+1}, j_{t+1}, y_{t+1}=1)\}})}{\Phi_t(\mathbf{0}_t; \Gamma_t^{\{\mathcal{S}_t, \mathcal{Y}_t(\mathcal{S}_t)\}})} + \frac{\Phi_{t+2}(\mathbf{0}_{t+2}; \tilde{\Omega}_{ij}^{\{\mathcal{S}_t, \mathcal{Y}_t(\mathcal{S}_t), (i_{t+1}, j_{t+1}, y_{t+1}=-1)\}})}{\Phi_t(\mathbf{0}_t; \Gamma_t^{\{\mathcal{S}_t, \mathcal{Y}_t(\mathcal{S}_t)\}})},
 \end{aligned} \tag{5.21}$$

which is the same with Eq. (5.14), so the proof is complete.  $\blacksquare$

*Proof of Corollary 5.1.* Starting from Eq. (5.21), we can determine the expression for the prediction probability  $\text{Pred}_t^{\{\mathcal{S}_t, \mathcal{Y}_t(\mathcal{S}_t)\}}(i > j)$  for any pair  $(i, j)$ . Consequently, the summation of prediction probabilities  $C_t(\pi_t^{\{\mathcal{S}_t, \mathcal{Y}_t(\mathcal{S}_t)\}})$  defined in Eq. (3.21) takes the form specified in Eq. (5.8).  $\blacksquare$

*Proof of Corollary 5.2.* From the definition of  $C_{t+1}(\cdot)$  in Eq. (3.21), we have:

$$\begin{aligned}
 C_{t+1}\left(\pi_{t+1}^{\{\mathcal{S}_t, \mathcal{Y}_t(\mathcal{S}_t), (i_{t+1}, j_{t+1}, y_{t+1})\}}\right) &= \\
 \sum_{\substack{\pi_t^{\{\mathcal{S}_t, \mathcal{Y}_t(\mathcal{S}_t), (i_{t+1}, j_{t+1}, y_{t+1})\}}(i) \\ > \pi_t^{\{\mathcal{S}_t, \mathcal{Y}_t(\mathcal{S}_t), (i_{t+1}, j_{t+1}, y_{t+1})\}}(j)}} \text{Pred}_{t+1}^{\{\mathcal{S}_t, \mathcal{Y}_t(\mathcal{S}_t), (i_{t+1}, j_{t+1}, y_{t+1})\}}(i > j).
 \end{aligned} \tag{5.22}$$

Then, from Eq. (5.14) and Eq. (5.22), we will have:

$$\begin{aligned}
 \sum_{s=\pm 1} \Pr(y_{t+1} = s | \mathcal{S}_t, \mathcal{Y}_t(\mathcal{S}_t), \mathbf{0}_N, I_N) C_{t+1}\left(\pi_{t+1}^{\{\mathcal{S}_t, \mathcal{Y}_t(\mathcal{S}_t), (i_{t+1}, j_{t+1}, y_{t+1}=s)\}}\right) \\
 = \sum_{\substack{\pi_t^{\{\mathcal{S}_t, \mathcal{Y}_t(\mathcal{S}_t), (i_{t+1}, j_{t+1}, y_{t+1})\}}(i) \\ > \pi_t^{\{\mathcal{S}_t, \mathcal{Y}_t(\mathcal{S}_t), (i_{t+1}, j_{t+1}, y_{t+1})\}}(j)}} \sum_{s=\pm 1} \frac{\Phi_{t+2}(\mathbf{0}_{t+2}; \tilde{\Omega}_{ij}^{\{\mathcal{S}_t, \mathcal{Y}_t(\mathcal{S}_t), (i_{t+1}, j_{t+1}, y_{t+1}=s)\}})}{\Phi_t(\mathbf{0}_t; \Gamma_t^{\{\mathcal{S}_t, \mathcal{Y}_t(\mathcal{S}_t)\}})}.
 \end{aligned} \tag{5.23}$$

Subtracting Eq. (5.8) from Eq. (5.23) will generate the desired results.  $\blacksquare$

## 5.7 Chapter Summary

In this chapter, we extend our batched version of the SUN Ranking algorithm to its active online counterpart, termed the SUN Active Ranking algorithm. We begin by reviewing previous online ranking frameworks and identifying their limitations. To address these shortcomings, and leveraging the known form of the ground-truth posterior, we introduce our online ranking framework based on the SUN distribution.

Furthermore, we provide a brief overview of the Bayesian Markov Decision Process as presented in Chen et al. [2016], and we select the next pair through the Knowledge Gradient method by maximizing the expectation of Kendall's  $\tau$  over the ground-truth posterior.

Finally, we discuss several interesting properties of the SUN Active Ranking algorithm, based on the inherent properties of the SUN distribution.

# Chapter 6 Approximation by Mean-Field Variational Inference

## 6.1 Introduction

While our SUN Ranking algorithms excel in estimating optimal rankings, as demonstrated in the experimental chapters (Chapter. 7 and Chapter. 8), they are subject to significant computational costs. In this chapter, we first delineate these computational challenges and subsequently propose how to mitigate them in this dissertation, alongside introducing our approximation approach.

The primary computational burden arises from computing multivariate normal CDFs, as demonstrated in Tables 7.1 and 7.2, primarily stemming from Eqs. (3.25), (3.29), and (5.4). The dimensionality of these CDFs escalates with the number of samples, imposing considerable computational overhead, as discussed in Durante [2019]. This challenge is exacerbated in subsequent iterations of the active learning scenario, where computational speed is paramount.

Although Algorithm 3 alleviates the need for direct computation of these CDFs, it introduces a secondary computational challenge by necessitating sampling from high-dimensional multivariate truncated normal distributions. The dimensionality of these distributions corresponds to the number of collected samples, presenting a challenge akin to that encountered in the computation of CDFs, as discussed in Fan et al. [2022].

The third computational challenge lies in the approximation scheme. Chen et al. [2016] employed the moment matching method to approximate a target function. However, in our framework, this method still requires computing the first and second moments of a given SUN distribution, entailing the computational challenge mentioned above (Sampling random numbers from the sophisticated SUN distribution). To address computational hurdles in our framework, we adopt the Mean-field variational inference method [Consonni and Marin, 2007] to approximate the posterior distribution  $(\boldsymbol{\theta}|\mathcal{S}_T, \mathcal{Y}_T(\mathcal{S}_T), \mathbf{0}_N, I_N)$  with a simple multivariate normal distribution. We will demonstrate later that this Mean-field variational inference method not only offers efficiency but also entails a straightforward sorting scheme.

The fourth computational challenge pertains to obtaining the optimal ranking through the maximization of Kendall's  $\tau$ , a known NP-hard problem as discussed in Sec. 3.3. However, this challenge can be readily addressed through the sorting of posterior means, as demonstrated in Theorems 3.1 and 6.1.

This chapter is organized as follows: We first introduce Variational Inference and its

Mean-field version (Sec. 6.2), after which we apply it to our SUN Ranking framework for the batched version (Sec. 6.3) or active online version (Sec. 6.4). Finally, we provide proofs of theorems in this chapter (Sec. 6.5).

## 6.2 Variational Inference and Mean-Field Family

In this section, we provide a brief introduction to Variational Inference (VI) or Variation Bayes (VB) method, which serves as an alternative to Markov Chain Monte Carlo (MCMC) for Bayesian learning [Jordan et al., 1999, Bishop et al., 2006, Blei et al., 2017]. VI approximates the true posterior distribution by a simpler family of distributions through an optimization problem. For consistency in notation, let's denote the prior of  $\theta$  as  $p(\theta)$  and the likelihood as  $p(\mathbf{y}|\theta)$ , where  $\mathbf{y}$  represents the observed data. Then, the posterior of  $\theta$  is given by

$$p(\theta|\mathbf{y}) \propto p(\theta)p(\mathbf{y}|\theta).$$

In contrast to approximation methods like MCMC, VI aims to approximate the posterior distribution  $p(\theta|\mathbf{y})$  via optimization. Specifically, given a family of distributions denoted as  $Q$ , VI seeks to find a distribution in  $Q$  that minimizes the Kullback-Leibler (KL) [Kullback and Leibler, 1951] divergence from  $p(\theta|\mathbf{y})$ , which can be formulated as:

$$\hat{q}(\theta) = \arg \min_{q(\theta) \in Q} \text{KL}(q(\theta) \parallel p(\theta|\mathbf{y})). \quad (6.1)$$

Although solving Eq. (6.1) directly is intractable, minimizing the KL divergence is equivalent to maximizing the Evidence Lower Bound (ELBO) [Blei et al., 2017], given by:

$$\text{ELBO}_{q(\theta)} = \mathbb{E}_{q(\theta)} \left[ \log \frac{p(\mathbf{y}|\theta)p(\theta)}{q(\theta)} \right]. \quad (6.2)$$

Thus, Eq. (6.1) can be reformulated as

$$\hat{q}(\theta) = \arg \max_{q(\theta) \in Q} \text{ELBO}_{q(\theta)},$$

which is typically solved using gradient ascent methods.

In practice, the posterior distribution often exhibits complexity, rendering direct utilization of Eq. (6.2) challenging. To address this, researchers introduce latent variables. Specifically, if we have  $T$  observations  $\mathbf{y}_T = (y_1, \dots, y_T)^\top$  along with corresponding latent variables  $\mathbf{z} = (z_1, \dots, z_T)^\top$ , the goal of VI in Eq. (6.1) becomes:

$$\hat{q}(\theta, \mathbf{z}) = \arg \min_{q(\theta, \mathbf{z}) \in Q} \text{KL}(q(\theta, \mathbf{z}) \parallel p(\theta, \mathbf{z}|\mathbf{y})).$$

By integrating out  $z$  in  $q(\theta, z)$ , we obtain the estimated  $\hat{q}(\theta)$ . Mean-field variational inference (MFVI) is a special case of VI, assuming  $Q$  belongs to the mean-field family, denoted as  $Q_{MF}$ , which takes the form:

$$Q_{MF} = \left\{ q_{MF}(\theta, z) : q_{MF}(\theta, z) = q_{MF}(\theta) \prod_{l=1}^T q_{MF}(z_l) \right\}.$$

This leads to easily obtaining  $\hat{q}(\theta)$  since  $\theta$  and  $z$  are assumed to be independent. With the definition of  $Q_{MF}$ , the goal function of MFVI becomes:

$$\hat{q}_{MF}(\theta, z) = \arg \min_{q(\theta, z) \in Q_{MF}} \text{KL}(q(\theta, z) \| p(\theta, z | \mathbf{y})). \quad (6.3)$$

Solving Eq. (6.3) is equivalent to maximizing the corresponding ELBO, which in the MFVI case will be:

$$\text{ELBO}_{q_{MF}(\theta, z)} = \mathbb{E}_{q_{MF}(\theta, z)} \left[ \log \frac{p(\theta, z, \mathbf{y}_T)}{q_{MF}(\theta, z)} \right]. \quad (6.4)$$

From Blei et al. [2017], we can use the coordinate ascent variational algorithm to maximize  $\text{ELBO}_{q_{MF}(\theta, z)}$ . At the  $s$ -th iteration, for example, we update  $q_{MF}^{(s)}(\theta)$  and  $q_{MF}^{(s)}(z)$  as follows:

$$\begin{aligned} q_{MF}^{(s)}(\theta) &\propto \exp \left[ \mathbb{E}_{q_{MF}^{(s-1)}(z)} \{ \log p(\theta | z, \mathbf{y}_T) \} \right], \\ q_{MF}^{(s)}(z) &\propto \exp \left[ \mathbb{E}_{q_{MF}^{(s)}(\theta)} \{ \log p(z | \theta, \mathbf{y}_T) \} \right], \end{aligned} \quad (6.5)$$

where the superscript  $(s)$  emphasizes the corresponding iteration steps.

Having introduced the general concepts of VI and MFVI, we now focus on applying the MFVI method to SUN Ranking algorithms.

### 6.3 SUN Ranking with Mean-Field Variational Inference

To begin, recalling the matrix form of  $\mathcal{S}_T$  and vector form of  $\mathcal{Y}_T(\mathcal{S}_T)$ , denoted as  $X_T$  and  $\mathbf{y}_T$  respectively, as shown below Eq. (3.16), we utilize them to represent the collected data for simplicity. In another perspective, as discussed in Albert and Chib [1993], the collected  $T$  comparison outcomes from TM model can be modeled as follows:

$$(y_l | \theta) = \begin{cases} 1 & \text{with probability } \Phi(X_T(l, :) \theta), \\ -1 & \text{with probability } \Phi(-X_T(l, :) \theta), \end{cases} \quad \text{for } l = 1, \dots, T, \text{ and } \theta \sim \mathcal{N}_N(\mathbf{0}_N, I_N),$$

with  $X_T(l, :)$  representing the  $l$ -th row of  $X_T$ . Then, the posterior distribution of  $\theta$  will be:

$$p(\theta | \mathbf{y}_T) = p(\theta) \prod_{l=1}^T \Phi(y_l(X_T(l, :) \theta)).$$

We then introduce latent variables  $\mathbf{z} = (z_1, \dots, z_T)^\top$  as in Albert and Chib [1993], where  $(z_l | \boldsymbol{\theta}) \sim \mathcal{N}(X_T(l, :) \boldsymbol{\theta}, 1)$  and each element in  $\mathbf{z}$  are independent. The comparison outcome  $y_l$  therefore is defined by:

$$y_l = \begin{cases} 1 & \text{if } z_l > 0 \\ -1 & \text{otherwise} \end{cases}. \quad (6.6)$$

It is worthwhile to notice that, with the introduced latent variable  $\mathbf{z}$ ,  $\int p(\boldsymbol{\theta}, \mathbf{z} | \mathbf{y}_T) d\mathbf{z}$  is actually our ground-truth posterior, i.e. SUN distribution. We will demonstrate this subsequently. From the definition of  $z_l$ ,  $y_l$  only depends on  $z_l$  and is conditionally independent of  $\boldsymbol{\theta}$ , i.e.,

$$p(y_l | z_l) = p(y_l | z_l, \boldsymbol{\theta}),$$

the probability density of  $p(y_l | z_l)$  can be represented as:

$$p(y_l | z_l, \boldsymbol{\theta}) = \mathbf{1}_{\{y_l=-1\}} \mathbf{1}_{\{z_l \leq 0\}} + \mathbf{1}_{\{y_l=1\}} \mathbf{1}_{\{z_l > 0\}}.$$

Then,

$$\begin{aligned} p(y_l, z_l, \boldsymbol{\theta}) &\propto p(y_l | z_l, \boldsymbol{\theta}) p(z_l | \boldsymbol{\theta}) p(\boldsymbol{\theta}) \\ &= (\mathbf{1}_{\{y_l=-1\}} \mathbf{1}_{\{z_l \leq 0\}} + \mathbf{1}_{\{y_l=1\}} \mathbf{1}_{\{z_l > 0\}}) \\ &\quad \times \phi(z_l; X_T(l, :) \boldsymbol{\theta}, 1) \phi_N(\boldsymbol{\theta}; \mathbf{0}_N, I_N). \end{aligned} \quad (6.7)$$

From the above equation, we obtain:

$$\begin{aligned} p(z_l, \boldsymbol{\theta} | y_l) &= C_{z_l, y_l} (\mathbf{1}_{\{y_l=-1\}} \mathbf{1}_{\{z_l \leq 0\}} + \mathbf{1}_{\{y_l=1\}} \mathbf{1}_{\{z_l > 0\}}) \\ &\quad \times \phi(z_l; X_T(l, :) \boldsymbol{\theta}, 1) \phi_N(\boldsymbol{\theta}; \mathbf{0}_N, I_N), \end{aligned}$$

where  $C_{z_l, y_l}$  is the corresponding normalization constant. Thus, integrating  $z_l$  out, we have:

$$\begin{aligned} p(\boldsymbol{\theta} | y_l) &= \begin{cases} C'_{z_l, y_l=1} \Phi(X_T(l, :) \boldsymbol{\theta}) \phi_N(\boldsymbol{\theta}; \mathbf{0}_N, I_N) & y_l = 1, \\ C'_{z_l, y_l=-1} \Phi(-X_T(l, :) \boldsymbol{\theta}) \phi_N(\boldsymbol{\theta}; \mathbf{0}_N, I_N) & y_l = -1, \end{cases} \\ &= C'_{z_l, y_l} \Phi(y_l X_T(l, :) \boldsymbol{\theta}) \phi_N(\boldsymbol{\theta}; \mathbf{0}_N, I_N), \end{aligned} \quad (6.8)$$

where  $C'_{z_l, y_l=-1}$ ,  $C'_{z_l, y_l=1}$ ,  $C_{z_l, y_l}$  are corresponding normalization constants. From the above expression, it is easy to see that  $p(\boldsymbol{\theta} | y_l)$  is simply the posterior distribution of  $\boldsymbol{\theta}$  with prior  $\mathcal{N}_N(\mathbf{0}_N, I_N)$  and one observation  $\Phi(y_l X_T(l, :) \boldsymbol{\theta})$ . Since  $z_l$  are independent for  $l = 1, \dots, T$ , and so does  $y_l$  (as  $y_l$  only depends on  $z_l$ ), we have:

$$p(\mathbf{z}, \boldsymbol{\theta} | \mathbf{y}_T) = \prod_{l=1}^T C_{z_l, y_l} (\mathbf{1}_{\{y_l=-1\}} \mathbf{1}_{\{z_l \leq 0\}} + \mathbf{1}_{\{y_l=1\}} \mathbf{1}_{\{z_l > 0\}}) \quad (6.9)$$

$$\times \phi(z_l; X_T(l,:) \boldsymbol{\theta}, 1) \phi_N(\boldsymbol{\theta}; \mathbf{0}_N, I_N), \quad (6.10)$$

from which integrating  $\mathbf{z}$  out, we obtain:

$$p(\boldsymbol{\theta} | \mathbf{y}_T) \propto \prod_{l=1}^T \Phi(y_l X_T(l,:) \boldsymbol{\theta}) \phi_N(\boldsymbol{\theta}; \mathbf{0}_N, I_N),$$

which is identical to the SUN posterior in Eq. (3.19).

Now we have demonstrated that,  $p(\boldsymbol{\theta} | \mathbf{y}_T)$  is the target distribution to approximate. We then will demonstrate how the MFVI method is carried out. From the density  $p(\mathbf{z}, \boldsymbol{\theta} | \mathbf{y}_T)$  in Eq. (6.9),  $p(z_l | \boldsymbol{\theta}, \mathbf{y}_T)$  and  $p(\boldsymbol{\theta} | \mathbf{z}, \mathbf{y}_T)$  have the following distributions:

$$(z_l | \boldsymbol{\theta}, \mathbf{y}_T) \sim \text{TN}(X_T(l,:) \boldsymbol{\theta}, 1, \mathbb{D}_{Z_l}), \quad \text{with } l = 1, \dots, T. \quad (6.11)$$

$$(\boldsymbol{\theta} | \mathbf{z}, \mathbf{y}_T) \sim \mathcal{N}_N((I_N + X_T^\top X_T)^{-1} X_T^\top \mathbf{z}, (I_N + X_T^\top X_T)^{-1}).$$

Here,  $\text{TN}(X_T(l,:) \boldsymbol{\theta}, 1, \mathbb{D}_{Z_l})$  represents a univariate truncated normal distribution, with the multivariate case defined in Eq. (3.30). Moreover,  $(z_l | \boldsymbol{\theta}, \mathbf{y}_T)$  follows a density function given by

$$p(z_l | \boldsymbol{\theta}, \mathbf{y}_T) = \frac{1}{B(\mathbb{D}_{Z_l})} \phi(X_T(l,:) \boldsymbol{\theta}, 1), \quad z_l \in \mathbb{D}_{Z_l},$$

where  $B(\mathbb{D}_{Z_l}) = \int_{z_l \in \mathbb{D}_{Z_l}} \phi(z_l; X_T(l,:) \boldsymbol{\theta}, 1) dz_l$ . Here,  $\mathbb{D}_{Z_l} = \{z_l : z_l > 0 \text{ if } y_{T,l} = 1, z_l \leq 0 \text{ if } y_{T,l} = -1\}$ , and  $y_{T,l}$  denotes the  $l$ -th element of  $\mathbf{y}_T$ .

Since the kernel of  $(z_l | \boldsymbol{\theta}, \mathbf{y}_T)$  and  $(\boldsymbol{\theta} | \mathbf{z}, \mathbf{y}_T)$  are normal or multivariate normal distribution, the coordinate ascent variational algorithm in Eq. (6.5) will be simple, for example, at iteration step  $s$

$$\begin{aligned} \log p(\boldsymbol{\theta} | \mathbf{z}, \mathbf{y}_T) &\propto -\frac{1}{2} \left( \boldsymbol{\theta} - (I_N + X_T^\top X_T)^{-1} X_T^\top \mathbf{z}^{(s-1)} \right)^\top (I_N + X_T^\top X_T) \\ &\quad \times \left( \boldsymbol{\theta} - (I_N + X_T^\top X_T)^{-1} X_T^\top \mathbf{z}^{(s-1)} \right), \end{aligned}$$

where taking expectation of  $\log p(\boldsymbol{\theta} | \mathbf{z}, \mathbf{y}_T)$  over  $\mathbf{z}^{(s-1)}$  will be

$$\begin{aligned} \mathbb{E}_{q_{\text{MF}}^{(s-1)}(\mathbf{z})} \log p(\boldsymbol{\theta} | \mathbf{z}, \mathbf{y}_T) &\propto -\frac{1}{2} \left( \boldsymbol{\theta} - (I_N + X_T^\top X_T)^{-1} X_T^\top \mathbb{E}_{q_{\text{MF}}^{(s-1)}(\mathbf{z})}[\mathbf{z}] \right)^\top (I_N + X_T^\top X_T) \\ &\quad \times \left( \boldsymbol{\theta} - (I_N + X_T^\top X_T)^{-1} X_T^\top \mathbb{E}_{q_{\text{MF}}^{(s-1)}(\mathbf{z})}[\mathbf{z}] \right) + C_{\mathbf{z}^{(s-1)}}, \end{aligned}$$

where  $C_{\mathbf{z}^{(s-1)}}$  is a constant that is not related to  $\boldsymbol{\theta}$ . From the above equation we know that

$$\begin{aligned} \exp \left\{ \mathbb{E}_{q_{\text{MF}}^{(s-1)}(\mathbf{z})} \log p(\boldsymbol{\theta} | \mathbf{z}, \mathbf{y}_T) \right\} &\propto \exp \left\{ -\frac{1}{2} \left( \boldsymbol{\theta} - (I_N + X_T^\top X_T)^{-1} X_T^\top \mathbb{E}_{q_{\text{MF}}^{(s-1)}(\mathbf{z})}[\mathbf{z}] \right)^\top (I_N + X_T^\top X_T) \right. \\ &\quad \left. \times \left( \boldsymbol{\theta} - (I_N + X_T^\top X_T)^{-1} X_T^\top \mathbb{E}_{q_{\text{MF}}^{(s-1)}(\mathbf{z})}[\mathbf{z}] \right) + C_{\mathbf{z}^{(s-1)}} \right\}. \end{aligned}$$

Since the kernel of  $\exp \left\{ \mathbb{E}_{q_{\text{MF}}^{(s-1)}(\mathbf{z})} \log p(\boldsymbol{\theta}|\mathbf{z}, \mathbf{y}_T) \right\}$  is multivariate normal, and we have  $q_{\text{MF}}^{(s)}(\boldsymbol{\theta}) \propto \exp \left[ \mathbb{E}_{q_{\text{MF}}^{(s-1)}(\mathbf{z})} \{ \log p(\boldsymbol{\theta}|\mathbf{z}, \mathbf{y}_T) \} \right]$  as shown in Eq. (6.5),  $q_{\text{MF}}^{(s)}(\boldsymbol{\theta})$  then can be updated as

$$q_{\text{MF}}^{(s)}(\boldsymbol{\theta}) \sim \mathcal{N}_N((I_N + X_T^\top X_T)^{-1} X_T^\top \mathbb{E}[\mathbf{z}^{(s-1)}], (I_N + X_T^\top X_T)^{-1}).$$

The updating scheme for  $q_{\text{MF}}^{(s)}(\mathbf{z}) = \prod_{l=1}^T q_{\text{MF}}^{(s)}(z_l)$  is similar to and simpler than the updating scheme of  $q_{\text{MF}}^{(s)}(\boldsymbol{\theta})$ . Taking  $q_{\text{MF}}^{(s)}(z_l)$  for example, at iteration step  $s$ , we have

$$\log(z_l|\boldsymbol{\theta}, \mathbf{y}_T) \propto -\frac{1}{2} (z_l - X_T(l,:) \boldsymbol{\theta})^2, \quad z_l \in \mathbb{D}_{Z_l}.$$

Then,

$$\mathbb{E}_{q_{\text{MF}}^{(s)}(\boldsymbol{\theta})} \log(z_l|\boldsymbol{\theta}, \mathbf{y}_T) \propto -\frac{1}{2} \left( z_l - X_T(l,:) \mathbb{E}_{q_{\text{MF}}^{(s)}(\boldsymbol{\theta})} [\boldsymbol{\theta}] \right)^2 + C_l^{(s)}, \quad z_l \in \mathbb{D}_{Z_l}.$$

Here  $C_l^{(s)}$  is a constant that do not dependent on  $z_l$ . Then we have

$$\exp \left\{ \mathbb{E}_{q_{\text{MF}}^{(s)}(\boldsymbol{\theta})} \log(z_l|\boldsymbol{\theta}, \mathbf{y}_T) \right\} \propto \exp \left\{ -\frac{1}{2} \left( z_l - X_T(l,:) \mathbb{E}_{q_{\text{MF}}^{(s)}(\boldsymbol{\theta})} [\boldsymbol{\theta}] \right)^2 + C_l^{(s)} \right\}, \quad z_l \in \mathbb{D}_{Z_l}.$$

Since the kernel in the above equation is univariate normal distribution, and  $z_l$  has its domain  $\mathbb{D}_{Z_l}$ , from  $q_{\text{MF}}^{(s)}(\mathbf{z}) \propto \exp \left[ \mathbb{E}_{q_{\text{MF}}^{(s)}(\boldsymbol{\theta})} \{ \log p(\mathbf{z}|\boldsymbol{\theta}, \mathbf{y}_T) \} \right]$  in Eq. (6.5), we know that  $z_l$  is still truncated normal distributed with the expression

$$q_{\text{MF}}^{(s)}(z_l) \sim \text{TN}(X_T(l,:) \mathbb{E}_{q_{\text{MF}}^{(s)}(\boldsymbol{\theta})} [\boldsymbol{\theta}], 1, \mathbb{D}_{Z_l}).$$

As for the ELBO defined in Eq. (6.4), assume we have finished the  $s$ -th iteration, then the specific form of ELBO will be [Fasano et al., 2022]:

$$\text{ELBO} \{ q_{\text{MF}}^{(s)}(\boldsymbol{\theta}, \mathbf{z}) \} = -\frac{1}{2} \left( (\bar{\mathbf{z}}^{(s)})^\top X_T V_T V_T^\top X_T^\top \bar{\mathbf{z}}^{(s)} + \sum_{l=1}^T \log \Phi(v_{\bar{\mathbf{z}}^{(s)}, l}) \right), \quad (6.12)$$

where  $v_{\bar{\mathbf{z}}^{(s)}, l}$  is the  $l$ -the element of  $v_{\bar{\mathbf{z}}^{(s)}}$ , with its expression being

$$v_{\bar{\mathbf{z}}^{(s)}} = \text{diag}(\mathbf{y}_T) X_T V_T X_T^\top \bar{\mathbf{z}}^{(s)},$$

and  $\bar{\mathbf{z}}^{(s)}$  is the mean vector of  $q_{\text{MF}}^{(s)}(\mathbf{z})$ , with its expression being

$$q_{\text{MF}}^{(s)}(\mathbf{z}) = \prod_{l=1}^T q_{\text{MF}}^{(s)}(z_l).$$

We summarize the MFVI method for SUN Ranking, and have the following iterative algorithm [Consonni and Marin, 2007]:

**Algorithm 5** Mean-field Variational Inference for SUN

**Input**  $X_T$  and  $y_T$  from  $\mathcal{S}_T, \mathcal{Y}(\mathcal{S}_T)$  as defined below Eq. (3.16).

**Output**  $q_{\text{MF}}(\boldsymbol{\theta}) \sim \mathcal{N}_N(\boldsymbol{\theta}_T^*, V_T)$ .

- 1: Initialize  $\bar{\mathbf{z}}^{(0)} \in \mathbb{R}^T$ ,  $s = 0$ .
- 2: **while** ELBO $\{q_{\text{MF}}^{(s)}(\boldsymbol{\theta}, \mathbf{z})\}$  in Eq. (6.12) is not convergent **do**
- 3:   Let  $s = s + 1$  and  $\bar{\boldsymbol{\theta}}^{(s)} = (I_N + X_T^\top X_T)^{-1} X_T^\top \bar{\mathbf{z}}^{(s-1)}$ .
- 4:   Let the  $l$ -th element of  $\bar{\mathbf{z}}^{(s)}$  being  $\bar{z}_l^{(s)} = X_T(l, :) \bar{\boldsymbol{\theta}}^{(s)} + y_{T,l} \frac{\phi(X_T(l, :) \bar{\boldsymbol{\theta}}^{(s)})}{\Phi(y_{T,l} X_T(l, :) \bar{\boldsymbol{\theta}}^{(s)})}$ , for  $l = 1, \dots, T$ .
- 5: **end while**
- 6: Obtain the converged  $\bar{\boldsymbol{\theta}}^{(s)}$  and denote it as  $\bar{\boldsymbol{\theta}}_T^*$ . Denote  $V_T := (I_N + X_T^\top X_T)^{-1}$ .

With  $\mathcal{N}_N(\boldsymbol{\theta}_T^*, V_T)$  to approximate the ground-truth posterior distribution, we can estimate the ranking based on the approximated objective  $\widehat{C}_T(\pi)$ :

$$\begin{aligned}\widehat{\pi}_T &\in \arg \max_{\pi} \widehat{C}_T(\pi) := \sum_{\pi(i) > \pi(j)} \widehat{\text{Pred}_T(i > j)} \\ &= \int_{\theta_i > \theta_j} \phi_N(\boldsymbol{\theta}; \bar{\boldsymbol{\theta}}_T^*, V_T) d\boldsymbol{\theta}.\end{aligned}\quad (6.13)$$

Indeed, we do not need to calculate  $\widehat{\text{Pred}_T}(i > j)$  to obtain the corresponding ranking. The next theorem shows that the estimated ranking in Eq. (6.13) can be obtained according to the sorting of  $\bar{\boldsymbol{\theta}}_T^*$ .

**Theorem 6.1.** *If  $\boldsymbol{\theta}$  follows a multivariate normal distribution generated from Algorithm 5 with density function  $\phi_N(\boldsymbol{\theta}; \bar{\boldsymbol{\theta}}_T^{(*)}, V_T)$ , then:*

$$\begin{aligned}\Pi_{\bar{\boldsymbol{\theta}}_T^{(*)}} &\triangleq \{\pi \mid \pi \text{ is a ranking with } \pi(i) > \pi(j) \text{ only if } \bar{\boldsymbol{\theta}}_{T,i}^{(*)} \geq \bar{\boldsymbol{\theta}}_{T,j}^{(*)}, \text{ for all } i, j \text{ pairs with } i \neq j\} \\ &= \arg \max_{\pi} \widehat{C}_T(\pi),\end{aligned}\quad (6.14)$$

where  $\bar{\boldsymbol{\theta}}_{T,i}^{(*)}$  and  $\bar{\boldsymbol{\theta}}_{T,j}^{(*)}$  indicate the  $i$ -th and  $j$ -th elements of the mean vector  $\bar{\boldsymbol{\theta}}_T^{(*)}$ .

For the proof of this theorem, please refer to Sec. 6.5. The choice of  $\mathcal{N}_N(\bar{\boldsymbol{\theta}}_T^{(*)}, V_T)$  to approximate the posterior distribution via the MFVI method is motivated by the local convergence property established for  $\bar{\boldsymbol{\theta}}_T^{(*)}$  in Wang and Titterington [2012]. According to Consonni and Marin [2007], with probability 1, as the sample number  $T$  approaches infinity,  $\bar{\boldsymbol{\theta}}_T^{(*)}$  locally converges to the ground-truth score  $\boldsymbol{\theta}$  defined in Eq. (3.1) (i.e.,  $\bar{\boldsymbol{\theta}}_T^{(*)}$  converges to the ground-truth score  $\boldsymbol{\theta}$  whenever the starting value is sufficiently near to it). Furthermore, according to Theorem 6.1, the proposed ranking from Eq. (6.13) will also locally converge to the ground-truth ranking  $\pi^*$ .

From the discussion above, we utilize MFVI to approximate the SUN for two main reasons:

- It can be easily implemented, as depicted in Algorithm 5, and it exhibits a locally convergent property, as shown in Wang and Titterington [2012].
- It offers a simple sorting scheme of the mean of the multivariate normal distribution, as proved in Theorem 6.1.

In summary, our SUN Ranking algorithm employing the MFVI method is outlined below:

---

**Algorithm 6** SUN Ranking Algorithm with Mean-field Variational Inference

**Input**  $X_T$  and  $y_T$  from  $\mathcal{S}_T, \mathcal{Y}(\mathcal{S}_T)$  as defined below Eq. (3.16).

**Output** The proposed estimated ranking  $\widehat{\pi}_T$ .

- 1: Obtain the estimated distribution  $\phi_N \left( \boldsymbol{\theta}; \bar{\boldsymbol{\theta}}_T^{(*)}, (I_N + X_T^\top X_T)^{-1} \right)$  from Algorithm 5.
  - 2: Obtain  $\widehat{\pi}_T$  from the sorting of  $\bar{\boldsymbol{\theta}}_T^{(*)}$ .
- 

## 6.4 SUN Active Ranking with Mean-Field Variational Inference

We can further expedite our active learning framework using the MFVI method. Specifically,  $\phi_N \left( \boldsymbol{\theta}; \bar{\boldsymbol{\theta}}_t^{(*)}, V_t \right)$  represents the approximated distribution for  $p(\boldsymbol{\theta} | \mathcal{S}_t, \mathcal{Y}_t(\mathcal{S}_t), \mathbf{0}_N, I_N)$  through Algorithm 5. We denote the estimated ranking  $\widehat{\pi}_t^{\{\mathcal{S}_t, \mathcal{Y}_t(\mathcal{S}_t)\}}$ , generated from Algorithm 6, emphasizing its dependence on the collected data  $\mathcal{S}_t, \mathcal{Y}_t(\mathcal{S}_t)$ . Additionally,  $\Pr(y_{t+1} = s | \mathcal{S}_t, \mathcal{Y}_t(\mathcal{S}_t), \mathbf{0}_N, I_N)$ , with  $s = \pm 1$ , can also be approximated. We define,

$$\begin{aligned} \hat{\Pr}(y_{t+1} = s | \mathcal{S}_t, \mathcal{Y}_t(\mathcal{S}_t), \mathbf{0}_N, I_N) &:= \int \Phi \left( \frac{s(\theta_i - \theta_j)}{\sqrt{2}} \right) \phi_N \left( \boldsymbol{\theta}; \bar{\boldsymbol{\theta}}_t^{(*)}, V_t \right) d\boldsymbol{\theta} \\ &= \Phi \left( \frac{s(\bar{\theta}_{t,i}^{(*)} - \bar{\theta}_{t,j}^{(*)})}{\sqrt{2 + A_{ij}^\top V_t A_{ij}}} \right), \end{aligned} \quad (6.15)$$

where  $A_{ij}$  is introduced below Eq. (3.28) and  $\bar{\theta}_{t,i}^{(*)}, \bar{\theta}_{t,j}^{(*)}$  denote the  $i$ -th and  $j$ -th elements of  $\bar{\boldsymbol{\theta}}_t^{(*)}$  separately. The integration result in Eq. (6.15) stems from Lemma 2.4.1 in Aziz [2011]. Then, Eq. (5.3) equipped with the MFVI method can be represented as:

$$(i_{t+1}, j_{t+1})_{KG} \approx \sum_{s=\pm 1} \arg \max_{(i,j)} \hat{\Pr}(Y_{ij} = s | \mathcal{S}_t, \mathcal{Y}_t(\mathcal{S}_t), \mathbf{0}_N, I_N) \widehat{C}_{t+1} \left( \widehat{\pi}_{t+1}^{\{\mathcal{S}_t, \mathcal{Y}_t(\mathcal{S}_t), (i,j, Y_{ij}=s)\}} \right). \quad (6.16)$$

Here  $\widehat{C}_{t+1}(\cdot)$  is defined in Eq. (6.13), and  $\widehat{\pi}_{t+1}^{\{\mathcal{S}_t, \mathcal{Y}_t(\mathcal{S}_t), (i,j, Y_{ij}=s)\}}$  is defined above Eq. (6.15).

In summary, the active learning framework employing the MFVI method is outlined

below:

---

**Algorithm 7** SUN Active Ranking with Mean-field Variational Inference

---

**Input** The budget of sampling number  $T$ .

**Output** The estimated ranking  $\widehat{\pi}_T$ .

- 1: **for**  $t = 0$  to  $T - 1$  **do**
  - 2:   Initialize the compared pair set  $\mathcal{S}_0 = \emptyset$  and the outcome set  $\mathcal{Y}_0(\mathcal{S}_0) = \emptyset$ .
  - 3:   Run Algorithm 5 to obtain the estimated multivariate normal distribution with the input  $\mathcal{S}_t \cup \{(i, j)\}$  and  $\mathcal{Y}_t(\mathcal{S}_t) \cup \{Y_{ij}\}$  for each  $(i, j)$  with  $i \neq j$  and  $Y_{ij} = \pm 1$ .
  - 4:   Select  $(i_{t+1}, j_{t+1})$  using Eq. (6.16).
  - 5:   Record the outcome  $y_{t+1}$ .
  - 6:   Renew the collected data with  $\mathcal{S}_{t+1} = \mathcal{S}_t \cup \{(i_{t+1}, j_{t+1})\}$ ,  $\mathcal{Y}_{t+1}(\mathcal{S}_{t+1}) = \mathcal{Y}_t(\mathcal{S}_t) \cup \{y_{t+1}\}$ .
  - 7: **end for**
  - 8: Obtain  $\widehat{\pi}_T$  from Algorithm 6, with the input  $\mathcal{S}_T$  and  $\mathcal{Y}_T(\mathcal{S}_T)$ .
- 

**Remark 6.1.** As an approximation to Algorithm 4, the primary aim of Algorithm 7 is to reduce the computational costs when the sample size is large. Therefore, practically one can integrate Algorithm 4 and Algorithm 7 for implementation. Specifically, during early iterations with small sample numbers, one can employ Algorithm 4; after reaching a large sample size, transitioning to Algorithm 7 can be advantageous to alleviate the computational burden.

## 6.5 Proofs in This Chapter

We will demonstrate proofs of Theorem 6.1 in this section.

*Proof of Theorem 6.1.* If all elements in  $\bar{\theta}_T^{(*)}$  are equal, then any ranking of  $\{1, 2, \dots, N\}$  will reach the upper bound of  $\widehat{C}_T(\pi)$  and Eq. (6.14) is satisfied.

We then assume there exists at least two elements in  $\bar{\theta}_T^{(*)}$  are not equal, and we first demonstrate that elements on the right-hand side of Eq. (6.14) belong to the left-hand side. Suppose a rank  $\hat{\pi}$  maximizes  $\widehat{C}_T(\pi)$ , and assume it does not belong to the left-hand side of Eq. (6.14), i.e., there exist indices  $s$  and  $k$  such that  $\bar{\theta}_{T,s}^{(*)} > \bar{\theta}_{T,k}^{(*)}$  and  $\hat{\pi}(s) < \hat{\pi}(k)$ . This assumption leads to a contradiction. Note that the estimated posterior distribution is a multivariate normal distribution denoted as  $\phi_N(\boldsymbol{\theta}; \bar{\theta}_T^{(*)}, V_T)$ . For any pair  $(i, j)$  with  $i \neq j$ :

$$\text{Pred}_T(i > j) = \int_{\theta_i > \theta_j} \phi_N(\boldsymbol{\theta}; \bar{\theta}_T^{(*)}, V_T) d\boldsymbol{\theta} = \Phi\left(\frac{\bar{\theta}_{T,i}^{(*)} - \bar{\theta}_{T,j}^{(*)}}{\sqrt{A_{ij}^\top V_T A_{ij}}}\right), \quad (6.17)$$

where  $A_{ij}$  is an  $N$ -dimensional vector with its  $i$ -th element set to 1,  $j$ -th element set to  $-1$ , and other elements set to 0. Then, from Eq. (6.17), we can conclude that

$$\widehat{\text{Pred}_T(i > j)} > 0.5 \text{ if and only if } \bar{\theta}_{T,i}^{(*)} > \bar{\theta}_{T,j}^{(*)}.$$

$$\widehat{\text{Pred}_T(i > j)} = 0.5 \text{ if and only if } \bar{\theta}_{T,i}^{(*)} = \bar{\theta}_{T,j}^{(*)}.$$

Since

$$\widehat{\text{Pred}_T(i > j)} + \widehat{\text{Pred}_T(j > i)} = 1,$$

we will have

$$\widehat{\text{Pred}_T(k > s)} < 0.5 < \widehat{\text{Pred}_T(s > k)}$$

we denote  $\hat{\pi}_T$  as the rank via the sorting of  $\bar{\theta}_T^{(*)}$ :

$$\hat{\pi}_T(i) > \hat{\pi}_T(j) \text{ if } \bar{\theta}_{T,i}^{(*)} > \bar{\theta}_{T,j}^{(*)} \text{ or } \bar{\theta}_{T,i}^{(*)} = \bar{\theta}_{T,j}^{(*)} \text{ with } i \neq j.$$

Then,

$$\begin{aligned} \widehat{C_T(\hat{\pi})} &= \sum_{\hat{\pi}(i) > \hat{\pi}(j)} \widehat{\text{Pred}_T(i > j)} < \sum_{(i,j), i \neq j} \max(\widehat{\text{Pred}_T(i > j)}, \widehat{\text{Pred}_T(j > i)}) \\ &= \widehat{C_T(\hat{\pi}_T)} = \sum_{\hat{\pi}_T(i) > \hat{\pi}_T(j)} \widehat{\text{Pred}_T(i > j)}, \end{aligned} \tag{6.18}$$

where the symbol  $<$  in the above equation arises from the fact that  $\widehat{\text{Pred}_T(s > k)} > \widehat{\text{Pred}_T(k > s)}$  while  $\widehat{C_T(\hat{\pi})}$  adopts  $\widehat{\text{Pred}_T(k > s)}$ . This contradiction arises because  $\hat{\pi}$  will not maximize  $\widehat{C_T(\pi)}$ .

We then prove that elements on the left-hand side of Eq. (6.14) belong to the right-hand side. Note that a rank  $\pi$  on the left-hand side satisfies:

$$\pi(i) > \pi(j) \text{ only if } \bar{\theta}_{T,i}^{(*)} \geq \bar{\theta}_{T,j}^{(*)}. \tag{6.19}$$

The summation of the prediction probability becomes:

$$\begin{aligned} \widehat{C_T(\pi)} &= \sum_{\pi(i) > \pi(j)} \widehat{\text{Pred}_T(i > j)} \\ &= \sum_{\bar{\theta}_{T,i}^{(*)} \geq \bar{\theta}_{T,j}^{(*)}} \widehat{\text{Pred}_T(i > j)} \\ &\stackrel{(1)}{=} \sum_{(i,j), i \neq j} \max(\widehat{\text{Pred}_T(i > j)}, \widehat{\text{Pred}_T(j > i)}) \\ &= \max_{\pi} \widehat{C_T(\pi)}, \end{aligned} \tag{6.20}$$

where “(1)” is due to Eq. (6.17), and the above equation ends our proof. ■

## 6.6 Chapter Summary

In this section, we tackle the computational challenges encountered by our SUN Ranking algorithm, despite benefiting from the known form of the ground-truth posterior. The potential heavy computational burden arises due to the computation of high-dimensional multivariate normal CDFs or sampling from high-dimensional multivariate truncated normal distributions.

To surmount this challenge, we initially consider the moment matching method proposed in Chen et al. [2016]. However, we find that this method is not suitable for our framework as it still requires the computation of the first and second moments of the corresponding SUN distribution, which in turn necessitates the computation of high-dimensional multivariate normal CDFs or sampling from high-dimensional multivariate truncated normal distributions.

Consequently, we shift our focus to the Variational Inference method, specifically the Mean-field variational inference method. We first introduce Variational Inference in its general form and then tailor it to suit our SUN Ranking algorithm. We employ this method not only for its simplicity but also for its local convergent property. Furthermore, by utilizing a multivariate normal distribution to approximate the SUN distribution, we prove that the estimated ranking from this multivariate normal distribution is simply the sorting of its mean.

Finally, we propose the MFVI method for both our batched and active online versions of SUN Ranking.



# Chapter 7 Experimental Validation on Simulated Data

While the SUN Ranking framework has been theoretically developed for both batched and active online scenarios, a thorough evaluation of its performance using simulated and real-world data is essential. This chapter is dedicated to assessing the effectiveness of our framework across both batched and active online versions, employing simulated datasets for validation.

Our exploration begins with an analysis of the SUN Ranking framework for batched data (Section 7.1), followed by its active online counterpart (Section 7.2). Throughout these experiments, we meticulously evaluate both the original framework and its corresponding MFVI-approximated version. Moreover, reproducible code are available at [https://github.com/zhenlipku/sun\\_ranking](https://github.com/zhenlipku/sun_ranking).

## 7.1 Simulation Study for SUN Ranking Algorithm

In this section, we demonstrate the effectiveness of our SUN Ranking algorithm for batched data using synthetic datasets.

### 7.1.1 Experimental Setting

We explore two scenarios using simulated data:

- **The TM Scenario:** In this scenario, the ground-truth comparison model is TM, given by Eq. (3.2). We consider  $N = 10$  items to be ranked. The ground-truth scores  $\theta$  are generated such that  $\theta_i \sim \text{Uniform}(0, 20)$  for each  $i$ .
- **The BTL Scenario:** In this scenario, the ground-truth comparison model is BTL, given by Eq. (3.4). Again, we consider  $N = 10$  items to be ranked. The ground-truth scores  $\theta$  are generated from a Dirichlet distribution, i.e.,  $\theta \sim \text{Dir}(\alpha)$  with  $\alpha_i = 1$  for each  $i$ .

### 7.1.2 Implementation Details

We implement two versions of our methods: SUN Ranking (Algorithm 2) and SUN Ranking MFVI (Algorithm 6). For SUN Ranking, we employ Monte Carlo integration by drawing  $12 \times 10^4$  independent samples from the corresponding SUN distribution. These samples are used to estimate prediction probabilities as well as the posterior mean. In the

MFVI version, we set the threshold for the convergence of the ELBO to  $10^{-2}$  and the maximum number of iterations to  $10^4$ . The experiments were conducted on an AMD Ryzen 3700X processor using MATLAB R2020A.

### 7.1.3 Compared Baselines

Our methods are compared to the following approaches, with detailed introductions provided in Section 3.2:

- **MLE of BTL** [Ford Jr, 1957]: This method assumes the likelihood function to be the BTL model, and the scores are estimated via MLE.
- **Borda Count** [Borda, 1781, Ammar and Shah, 2011]: This method estimates the scores of items based on the number of votes they receive. In other words, the more an item is preferred, the higher its score.
- **HodgeRank** [Jiang et al., 2011]: This method is a generalization of Borda Count and solves a least squares problem to estimate scores.
- **Rank Centrality** [Negahban et al., 2016]: This method utilizes a transition matrix to model comparisons, estimating item scores when the transition matrix has converged.

### 7.1.4 Kendall's $\tau$ Comparison

To model the batched data, we sample compared pairs uniformly. For each method, we repeat the experiment 25 times to mitigate the impact of randomness. The results are presented as the median of Kendall's  $\tau$  across 25 runs, accompanied by the range spanning from the 0.25th to the 0.75th quantile values, as shown in Fig. 7.1 and Fig. 7.2.

Although Kendall's  $\tau$ , denoted as  $\tau(\pi, \pi^*)$  in Eq. (3.6), differs from  $\tau^0(\pi, \pi^*)$  in Eq. (3.7), which is utilized in computational software such as MATLAB, they are essentially the same since  $\tau^0(\pi, \pi^*) = 2\tau(\pi, \pi^*) - 1$ . Hence, in the experimental section, unless otherwise stated, Kendall's  $\tau$  in the  $y$ -axis label is  $\tau^0(\pi, \pi^*)$ .

For the TM setting, as shown in Fig. 7.1, where the x-axis represents the sampled numbers, and the y-axis represents Kendall's  $\tau$ , it is evident that our SUN Ranking and SUN Ranking MFVI outperform other competitors. This result is expected since the ground-truth model is TM, which aligns with the setting modeled in our framework. Interestingly, SUN Ranking MFVI exhibits better performance than SUN Ranking when comparing the median curve (their error bars are tangled together). This could be attributed to the fact that we only sample  $12 \times 10^4$  samples for the Monte Carlo integration throughout the entire process. The sample number may not be large enough, as the dimension of the multivariate normal CDF grows with

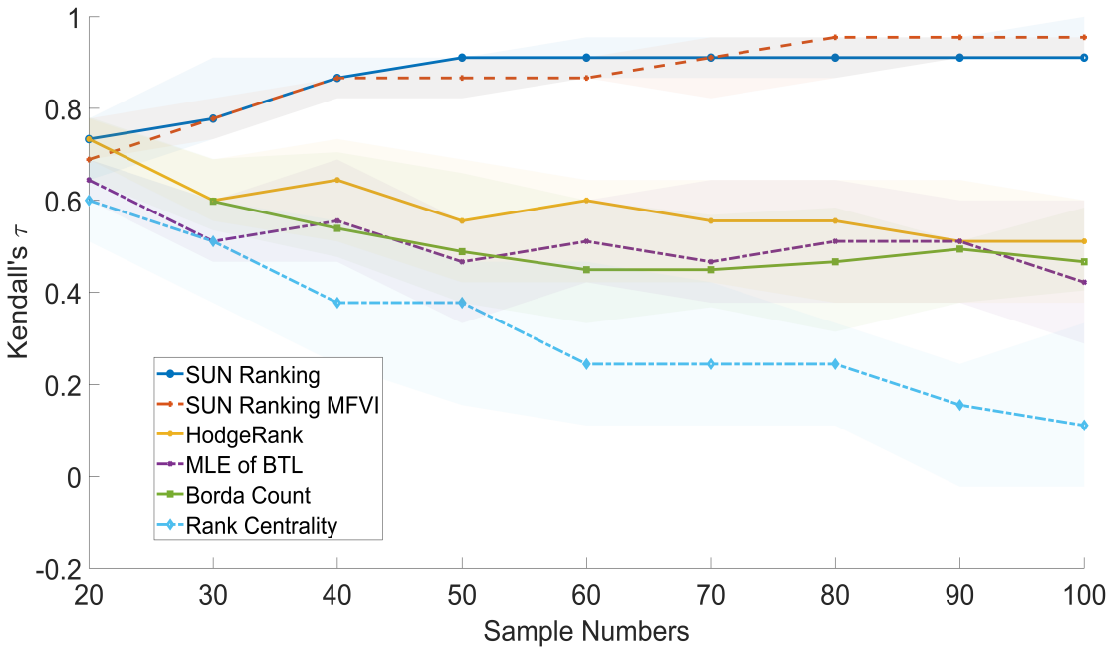


Figure 7.1 Error bar figure of batched ranking methods with the ground-truth model being TM.

an increase in the number of samples, potentially leading to estimation errors that hinder the performance of SUN Ranking.

In the BTL setting, depicted in Fig. 7.2, where the x-axis and y-axis retain the same interpretation as in Fig. 7.1, it becomes apparent that the median curve of our SUN Ranking and SUN Ranking MFVI outperforms other methods when comparing median curves. This highlights the robustness of our Bayesian ranking framework, even under the incorrect likelihood assumption. For SUN Ranking MFVI, the target distribution for approximation remains the ground-truth posterior throughout the entire process, ensuring accurate its Kendall's  $\tau$  performance. HodgeRank's performance can be elucidated by Rajkumar and Agarwal [2014b], which demonstrates its capability to recover the ground-truth ranking in the BTL setting. Similarly, the consistency of MLE of BTL is demonstrated in Bong and Rinaldo [2022].

### 7.1.5 Computational Costs

To provide insight into the computational costs, we present the computation time for a single trial of each method in Table 7.1. Despite the superior performance of our SUN Ranking in terms of Kendall's  $\tau$ , it may incur higher computational costs, especially when the sample number  $T$  is large.

It is noteworthy that although our SUN Ranking algorithm enjoys robustness and high

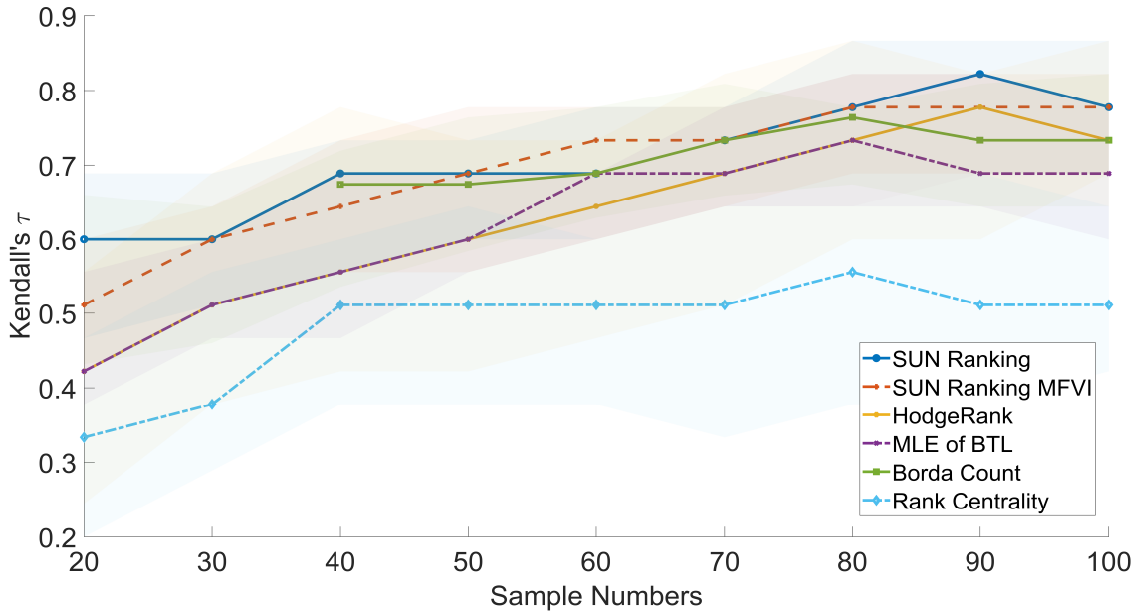


Figure 7.2 Error bar figure of batched ranking methods with the ground-truth model being BTL.

Table 7.1 Computational time of one trial for batched ranking algorithms (seconds).

Algorithms	$T = 10$	$T = 20$	$T = 50$
Rank Centrality	0.003	0.005	0.008
MLE of BTL	<b>0.001</b>	0.164	0.313
Borda Count	0.003	0.005	<b>0.007</b>
HodgeRank Supervised	<b>0.001</b>	<b>0.002</b>	0.009
SUN Ranking	0.292	0.836	6.442
SUN Ranking MFVI	0.002	0.006	0.01

Kendall  $\tau$  performance, it is the slowest algorithm. This can be attributed to the sophisticated form of the posterior, and the proposed estimated ranking from this sophisticated form is time-consuming as discussed earlier. On the other hand, SUN Ranking MFVI is comparable to other methods in speed and still possesses high Kendall's  $\tau$  performance, which demonstrates the effectiveness of our SUN Ranking MFVI method in simulated data.

## 7.2 Simulation Study for SUN Active Ranking Algorithm

In this section, we showcase the efficacy of our SUN Active Ranking algorithms employing simulated datasets.

### 7.2.1 Experimental Settings and Implementation Details

Similar to the batched version, we investigate two scenarios:

- **The TM Scenario:** In this scenario, the ground-truth comparison model is TM, given by Eq. (3.2). We consider  $N = 10$  items to be ranked. The ground-truth scores  $\theta$  are generated such that  $\theta_i \sim \text{Uniform}(0, 20)$  for each  $i$ .
- **The BTL Scenario:** In this scenario, the ground-truth comparison model is BTL, given by Eq. (3.4). Again, we consider  $N = 10$  items to be ranked. The ground-truth scores  $\theta$  are generated from a Dirichlet distribution, i.e.,  $\theta \sim \text{Dir}(\alpha)$  with  $\alpha_i = 1$  for each  $i$ .

We implement two variants of our methods: SUN Active Ranking (Algorithm 4) and SUN Active Ranking MFVI (Algorithm 7). In the MFVI version, we set the convergence threshold of the ELBO to  $10^{-2}$  and the maximum number of iterations to  $10^4$ . The experiments were conducted on an AMD Ryzen 3700X processor using MATLAB R2020A.

### 7.2.2 Compared Baselines

Our method is compared to the following approaches, with details provided in Sec. 5.2:

1. **Crowd-BT** [Chen et al., 2013]: This method iteratively selects pairs to maximize the expected information gain (EIG). It employs moment matching method to approximate the posterior distribution and subsequently generates estimated rankings based on the sorting of the mean of the estimated posterior.
2. **AKG** [Chen et al., 2016]: Similar to ours, this method iteratively selects pairs to optimize the expectation of Kendall’s  $\tau$ . Different from our method with a closed-form posterior, it approximates the posterior via moment matching in each iteration, and the estimated ranking is proposed from the approximated distribution.
3. **HodgeRank Active Supervised** [Xu et al., 2018a]: This method addresses a Maximum A Posterior (MAP) problem through ridge regression. It selects pairs for comparison by maximizing the EIG, with the final ranking estimated according to the posterior mean.

### 7.2.3 Kendall’s $\tau$ Comparison

Similarly, each method was subjected to 25 repetitions of the experiment to alleviate the influence of randomness. The results are depicted as the median of Kendall’s  $\tau$  across 25 runs, supplemented by the range spanning from the 0.25th to the 0.75th quantile values, as

illustrated in Fig. 7.3 and Fig. 7.4.

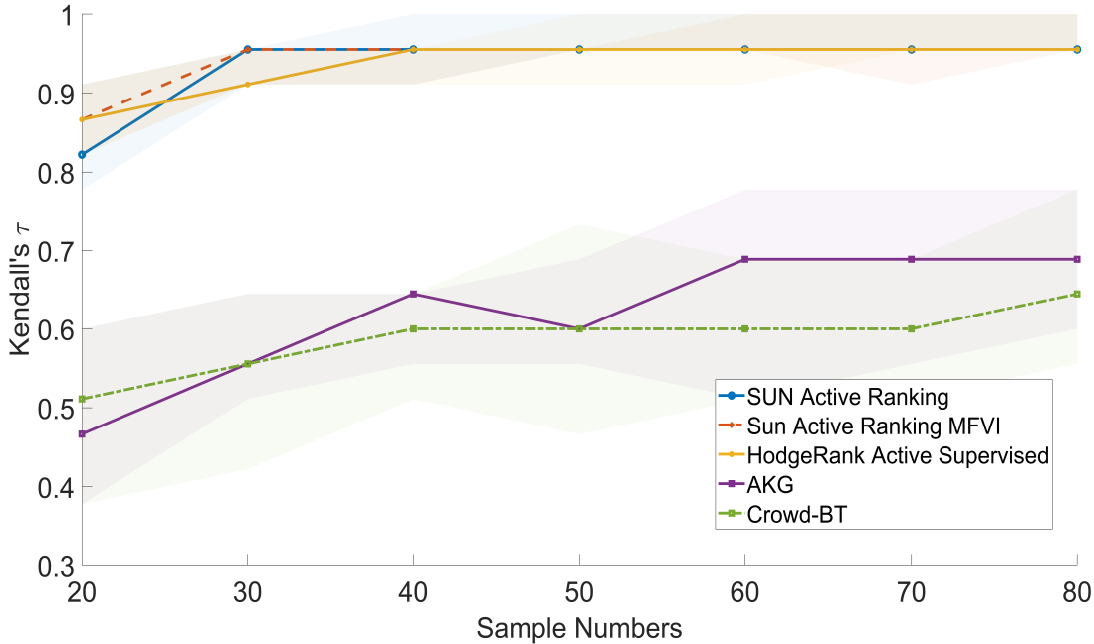


Figure 7.3 Error bar figure of active online ranking methods with the ground-truth model being TM.

Our SUN Active Ranking consistently outperforms other baselines for both the TM and BTL models. Specifically, under the TM model illustrated in Fig. 7.3, our methods significantly outperform Crowd-BT and AKG, mainly because these two methods adopt the BTL model instead of the TM model. Comparing with HodgeRank Active Supervised, our algorithm’s median curve converges more rapidly. This improved convergence rate can be attributed to our method’s direct optimization of the expectation of Kendall’s  $\tau$ , which measures ranking accuracy, rather than the EIG adopted by HodgeRank Active Supervised. Besides, the 0.25th quantile of our SUN Active Ranking is no less than the median of HodgeRank Active Supervised after convergence. This enhanced Kendall’s  $\tau$  performance can be attributed to the fact that our algorithm is firmly anchored in the ground-truth posterior, while HodgeRank Active Supervised relies on ridge regression, which may introduce bias in item score estimation.

Under the BTL model illustrated in Fig. 7.4, our method consistently outperforms HodgeRank Active Supervised, demonstrating the robustness of our approach. Surprisingly, even when considering the BTL model, our methods exhibit superior performance compared to Crowd-BT and AKG, both grounded in the BTL model. This unexpected result can be attributed to the fact that both AKG and Crowd-BT rely on moment matching to approximate a target distribution, which deviates from the ground-truth posterior with more than one sample. As

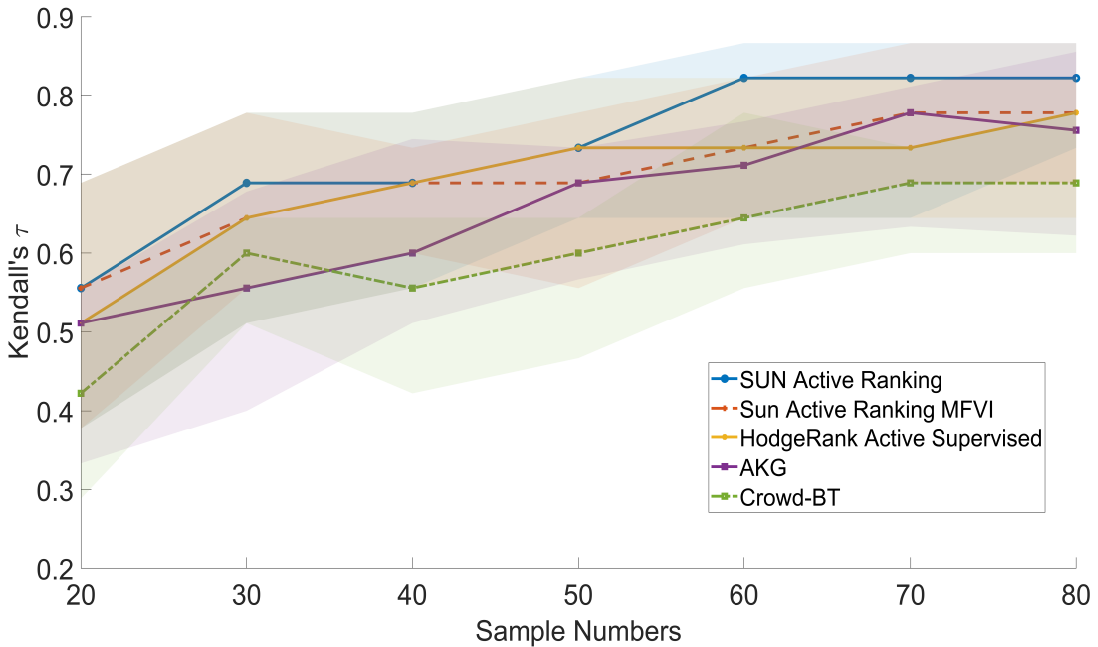


Figure 7.4 Error bar figure of active online ranking methods with the ground-truth model being BTL.

the number of samples grows, the cumulative effect of such an approximation may lead to significant deviations between the approximated posterior and the ground-truth posterior. In contrast, our method directly derives rankings based on the closed-form posterior distribution.

Besides, it is interesting to note that our SUN Active Ranking MFVI, although an approximated algorithm, still achieves better or comparable Kendall's  $\tau$  value than other methods. This can be attributed to the fact that the target distribution for approximation is the known form of the ground-truth posterior throughout the entire process, and such an approximated distribution has a minimum KL divergence between the target distribution in the mean-field family, which ensures its robustness and performance empirically.

#### 7.2.4 Computational Costs

To provide insight into the computational costs, similar to the batched experiments, we present the computation time for a single trial of each method in Table 7.2, as in Sec. 7.1.5. Despite the superior performance of our SUN Active Ranking in terms of Kendall's  $\tau$ , it may incur higher computational costs especially when the sample number  $T$  is large, which is discussed in Chap. 6. In contrast, methods like Crowd-BT and AKG, which employ posterior approximation, can be much more efficient since their rankings are based on a simple estimated posterior throughout the entire process. Additionally, HodgeRank Active Supervised, although

it may introduce bias in item score estimation, utilizes a closed-form posterior that is a simple multivariate normal distribution, enabling computational efficiency.

It is noteworthy that SUN Active Ranking MFVI outperforms the other methods in terms of computational speed in the simulated setting, making it a suitable choice when computational efficiency is a priority. Conversely, our SUN Active Ranking method requires more time due to its higher computational demands. This trade-off suggests that if one seeks more accurate estimated rankings and is willing to address the computational burden through techniques such as parallel computing, then SUN Active Ranking becomes a valuable choice.

Table 7.2 Computational time of one trial for active online ranking algorithms (seconds).

Algorithms	$T = 10$	$T = 20$	$T = 50$
AKG	0.097	0.168	0.376
Crowd-BT	0.750	0.770	0.873
HodgeRank Active Supervised	0.740	0.759	0.788
SUN Active Ranking	1.519	4.756	82.451
SUN Active Ranking MFVI	<b>0.096</b>	<b>0.150</b>	<b>0.362</b>

### 7.3 Chapter Summary

This chapter presents an evaluation of the SUN Ranking algorithm using simulated data generated from both the TM model (Fig. 7.1) and the BTL model (Fig. 7.2), demonstrating the algorithm’s robustness across different comparison models. In both scenarios, our SUN-based Bayesian framework achieves state-of-the-art results in Kendall’s  $\tau$ , underscoring its efficacy and robustness, even under misspecified comparison models such as the BTL scenario.

However, it is important to note that while our SUN Ranking algorithm excels in Kendall’s  $\tau$  performance, it may incur heavy computational burden, as evidenced by the computational costs depicted in Table 7.1. This computational complexity arises from the intricacies of high-dimensional CDFs of the multivariate normal distribution in the SUN-distributed posterior. Direct computation or sampling using Monte Carlo integration can be time-consuming, as discussed in Chapter 6.

To mitigate this issue, we introduce the SUN Ranking MFVI method as an approximate algorithm, which achieves comparable results to the original version while significantly reducing computational costs, as demonstrated in Table 7.1 and Figs. 7.1 and 7.2. This highlights the effectiveness of the approximation scheme via MFVI, which minimizes the Kullback-Leibler divergence in the mean-field family and utilizes a simple iterative scheme (Algorithm

5), and finally the straightforward sorting scheme of the posterior mean, as demonstrated in Theorem 6.1.

In the Active Online Ranking scenario, our algorithms are similarly evaluated on different comparison models, i.e., the TM model (Fig. 7.3) and the BTL model (Fig. 7.4). As observed in the batched data experiments, our SUN Active Ranking achieves state-of-the-art results in both scenarios, highlighting its effectiveness and robustness. However, our SUN Active Ranking also suffers from high computational burden, as depicted in Table 7.2, for reasons mentioned above. Hence, the SUN Active Ranking MFVI serves as a viable alternative, achieving comparable results while drastically reducing computational time, as depicted in Table 7.2.

These findings validate the effectiveness of our SUN Ranking MFVI method, indicating that when computational burden is paramount, the MFVI approximated version is preferable, while when accuracy is the primary concern, the original version remains a reasonable choice.



# Chapter 8 Real-World Applications

While we have demonstrated the utility and robustness of our SUN Ranking framework in simulated settings, it is imperative to assess its practical efficacy on real-world datasets. This chapter aims to elucidate the framework’s applicability in real-world scenarios.

We evaluate the SUN Ranking framework across various real-world applications, leveraging authentic datasets. We begin by examining its performance in a batched setting (Sec. 8.1), followed by its adaptation for active online learning (Sec. 8.2). Throughout these experiments, we compare both the original version and its MFVI-approximated counterpart. Furthermore, reproducible code is available at [https://github.com/zhenlipku/sun\\_ranking](https://github.com/zhenlipku/sun_ranking).

## 8.1 Real-World Applications for SUN Ranking Algorithm

In this section, we evaluate the performance of our method on real-world datasets: the *Reading Difficulty Dataset*, the *Imagine Quality Assessment* (IQA) dataset, and the *Visual Quality Assessment* (VQA) dataset, which we will introduce in detail subsequently. We implement both the SUN Ranking algorithm and its MFVI version (Algorithms 2 and 6) on these datasets. The baseline methods for comparison remain the same as those discussed in Section 7.1.3.

### 8.1.1 Applications and Datasets

**Reading Difficulty** [Collins-Thompson and Callan, 2004, Chen et al., 2013, 2016]: Pairwise comparison data concerning reading difficulty is extensively utilized across diverse domains, with a significant application in the realm of education. Specifically, in educational contexts, this data serves as a pivotal tool in crafting instructional materials and exercises tailored to learners’ individual proficiency levels. By leveraging pairwise comparisons, educators can adeptly match learners with texts commensurate to their current aptitude, thereby fostering more impactful and personalized learning engagements.

The reading difficulty dataset was collected from CrowdFlower<sup>①</sup> and comprises 491 documents, each assigned a reading difficulty score ranging from 1 to 12 (integer values). A higher score indicates greater difficulty in reading. The dataset encompasses a total of 7,898 pairwise comparison samples, where workers determined which document is more challenging

---

<sup>①</sup> <http://www.crowdflower.com>

to read in each pair. For simplicity, we select the first 50 documents ( $N = 50$ ) along with the corresponding 692 pairwise comparison samples from within these documents. To assess the effectiveness of an estimated ranking  $\pi$ , we compute the accuracy as defined in Chen et al. [2016]:

$$\text{Accuracy}(\pi, \pi^*) = \frac{2}{N(N-1)} \sum_{\pi(i) > \pi(j)} \mathbf{1}_{\{\theta_i \geq \theta_j\}}. \quad (8.1)$$

It is worth noting that the  $\text{Accuracy}(\pi, \pi^*)$  defined in Eq. (8.1) extends Kendall's  $\tau$  ( $\tau(\pi, \pi^*)$ ) defined in Eq. (3.6). Specifically,

$$\text{Accuracy}(\pi) = \tau(\pi, \pi^*) \text{ if elements in } \theta \text{ have non-identical values.}$$

**VQA and IQA:** Pairwise comparison data plays an essential role in IQA, serving as a fundamental tool for assessing and enhancing image quality in diverse domains including medical imaging, multimedia content delivery, and advertising. Through comparisons between compressed images and their uncompressed counterparts, practitioners can meticulously adjust compression parameters to achieve a delicate balance between minimizing quality degradation and reducing file sizes.

The IQA dataset, as utilized in Xu et al. [2018a], incorporates 43,266 pairwise comparisons. This dataset comprises 15 reference images [IVC:2005, Live:2008], each paired with 16 distinct distortions ( $N = 16$ ).

Pairwise comparison data is instrumental in the realm of VQA, serving as a pivotal tool for fine-tuning video compression algorithms and encoding methodologies. Through meticulous evaluation of perceived quality disparities between compressed and original video content, developers can strategically optimize compression parameters to deliver superior video playback experiences, all while efficiently managing bandwidth utilization and storage demands.

The VQA dataset, drawn from previous studies [Xu et al., 2011, 2018a], originates from the LIVE dataset [Live:2008]. It consists of 10 unique reference videos, each paired with 16 distinct distorted versions (resulting in  $N = 16$ ), totaling 43,266 pairwise comparisons.

### 8.1.2 Implementation Details

For our SUN Ranking MFVI, we still set the convergence threshold of ELBO at  $10^{-2}$ , and the maximum number of iteration steps to  $10^4$ . The experiments were conducted on an AMD Ryzen 3700X processor using MATLAB R2020A.

### 8.1.3 Result Analysis for Reading Difficulty Dataset

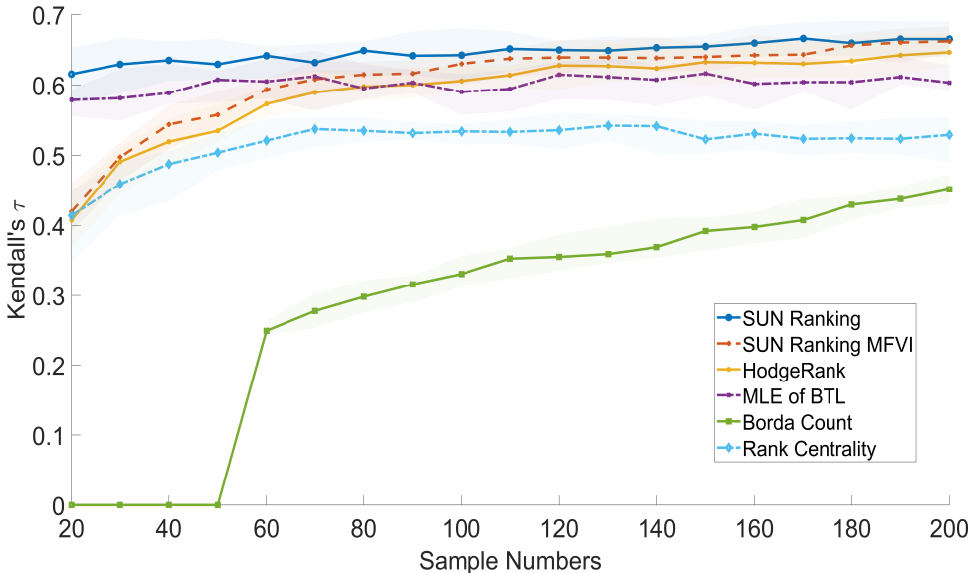


Figure 8.1 Error bar figure of batched ranking methods in the reading difficulty dataset.

For the Reading Difficulty dataset, the results are illustrated in Fig. 8.1. Each method underwent 25 repetitions of the experiment to mitigate the influence of randomness. The results are presented as the median of Accuracy (defined in Eq. (8.1)) across 25 runs, accompanied by the range spanning from the 0.25th to the 0.75th quantile values.

Our SUN Ranking and SUN Ranking MFVI consistently outperform other methods in terms of median values. This indicates the effectiveness of our framework in recovering the ground-truth in real-world datasets.

Interestingly, for sample numbers less than 60, the 0.25th quantile value of our SUN Ranking exceeds the median value of other methods. This underscores the ability of our Bayesian framework to recover the ranking even with a small sample size. This can be attributed to our knowledge of the ground-truth posterior distribution, upon which our proposed ranking is based.

Furthermore, SUN Ranking MFVI achieves higher median values than other competitors and exhibits comparable performance to SUN Ranking. This can be attributed to the fact that the target distribution for MFVI approximation is the ground-truth posterior regardless of the input data. The effectiveness of this approximation is demonstrated by its faster computational speed compared to SUN Ranking, as shown in Table 7.1. Moreover, the higher 0.25th quantile value of SUN Ranking MFVI compared to the median value of other methods further confirms its effectiveness.

### 8.1.4 Result Analysis for IQA and VQA Datasets

Given the absence of ground-truth scores in these datasets, we employ the HodgeRank estimator [Jiang et al., 2011], which has been widely used [Ghadiyaram and Bovik, 2015, Li et al., 2016, Xu et al., 2018a] to estimate the global ranking from paired comparison data, due to its effectiveness and theoretical robustness in establishing the global ranking. Similar to the Reading Difficulty dataset, we use Accuracy( $\pi, \pi^*$ ) to evaluate the estimated ranking.

Furthermore, in this scenario, Accuracy( $\pi, \pi^*$ ) as defined in Eq. (8.1) becomes Kendall’s  $\tau$  (essentially the same as  $\tau^0(\pi, \pi^*)$  defined in Eq. (3.7), so we will use  $\tau^0(\pi, \pi^*)$  in IQA and VQA datasets) when the ground-truth scores estimated via HodgeRank differ between elements, as observed in VQA and IQA datasets. For computational efficiency, we only implement the MFVI version of our SUN Ranking algorithm. Since the ground-truth scores are estimated via HodgeRank, we omit this algorithm in the Kendall’s  $\tau$  comparison for fairness.

The results for IQA datasets are illustrated in Fig. 8.2. Similarly, an error bar figure is presented. The curve represents the median of 25 trials, and the error bars range from the 0.25th quantile to the 0.75th quantile. Comparing the median values, our SUN Ranking algorithm achieves the highest Kendall’s  $\tau$  value in all IQA datasets, showcasing its effectiveness and robustness, especially given that the ground-truth scores are estimated via another pairwise comparison method (HodgeRank). Although the curve of SUN Ranking exhibits similar performance to that of Borda Count when the sample number is large, Borda Count fails to produce a Kendall’s  $\tau$  value in small samples, as it requires all items to be compared to propose estimated scores. This finding underscores the efficiency of our framework in small sample scenarios. Furthermore, the fact that our 0.25th quantile value surpasses that of Rank Centrality in some IQA datasets at small sample numbers suggests the potential superiority of our algorithm. Concerning Maximum Likelihood Estimation (MLE), our algorithm outperforms it in all IQA datasets, likely due to the unsuitability of the estimated score for the MLE framework.

The results for the VQA dataset are illustrated in Fig. 8.3, where the curve represents the mean and error bars span from the 0.25th to the 0.75th quantile. Similar to the IQA datasets, our SUN Ranking algorithm consistently achieves either the highest or comparable median value of Kendall’s  $\tau$ . While, in some cases, the Borda Count method attains the same median value for sample sizes larger than 60, it necessitates the inclusion of all items in comparisons, rendering it impractical for scenarios with limited sample sizes. This underscores the efficiency and robustness of our method, particularly in settings with constrained sample numbers.

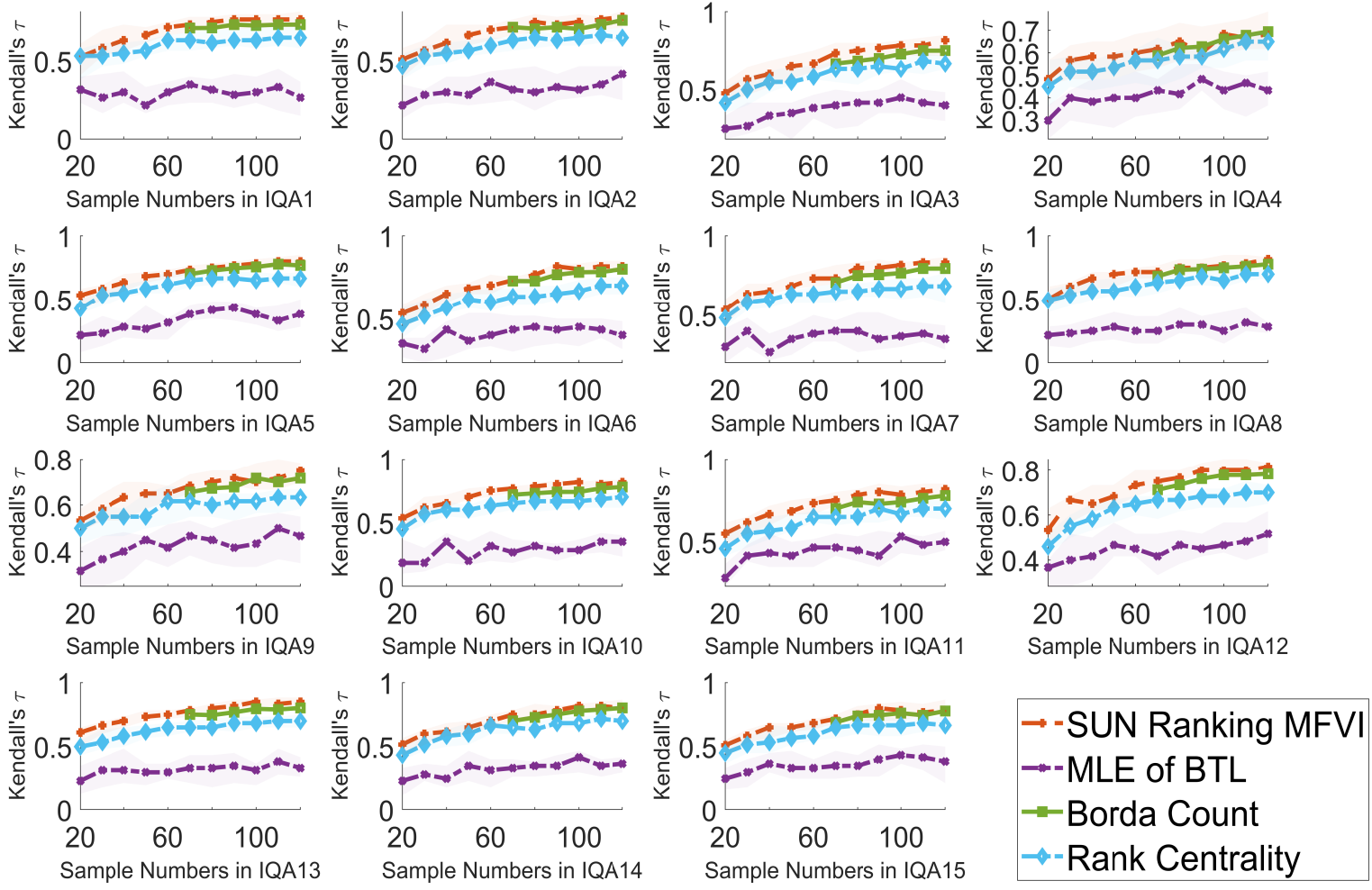


Figure 8.2 Error bar figures of batched ranking methods in IQA datasets.

## 8.2 Real-World Experiments for SUN Active Ranking Algorithm

In this section, akin to the batched version algorithms, we continue to evaluate the performance of our method on real-world datasets, including the Reading Difficulty dataset, as well as the IQA and VQA datasets. To ensure computational efficiency, as exemplified in Table 7.2, we exclusively employ the SUN Active Ranking MFVI algorithm (Algorithm 7) with real-world data. The baseline methods for comparison remain consistent with those discussed in Section 7.2.2.

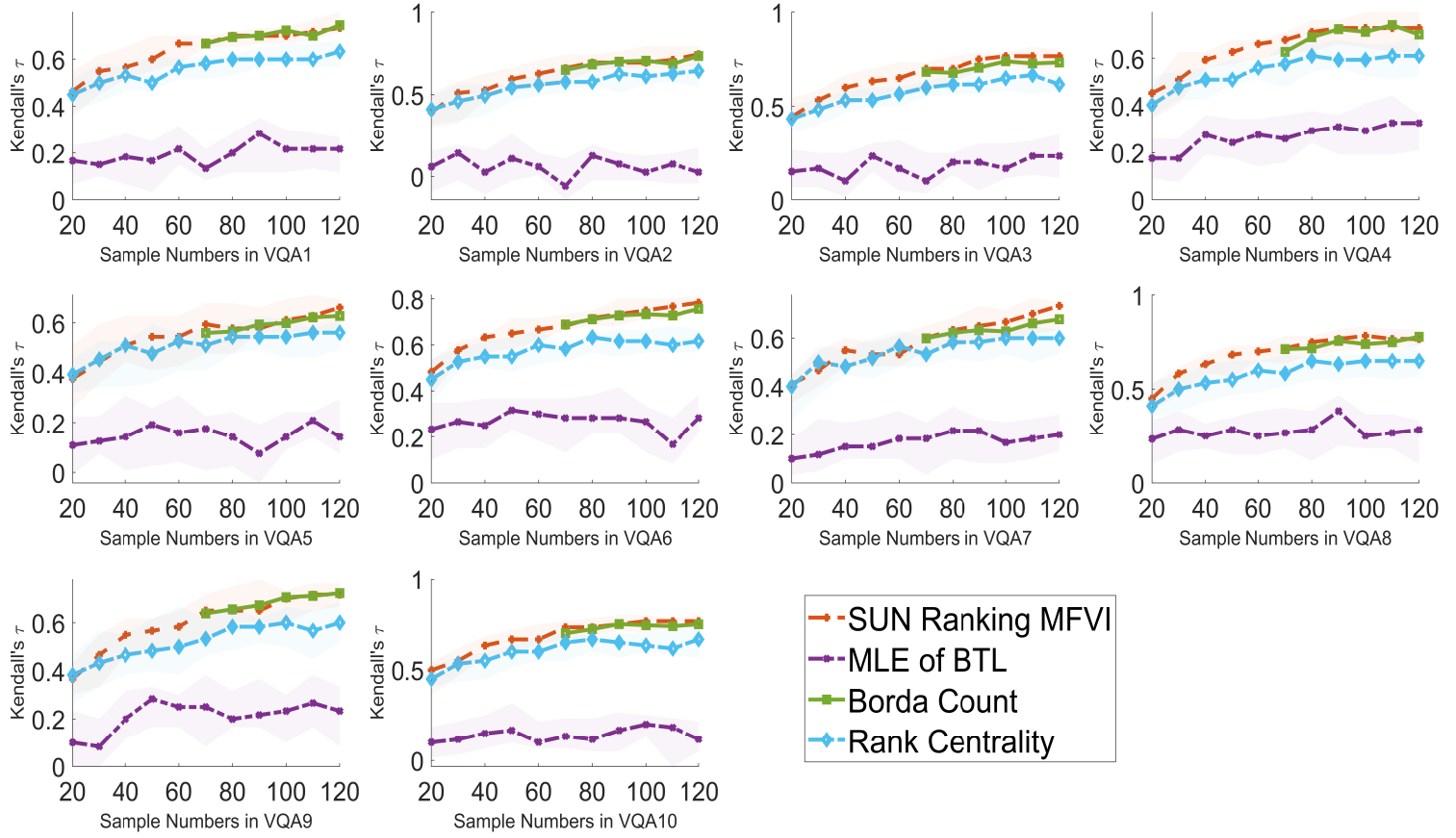


Figure 8.3 Error bar figures of batched ranking methods in VQA datasets.

### 8.2.1 Implementation Details

For our SUN Active Ranking MFVI, we maintain the convergence threshold of the ELBO at  $10^{-2}$  and the maximum number of iteration steps at  $10^4$ . The experiments were conducted on an AMD Ryzen 3700X processor using MATLAB R2020A.

### 8.2.2 Results Analysis

Similar to previous sections, we report the median, together with the error bar from the 25th quantile to the 75th quantile over 25 independent trials for each dataset.

For the Reading Difficulty dataset as depicted in Fig. 8.4, our SUN Active Ranking MFVI consistently demonstrates superior performance compared to other methods. Notably, the 0.25th quantile achieves a higher accuracy value (defined in Eq. (8.1)) than the median value obtained by other methods. This outcome underscores the efficacy of our SUN Active Ranking MFVI method in real-world applications, indicating that the approximation via MFVI is both

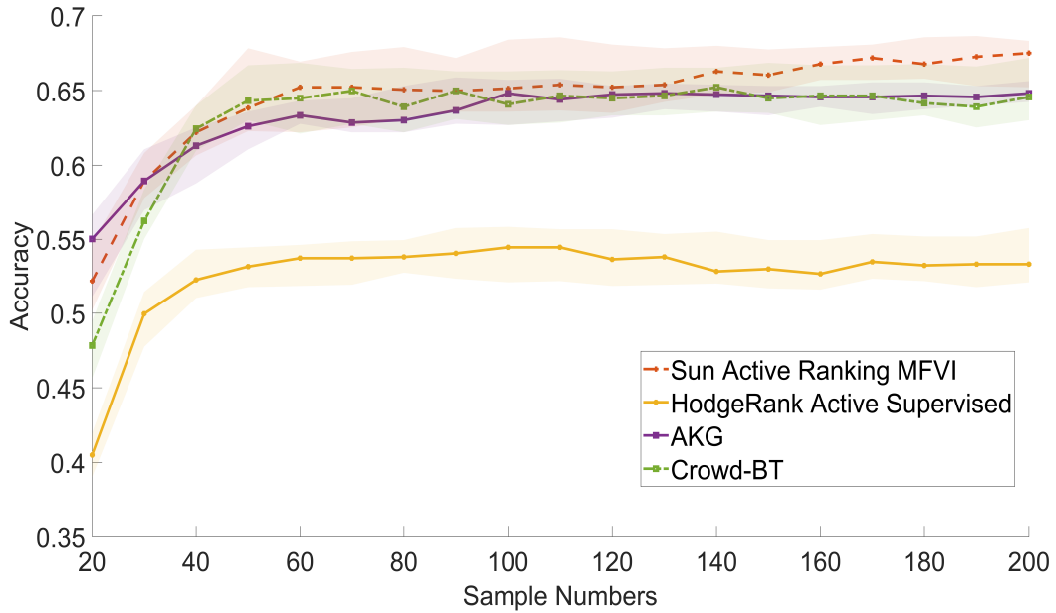


Figure 8.4 Error bar figure of active online ranking methods in the reading difficulty dataset.

reasonable and effective.

In the IQA dataset (refer to Fig. 8.5) and the VQA dataset (refer to Fig. 8.6), the median curve (measured via  $\tau^0(\pi, \pi^*)$  as discussed in Sec. 8.1.4) of our SUN Active Ranking MFVI method is comparable to that of HodgeRank Active Supervised and surpasses that of AKG and Crowd-BT. When we mention "comparable results," it indicates that in most instances, the median curve of our method closely aligns with that of HodgeRank Active Supervised.

It's worth noting that the ground-truth score is estimated via the HodgeRank estimator, which is more aligned with the objective of the HodgeRank Active Supervised method. This result further emphasizes the robustness of our SUN Active Ranking approach in real-world practices.

### 8.3 Chapter Summary

In this section, we apply our SUN Ranking framework for ranking, both in the batched and active online versions, on real-world datasets.

For the batched version, our SUN Ranking achieves higher Kendall's  $\tau$  values compared to other competitors in the reading difficulty dataset, demonstrating the effectiveness of our SUN Ranking algorithm in the educational field. Particularly noteworthy is that in small sample cases, the 0.25 quantile value of the SUN Ranking algorithm exceeds the median value of other methods, indicating the potential superiority of our approach, especially under limited

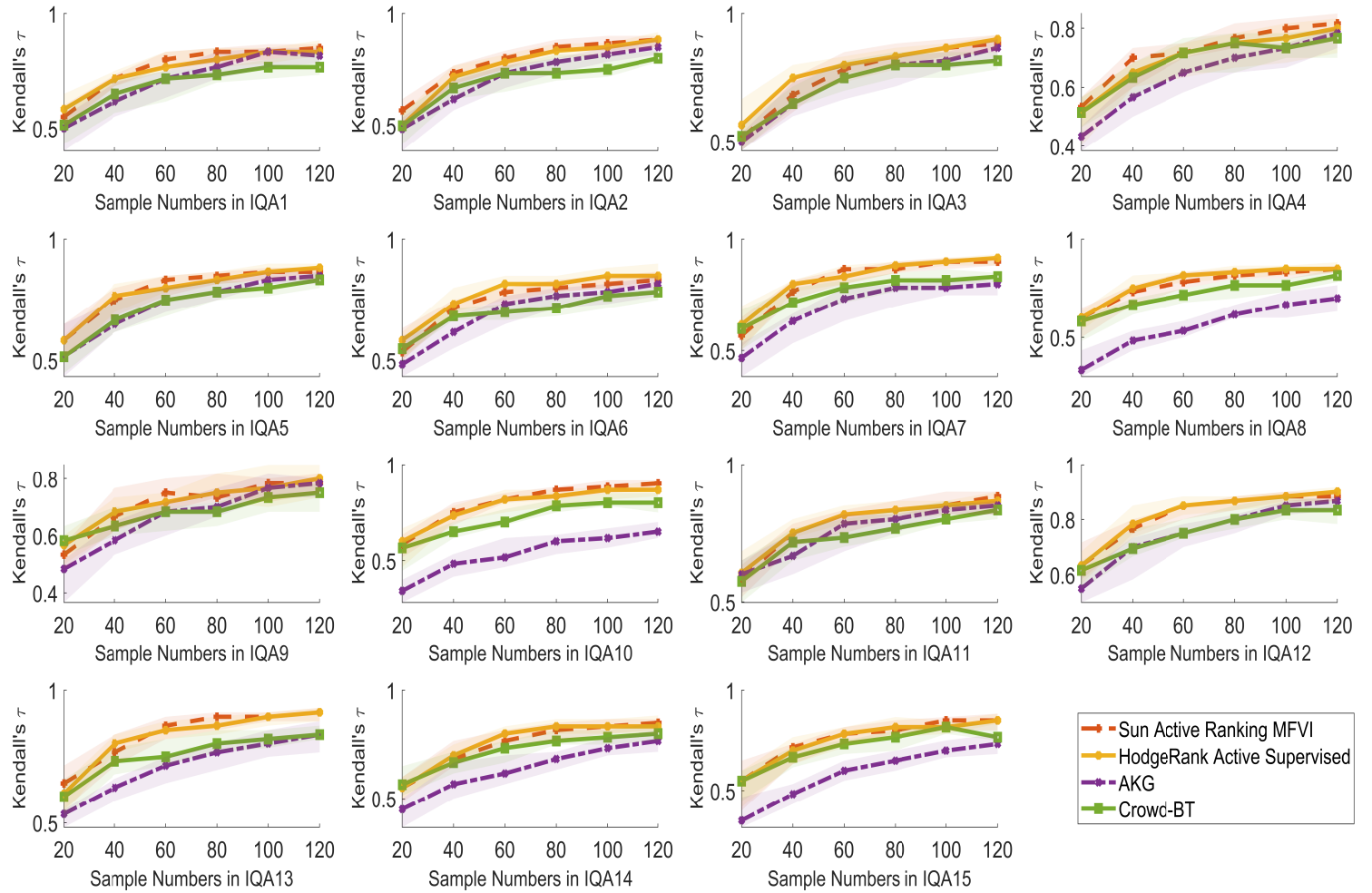


Figure 8.5 Error bar figures of active online ranking methods in IQA datasets.

sample constraints.

However, it is important to note that while the original SUN Ranking algorithm demonstrates the best performance, it may suffer from a heavy computational burden due to its reliance on the sophisticated posterior, i.e., the SUN distribution. This heavy computational burden is depicted in Table 7.1 and Table 7.2.

The SUN Ranking MFVI therefore serves as a compensatory method in this regard. In the reading difficulty dataset, our MFVI version achieves the same value of Kendall's  $\tau$  after 180 samples compared to the original version, showcasing its utility and good performance for approximation.

In the active online ranking scenario, similar trends are observed. Our SUN Active

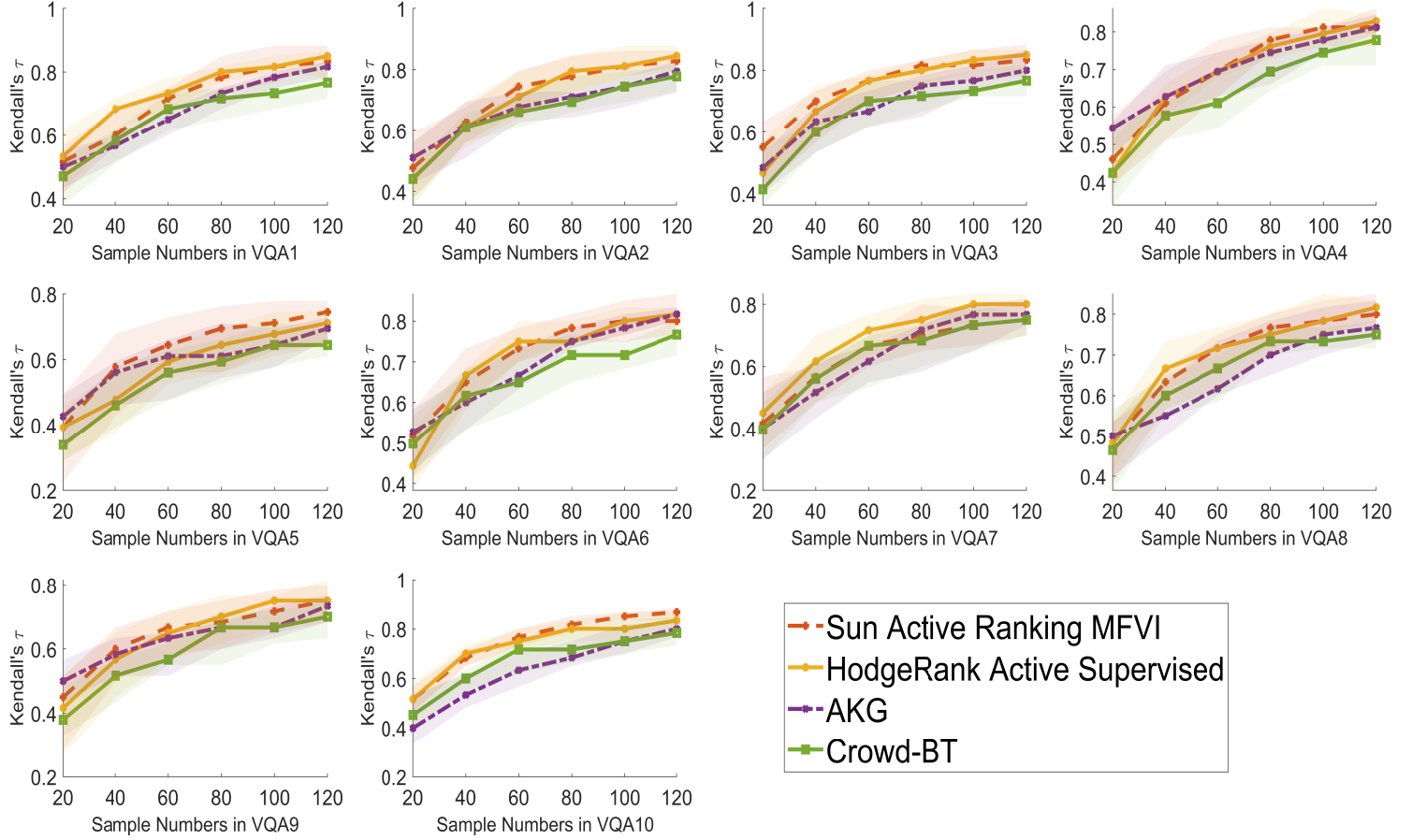


Figure 8.6 Error bar figures of active online ranking methods in VQA datasets.

Ranking MFVI achieves the highest value of Kendall's  $\tau$ ; additionally, its 0.25th quantile value is higher than the median value of other methods, showing its potential advantages over other methods. Furthermore, in IQA and VQA datasets, the performance, which achieves state-of-the-art results in some cases and comparable results in others, demonstrates its robustness under different conditions. Considering that the ground-truth scores in IQA and VQA datasets are estimated via HodgeRank, the results further emphasize the robustness of our framework.

In summary, similar to the results of simulated data scenarios, our findings present a trade-off: if one prioritizes accuracy, SUN Ranking without MFVI is the better choice, but if computational speed is important, then the MFVI version is a reasonable alternative. Our practical use of the MFVI version highlights its accuracy, robustness, and efficiency.



## Chapter 9 Conclusions and Future Work

In conclusion, this dissertation presents a pioneering Bayesian conjugate framework built upon the Thurstone-Mosteller model, featuring a posterior distribution adhering to the unified skew-normal (SUN) distribution. The optimal ranking in our Bayesian framework involves maximizing the expectation of Kendall's  $\tau$  correlation coefficient over the SUN posterior, thereby facilitating accurate ranking inferences. Under certain empirically observed conditions, the resulting ranking simplifies to the sorting of the posterior mean. By maximizing the objective function and leveraging the known form of the posterior distribution, we extend our algorithm from offline to an active online ranking strategy using the knowledge gradient method. Additionally, to address computational challenges with large samples, we propose an approximated version of our framework using the Mean-field Variational Inference method, significantly enhancing computational speeds while maintaining high Kendall's  $\tau$  performance. Our methods consistently outperform or achieve comparable results to baseline methods across different scenarios, including simulated data and real-world datasets, highlighting the efficacy and efficiency of our approach.

Despite the significant progress made, several promising avenues for future research remain open. For instance, there is a need to establish sufficient and necessary conditions for the absence of loops when determining the optimal ranking based on the expectation of Kendall's  $\tau$  correlation coefficient. This endeavor may involve evaluating complex and non-closed-form multivariate normal cumulative distribution functions. Furthermore, extending our framework to incorporate variations in annotator reliability on crowdsourcing platforms while preserving conjugate properties would enhance its applicability to real-world scenarios with diverse annotator expertise. Additionally, in the context of Variational Inference, exploring other families of distributions beyond the multivariate normal could be pursued to improve approximation accuracy without sacrificing computational efficiency.



## Reference

- J-C de Borda. Mémoire sur les élections au scrutin: Histoire de la facadémie royale des sciences. *Paris, France*, 12, 1781.
- Linas Baltrunas, Tadas Makcinskas, and Francesco Ricci. Group recommendations with rank aggregation and collaborative filtering. In *Proceedings of the fourth ACM conference on Recommender systems*, pages 119–126, 2010.
- Ritu Meena and Kamal K Bharadwaj. Group recommender system based on rank aggregation—an evolutionary approach. In *Mining Intelligence and Knowledge Exploration: First International Conference, MIKE 2013, Tamil Nadu, India, December 18-20, 2013. Proceedings*, pages 663–676. Springer, 2013.
- Meike Zehlike, Ke Yang, and Julia Stoyanovich. Fairness in ranking, part ii: Learning-to-rank and recommender systems. *ACM Computing Surveys*, 55(6):1–41, 2022.
- Michał Bałchanowski and Urszula Boryczka. A comparative study of rank aggregation methods in recommendation systems. *Entropy*, 25(1):132, 2023.
- Cynthia Dwork, Ravi Kumar, Moni Naor, and Dandapani Sivakumar. Rank aggregation methods for the web. In *Proceedings of the 10th international conference on World Wide Web*, pages 613–622, 2001.
- Ronny Lempel and Shlomo Moran. Rank-stability and rank-similarity of link-based web ranking algorithms in authority-connected graphs. *Information Retrieval*, 8(2):245–264, 2005.
- Fabrizio Lamberti, Andrea Sanna, and Claudio Demartini. A relation-based page rank algorithm for semantic web search engines. *IEEE Transactions on Knowledge and Data Engineering*, 21(1):123–136, 2008.
- Nir Ailon, Moses Charikar, and Alantha Newman. Aggregating inconsistent information: ranking and clustering. *Journal of the ACM (JACM)*, 55(5):1–27, 2008.
- Konstantinos Pelechrinis, Evangelos Papalexakis, and Christos Faloutsos. Sportsnetrank: Network-based sports team ranking. 2016.
- Tom Minka, Ryan Cleven, and Yordan Zaykov. Trueskill 2: An improved bayesian skill rating system. *Technical Report*, 2018.
- Pinhan Chen, Chao Gao, and Anderson Y Zhang. Optimal full ranking from pairwise comparisons. *The Annals of Statistics*, 50(3):1775–1805, 2022.
- Xi Chen, Kevin Jiao, and Qihang Lin. Bayesian decision process for cost-efficient dynamic ranking via crowdsourcing. *The Journal of Machine Learning Research*, 17(1):7617–7656, 2016.
- Xiaoye Jiang, Lek-Heng Lim, Yuan Yao, and Yinyu Ye. Statistical ranking and combinatorial hodge theory. *Mathematical Programming*, 127(1):203–244, 2011.
- Peter Emerson. The original borda count and partial voting. *Social Choice and Welfare*, 40:353–358, 2013.
- Arun Rajkumar and Shivani Agarwal. A statistical convergence perspective of algorithms for rank aggregation from pairwise data. In *International Conference on Machine Learning*, pages 118–126, 2014a.
- Sahand Negahban, Sewoong Oh, and Devavrat Shah. Iterative ranking from pair-wise comparisons. *Advances in neural information processing systems*, 25, 2012.

Hossein Azari Soufiani, William Chen, David C Parkes, and Lirong Xia. Generalized method-of-moments for rank aggregation. *Advances in Neural Information Processing Systems*, 26, 2013.

Jing Li, Rafal Mantiuk, Junle Wang, Suiyi Ling, and Patrick Le Callet. Hybrid-mst: A hybrid active sampling strategy for pairwise preference aggregation. In *Advances in Neural Information Processing Systems*, pages 3475–3485, 2018.

Aliaksei Mikhailiuk, Clifford Wilmot, Maria Perez-Ortiz, Dingcheng Yue, and Rafał K Mantiuk. Active sampling for pairwise comparisons via approximate message passing and information gain maximization. In *2020 25th International Conference on Pattern Recognition (ICPR)*, pages 2559–2566. IEEE, 2021.

Qianqian Xu, Jiechao Xiong, Xi Chen, Qingming Huang, and Yuan Yao. Hodgerank with information maximization for crowdsourced pairwise ranking aggregation. In *Thirty-Second AAAI Conference on Artificial Intelligence*, 2018a.

Xi Chen, Paul N Bennett, Kevyn Collins-Thompson, and Eric Horvitz. Pairwise ranking aggregation in a crowdsourced setting. In *Proceedings of the sixth ACM international conference on Web search and data mining*, pages 193–202. ACM, 2013.

Maurice G Kendall. A new measure of rank correlation. *Biometrika*, 30(1/2):81–93, 1938.

Daniele Durante. Conjugate Bayes for probit regression via unified skew-normal distributions. *Biometrika*, 106(4):765–779, 08 2019. ISSN 0006-3444. doi: 10.1093/biomet/asz034. URL <https://doi.org/10.1093/biomet/asz034>.

Reinaldo B Arellano-Valle and Adelchi Azzalini. On the unification of families of skew-normal distributions. *Scandinavian Journal of Statistics*, 33(3):561–574, 2006.

Bo Wang and D Titterington. Convergence and asymptotic normality of variational bayesian approximations for exponential family models with missing values. *arXiv preprint arXiv:1207.4159*, 2012.

Adelchi Azzalini and A Dalla Valle. The multivariate skew-normal distribution. *Biometrika*, 83(4):715–726, 1996.

Adelchi Azzalini and Antonella Capitanio. Statistical applications of the multivariate skew normal distribution. *Journal of the Royal Statistical Society: Series B (Statistical Methodology)*, 61(3):579–602, 1999.

Graciela González et al. The closed skew-normal distribution. In *Skew-Elliptical Distributions and Their Applications*, pages 39–56. Chapman and Hall/CRC, 2004.

Arjun K Gupta and John T Chen. A class of multivariate skew-normal models. *Annals of the Institute of Statistical Mathematics*, 56:305–315, 2004.

S Kocherlakota and K Kocherlakota. Generalized variance. *Encyclopedia of Statistical Sciences*, 2004.

Arjun K Gupta, Graciela González-Farias, and J Armando Domínguez-Molina. A multivariate skew normal distribution. *Journal of multivariate analysis*, 89(1):181–190, 2004.

Shanti S Gupta and Klaus J Miescke. Bayesian look ahead one-stage sampling allocations for selection of the best population. *Journal of statistical planning and inference*, 54(2):229–244, 1996.

Mohammad Abdus Samad Aziz. *Study of unified multivariate skew normal distribution with applications in finance and actuarial science*. PhD thesis, Bowling Green State University, 2011.

- Adelchi Azzalini and Antonella Bacchieri. A prospective combination of phase ii and phase iii in drug development. *Metron*, 68:347–369, 2010.
- Roberto Colombi. Closed skew normal stochastic frontier models for panel data. *Advances in Theoretical and Applied Statistics*, pages 177–186, 2013.
- Roberto Colombi, Subal C Kumbhakar, Gianmaria Martini, and Giorgio Vittadini. Closed-skew normality in stochastic frontiers with individual effects and long/short-run efficiency. *Journal of Productivity Analysis*, 42:123–136, 2014.
- Denis Allard and Philippe Naveau. A new spatial skew-normal random field model. *Communications in Statistics - Theory and Methods*, 36(9):1821–1834, 2007.
- Kjartan Rimstad and Henning Omre. Skew-gaussian random fields. *Spatial Statistics*, 10:43–62, 2014.
- Parisa Zarrin, Mohsen Maleki, Zahra Khodadai, and Reinaldo B Arellano-Valle. Time series models based on the unrestricted skew-normal process. *Journal of Statistical Computation and Simulation*, 89(1):38–51, 2019.
- Mamadou S Diallo and JNK Rao. Small area estimation of complex parameters under unit-level models with skew-normal errors. *Scandinavian Journal of Statistics*, 45(4):1092–1116, 2018.
- Augusto Fasano, Daniele Durante, and Giacomo Zanella. Scalable and accurate variational bayes for high-dimensional binary regression models. *Biometrika*, 109(4):901–919, 2022.
- Augusto Fasano and Daniele Durante. A class of conjugate priors for multinomial probit models which includes the multivariate normal one. *The Journal of Machine Learning Research*, 23(1):1358–1383, 2022.
- Niccolò Anceschi, Augusto Fasano, Daniele Durante, and Giacomo Zanella. Bayesian conjugacy in probit, tobit, multinomial probit and extensions: A review and new results. *Journal of the American Statistical Association*, 118(542):1451–1469, 2023.
- Louis L Thurstone. A law of comparative judgment. *Psychological review*, 34(4):273, 1927.
- Ralph Allan Bradley and Milton E Terry. Rank analysis of incomplete block designs: I. the method of paired comparisons. *Biometrika*, 39(3/4):324–345, 1952.
- R. Duncan Luce. Individual choice behavior: A theoretical analysis. *Journal of the American Statistical Association*, 67(1):1–15, 2005.
- Ammar Ammar and Devavrat Shah. Ranking: Compare, don’t score. In *2011 49th Annual Allerton Conference on Communication, Control, and Computing (Allerton)*, pages 776–783. IEEE, 2011.
- S Negahban, S Oh, and D Shah. Rank centrality: Ranking from pairwise com-parisons. *Operations research*, 65(1):266–287, 2016.
- Colin L Mallows. Non-null ranking models. i. *Biometrika*, 44(1/2):114–130, 1957.
- Wenpin Tang. Mallows ranking models: maximum likelihood estimate and regeneration. In *International Conference on Machine Learning*, pages 6125–6134. PMLR, 2019.
- Ralf Herbrich, Tom Minka, and Thore Graepel. Trueskill™: A bayesian skill rating system. In B. Schölkopf, J. Platt, and T. Hoffman, editors, *Advances in Neural Information Processing Systems*, volume 19.

- MIT Press, 2006. URL [https://proceedings.neurips.cc/paper\\_files/paper/2006/file/f44ee263952e65b3610b8ba51229d1f9-Paper.pdf](https://proceedings.neurips.cc/paper_files/paper/2006/file/f44ee263952e65b3610b8ba51229d1f9-Paper.pdf).
- Robin L Plackett. The analysis of permutations. *Journal of the Royal Statistical Society Series C: Applied Statistics*, 24(2):193–202, 1975.
- Yuxin Chen and Changho Suh. Spectral MLE: Top-k rank aggregation from pairwise comparisons. In *International Conference on Machine Learning*, pages 371–380. PMLR, 2015.
- Shengbo Guo and Scott Sanner. Real-time multiattribute bayesian preference elicitation with pairwise comparison queries. In *Proceedings of the Thirteenth International Conference on Artificial Intelligence and Statistics*, pages 289–296. JMLR Workshop and Conference Proceedings, 2010.
- Laura Priekule and Stephan Meisel. A bayesian ranking and selection problem with pairwise comparisons. In *2017 Winter Simulation Conference (WSC)*, pages 2149–2160. IEEE, 2017.
- Jianqing Fan, Zhipeng Lou, Weichen Wang, and Mengxin Yu. Ranking inferences based on the top choice of multiway comparisons. *arXiv preprint arXiv:2211.11957*, 2022.
- Qianqian Xu, Jiechao Xiong, Qingming Huang, and Yuan Yao. Online hodgerank on random graphs for crowdsourceable qoe evaluation. *IEEE Transactions on Multimedia*, 16(2):373–386, 2013.
- Ali Baharev, Hermann Schichl, Arnold Neumaier, and Tobias Achterberg. An exact method for the minimum feedback arc set problem. *Journal of Experimental Algorithms (JEA)*, 26:1–28, 2021.
- RB Bapat, D Kalita, and S Pati. On weighted directed graphs. *Linear Algebra and its Applications*, 436(1):99–111, 2012.
- John W Moon. *Topics on tournaments in graph theory*. Courier Dover Publications, 2015.
- Sangmin Byeon and Woojoo Lee. Directed acyclic graphs for clinical research: a tutorial. *Journal of Minimally Invasive Surgery*, 26(3):97, 2023.
- Sounaka Mishra and Kripasindhu Sikdar. On approximability of linear ordering and related np-optimization problems on graphs. *Discrete Applied Mathematics*, 136(2-3):249–269, 2004.
- Rafael Martí and Gerhard Reinelt. *The linear ordering problem: exact and heuristic methods in combinatorial optimization*, volume 175. Springer Science & Business Media, 2011.
- Reinaldo B Arellano-Valle and Adelchi Azzalini. Some properties of the unified skew-normal distribution. *Statistical Papers*, 63(2):461–487, 2022.
- Zdravko I Botev. The normal law under linear restrictions: simulation and estimation via minimax tilting. *Journal of the Royal Statistical Society Series B: Statistical Methodology*, 79(1):125–148, 2017.
- Ritesh Noothigattu, Dominik Peters, and Ariel D Procaccia. Axioms for learning from pairwise comparisons. *Advances in Neural Information Processing Systems*, 33:17745–17754, 2020.
- John Adrian Bondy, Uppaluri Siva Ramachandra Murty, et al. *Graph theory with applications*, volume 290. Macmillan London, 1976.
- Edward A Bender and S Gill Williamson. *Lists, decisions and graphs*. S. Gill Williamson, 2010.
- Qianqian Xu, Jiechao Xiong, Xinwei Sun, Zhiyong Yang, Xiaochun Cao, Qingming Huang, and Yuan Yao. A margin-based mle for crowdsourced partial ranking. In *Proceedings of the 26th ACM international conference on Multimedia*, pages 591–599, 2018b.

- Natalia A Bochkina and Peter J Green. The bernstein–von mises theorem and nonregular models. 2014.
- Robin L Plackett. A reduction formula for normal multivariate integrals. *Biometrika*, 41(3/4):351–360, 1954.
- Aad W Van der Vaart. *Asymptotic statistics*, volume 3. Cambridge university press, 2000.
- Alexander Ly, Maarten Marsman, Josine Verhagen, Raoul PPP Grasman, and Eric-Jan Wagenmakers. A tutorial on fisher information. *Journal of Mathematical Psychology*, 80:40–55, 2017.
- Jun Shao. *Mathematical statistics*. Springer Science & Business Media, 2003.
- Thomas Pfeiffer, Xi Gao, Yiling Chen, Andrew Mao, and David Rand. Adaptive polling for information aggregation. In *Proceedings of the AAAI Conference on Artificial Intelligence*, volume 26, pages 122–128, 2012.
- Solomon Kullback and Richard A Leibler. On information and sufficiency. *The annals of mathematical statistics*, 22(1):79–86, 1951.
- Peter Frazier, Warren Powell, and Savas Dayanik. A knowledge-gradient policy for sequential information collection. *SIAM J. Control and Optimization*, 47:2410–2439, 01 2008. doi: 10.1137/070693424.
- Warren B Powell. The knowledge gradient for optimal learning. *Wiley Encyclopedia of Operations Research and Management Science*, 2010.
- Guido Consonni and Jean-Michel Marin. Mean-field variational approximate bayesian inference for latent variable models. *Computational Statistics & Data Analysis*, 52(2):790–798, 2007.
- Michael I Jordan, Zoubin Ghahramani, Tommi S Jaakkola, and Lawrence K Saul. An introduction to variational methods for graphical models. *Machine learning*, 37:183–233, 1999.
- Christopher M Bishop et al. Pattern recognition and machine learning: springer new york. 2006.
- David M Blei, Alp Kucukelbir, and Jon D McAuliffe. Variational inference: A review for statisticians. *Journal of the American statistical Association*, 112(518):859–877, 2017.
- James H Albert and Siddhartha Chib. Bayesian analysis of binary and polychotomous response data. *Journal of the American statistical Association*, 88(422):669–679, 1993.
- Lester R Ford Jr. Solution of a ranking problem from binary comparisons. *The American Mathematical Monthly*, 64(8P2):28–33, 1957.
- A. Rajkumar and S. Agarwal. A statistical convergence perspective of algorithms for rank aggregation from pairwise data. In *International Conference on International Conference on Machine Learning*, 2014b.
- Heejong Bong and Alessandro Rinaldo. Generalized results for the existence and consistency of the mle in the bradley-terry-luce model. In *International Conference on Machine Learning*, pages 2160–2177. PMLR, 2022.
- Kevyn Collins-Thompson and James P Callan. A language modeling approach to predicting reading difficulty. In *Proceedings of the human language technology conference of the North American chapter of the association for computational linguistics: HLT-NAACL 2004*, pages 193–200, 2004.
- IVC:2005. Subjective quality assessment irccyn/ivc database. <http://www2.irccyn.ecnantes.fr/ivcdb/>.

Live:2008. Live image and video quality assessment database. [http://live.ece.utexas.edu/research/quality/live\\_video.html](http://live.ece.utexas.edu/research/quality/live_video.html).

Qianqian Xu, Tingting Jiang, Yuan Yao, Qingming Huang, Bowei Yan, and Weisi Lin. Random partial paired comparison for subjective video quality assessment via hogerank. In *Proceedings of the 19th ACM international conference on Multimedia*, pages 393–402, 2011.

Deepti Ghadiyaram and Alan C Bovik. Massive online crowdsourced study of subjective and objective picture quality. *IEEE Transactions on Image Processing*, 25(1):372–387, 2015.

Guoliang Li, Jiannan Wang, Yudian Zheng, and Michael J Franklin. Crowdsourced data management: A survey. *IEEE Transactions on Knowledge and Data Engineering*, 28(9):2296–2319, 2016.

## Appendix A Code Implementation

In this appendix, we provide a comprehensive guide for implementing the code used in our experiments. We recommend using MATLAB version 2020A or later, with the Parallel Computing Toolbox installed. The subsequent sections cover various aspects of the implementation.

### A.1 Implementation Description

To implement the code in this dissertation, please visit the following URL: [https://github.com/zhenlipku/sun\\_ranking](https://github.com/zhenlipku/sun_ranking). Download the ZIP file, unzip it, and you will find five folders within the “codes” directory.

- The “codes\sun\_ranking\_simu” folder contains the code for the simulated experiments using our original SUN Ranking algorithm, as discussed in Chapter 7. The main function is “sun\_ranking\_active\_simu.m”.
- The “codes\sun\_ranking\_mfvi\_simu” folder includes the code for the MFVI estimated version of our SUN Ranking algorithm, also detailed in Chapter 7. The main function is “sun\_ranking\_active\_mfvi.m”.
- The remaining three folders, “codes\reading\_difficulty”, “codes\iqa”, and “codes\vqa”, contain the code for the corresponding real-world datasets discussed in Chapter 8. The main functions for these datasets are “sun\_ranking\_active\_mfvi\_reading.m”, “sun\_ranking\_active\_mfvi\_iqa.m”, and “sun\_ranking\_active\_mfvi\_vqa.m”, respectively.

### A.2 Function Descriptions

To help readers better understand our MATLAB codes, we briefly describe each function and its purpose below.

- **com\_mean:** Computes the mean of a SUN distribution.
- **com\_prob:** Computes all  $\text{Pred}_T(i > j)$  for all possible pairs of a given SUN distribution.
- **com\_prob\_mean:** Calls **com\_mean** and **com\_prob** as a summarization.
- **drchrnd:** Generates random numbers from a Dirichlet distribution.
- **est\_para\_mf:** Generates parameters of a multivariate normal distribution via the MFVI method, approximating a SUN distribution (Algorithm 5).

- `est_prob_compute`: Computes the prediction probabilities when the posterior distribution is approximated via the MFVI method, i.e., the maximization of  $\widehat{C}_T(\pi)$  defined in Eq. (6.13).

- `est_tran_prob_compute`: Computes the estimated transitional probabilities when the posterior distribution is approximated via the MFVI method, i.e.,  $\hat{\Pr}(y_{t+1} = s | \mathcal{S}_t, \mathcal{Y}_t(\mathcal{S}_t), \mathbf{0}_N, I_N)$  in Eq. (6.15).

- `generateG`: Generates parameters of a SUN distribution with the imputed compared pairs and their outcomes.

- `max_prob`: Computes the summation of the maximized prediction probabilities of a SUN distribution, i.e., the upper bound of  $C_T(\pi)$  in Eq. (3.23).

- `mvrandn`: Generates random numbers from multivariate normal distributions with the corresponding input parameters.

- `mvncdf_fast`: Computes the value of multivariate normal CDFs.

- `rank_ver`, `if_loop_exist`, and `if_forms_a_rank`: Check whether loops exist, forming Algorithm 1.

- `sundraw`: Generates random numbers from a SUN distribution (Algorithm 3).

- `tran_prob_compute`: Generates transitional probabilities of a given SUN distribution and a given  $i, j$  pair, i.e.,  $\Pr(Y_{ij} = \pm 1 | \mathcal{S}_t, \mathcal{Y}_t(\mathcal{S}_t), \mathbf{0}_N, I_N)$  in Eq. (5.4).

### A.3 Function Details

In this section, we provide a detailed introduction to the core components of our code, specifically focusing on the KG policy in the SUN Active Ranking algorithm (Algorithm 4). This example aims to help readers better understand our code. The KG policy in Eq. (5.5) is implemented as follows:

```

1    outcomes = zeros(m, 1);
2    % m is the number of all possible pairs, i.e., m = N*(N-1)/2 for N items.
3    parfor k = 1:m
4        % Parallel computing
5        i = data(k, 1);
6        j = data(k, 2);
7        % data is a set of all possible pairs given previously. In the k-
8        % th iteration, we pick the k-th pair.
9        trans_prob = tran_prob_compute(i, j, x, y) / Denominator0;
    % Denominator0 is the normalization constant of a SUN distribution
    % computed above. The function ‘‘tran_prob_compute’’ computes

```

```
the transitional probability introduced in the previous section  
.  
10    outcomes(k) = trans_prob * max_prob(x, y, i, j, data) + (1 -  
         trans_prob) * max_prob(x, y, j, i, data);  
11    % For the k-th pair, we compute its possible expectation of  
         Kendall's tau over the posterior, using the functions ''  
         tran_prob_compute'' and ''max_prob'' introduced in the previous  
         section.  
12
```

Listing A.1 KG policy in Eq. (5.5)

The maximization of “outcomes” in the above code represents the KG policy in Eq. (5.5). For the batched version, pairs can be randomly selected for comparison.



## Acknowledgment

I extend my heartfelt gratitude to my advisor, Professor Yuan Yao, for his unwavering support, invaluable guidance, and insightful suggestions throughout this research journey. I am particularly grateful for his patience. His supervision has been exemplary, and I am truly fortunate to have had the opportunity to work under his mentorship.

I extend my sincere appreciation to Professor Wei Lin for generously sharing his expertise and providing valuable advice throughout the preparation of my dissertation.

Special thanks are due to Professor Yizhou Wang for providing the funding that supported my research endeavors.

I am grateful to Professor Qianqian Xu for introducing me to the researching field of my dissertation and providing precious advice that greatly contributed to my research.

I also express my gratitude to Doctor Xinwei Sun for his insightful discussions and invaluable advice, which significantly contributed to my research.

Lastly, I would like to express my gratitude to all my colleagues and friends who have supported and encouraged me throughout this journey.



# 北京大学学位论文原创性声明和使用授权说明

## 原创性声明

本人郑重声明：所呈交的学位论文，是本人在导师的指导下，独立进行研究工作所取得的成果。除文中已经注明引用的内容外，本论文不含任何其他个人或集体已经发表或撰写过的作品或成果。对本文的研究做出重要贡献的个人和集体，均已在文中以明确方式标明。本声明的法律结果由本人承担。

论文作者签名：李缘

日期：2024年5月31日

## 学位论文使用授权说明

(必须装订在提交学校图书馆的印刷本)

本人完全了解北京大学关于收集、保存、使用学位论文的规定，即：

- 按照学校要求提交学位论文的印刷本和电子版本；
- 学校有权保存学位论文的印刷本和电子版，并提供目录检索与阅览服务，在校园网上提供服务；
- 学校可以采用影印、缩印、数字化或其它复制手段保存论文；
- 因某种特殊原因需要延迟发布学位论文电子版，授权学校一年两年三年以后，在校园网上全文发布。

(保密论文在解密后遵守此规定)

论文作者签名：李缘

导师签名：

日期：2024年5月31日





## 学位论文答辩委员会名单

<b>论文题目</b>	基于SUN分布的Thurstone-Mosteller排序模型的共轭贝叶斯学习方法			
<b>作 者</b>	李臻			
<b>专 业</b>	统计学			
<b>答辩委员会成员</b>	<b>姓 名</b>	<b>专业技术职称</b>	<b>从事专业</b>	<b>工作单位</b>
主席	王亦洲	教授	计算机应用技术	北京大学
委员	邓明华	教授	概率论与数理统计	北京大学
	李丰	副教授	概率论与数理统计	中央财经大学
	林伟	研究员	统计学	北京大学
	孙鑫伟	副研究员	概率论与数理统计	复旦大学



# 北京大学博士学位论文答辩委员会决议书

(本表由博士答辩委员会秘书填写,一式两份,一份存学校档案,一份存研究生个人档案)

院、系: 数学科学学院

专业: 统计学

姓名: 李臻

研究方向: 统计机器学习, 互联网搜索

学号: 1601110060

导师姓名: 姚远

**学位论文题目:** 基于SUN分布的Thurstone-Mosteller排序模型的共轭贝叶斯学习方法

答辩委员会对学位论文和答辩情况的学术评语 (主要就论文选题意义, 创新性成果及学术水平; 论文存在的主要不足之处, 以及博士生答辩情况等方面)。

排序模型与算法是统计机器学习领域的一个重要问题, 本论文研究了基于SUN分布的Thurstone-Mosteller排序模型的共轭贝叶斯学习方法。选题具有重要的理论意义和实际应用价值。

本论文的主要贡献和创新点如下:

1. 系统地研究了在Thurstone-Mosteller模型和高斯先验分布的情况下, 给出了后验概率分布的闭形式, 提出了一种新的共轭贝叶斯决策框架。证明了在非对称条件下, 最优排序即为后验分布的均值排序。

2. 引入了知识梯度, 将基于静态数据的算法推广到主动采样算法, 提高了主动采样算法的效率。

3. 引入了平均场变分推理的近似方法, 提高了排序参数后验的估计效率, 保证了结果的稳健性。  
上述实验结果提供了开源代码。

论文工作表明作者掌握了本学科坚实宽广的基础理论和系统深入的专门知识, 具有独立从事科研工作能力。学位论文结构完整、逻辑清晰、满足写作与学术规范。论文答辩表达清楚, 回答问题正确。

答辩委员会经过讨论和无记名投票表决, 认为论文达到了博士学位论文水平, 一致同意通过李臻博士论文答辩, 建议授予其理学博士学位。

答辩委员会表决结果: 实到答辩委员: 5 人,

同意博士毕业者 5 人, 不同意博士毕业者 0 人, 结论为 准予毕业

同意建议授予博士学位者 5 人, 不同意建议授予博士学位者 0 人, 结论为 建议授予学位

答辩时间: 2024 年 05 月 29 日 9 时

答辩委员会主席 (签字):

委员 (签字):

本表不得折叠、不得跨页



## 提交终版学位论文承诺书

本人郑重承诺，所呈交的学位论文为最终版学位论文。本人知晓，该版学位论文将用于校学位评定委员会审议学位、国家和北京市学位论文抽检。论文版本呈交错误带来的结果将由本人承担。

论文作者签名：李臻

日期：2024年 6月 3日

